

Multi-dimensional Image Analysis

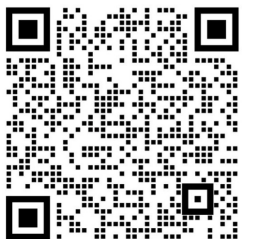
# IMARIS

Introduction and Applications

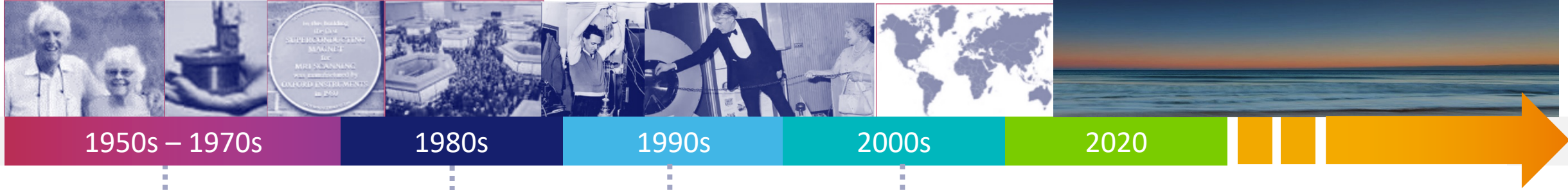
**April Hu**

Sales Engineer

[April.hu@andor.com](mailto:April.hu@andor.com)



# Our History



1950s – 1970s

1980s

1990s

2000s

2020

## Foundations

**Founded 1959:**  
Oxford Instruments is the first commercial spinout from Oxford University

Oxford Instruments develops the world's first superconducting magnet



## World Firsts

**1980:** Oxford Instruments delivers the world's first MRI system

**1983:** Floated on the London Stock Exchange



## Expansion

The Group expands its global presence opening offices in Japan and China

Broadens portfolio across Semiconductor processing, Analytical Techniques & Medical instrumentation



## Acceleration

Nanotechnology Tools strategy & focus drives growth

**2016:** Horizon Strategy

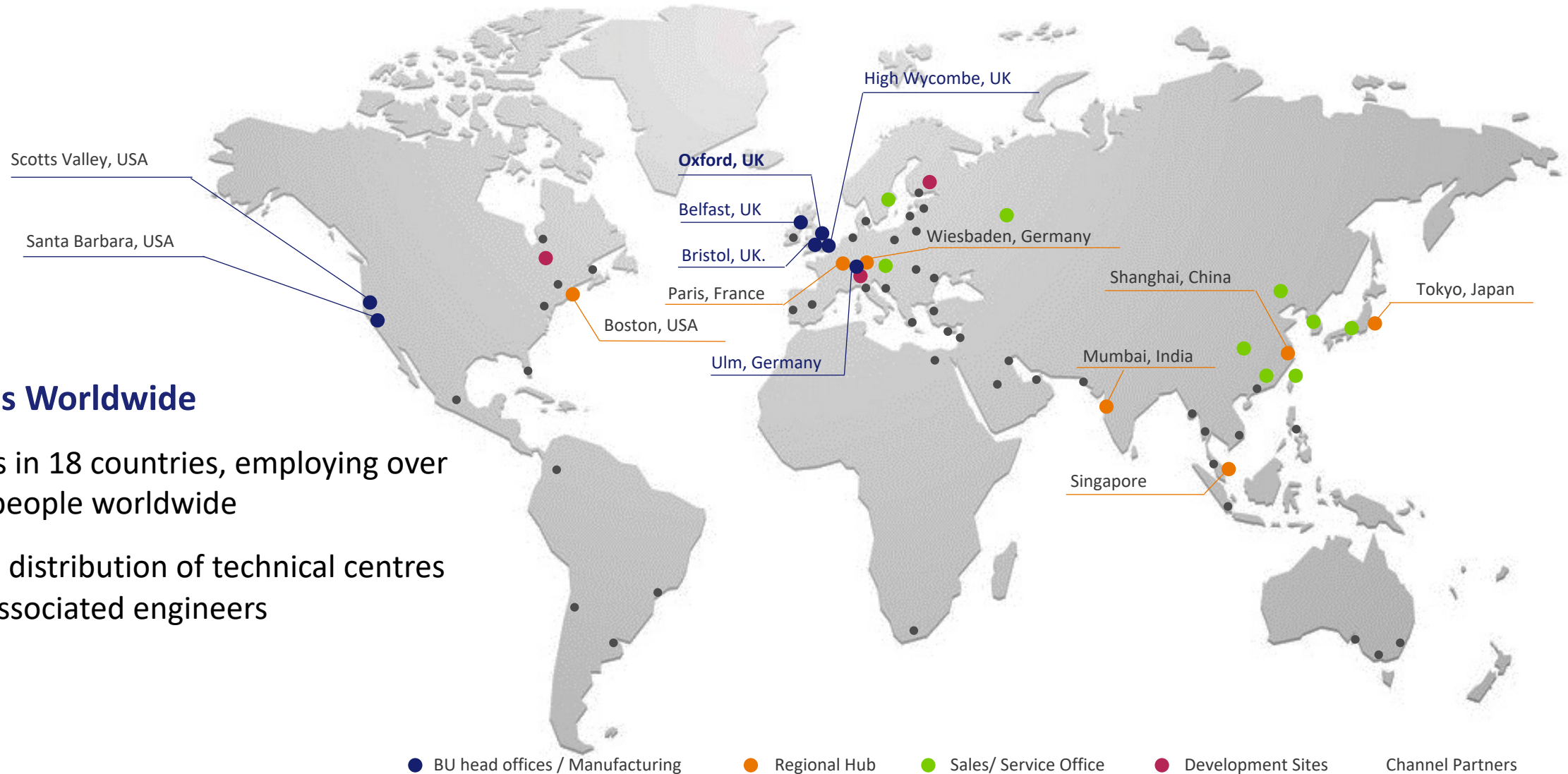


Our core purpose is to support our customers in addressing some of the world's most pressing challenges:

- enabling a greener economy
- increased connectivity
- improved health
- leaps in scientific understanding.

We are a leading provider of high technology products and services to the world's foremost industrial companies and scientific research communities to image, analyse, and manipulate materials down to the atomic and molecular level.

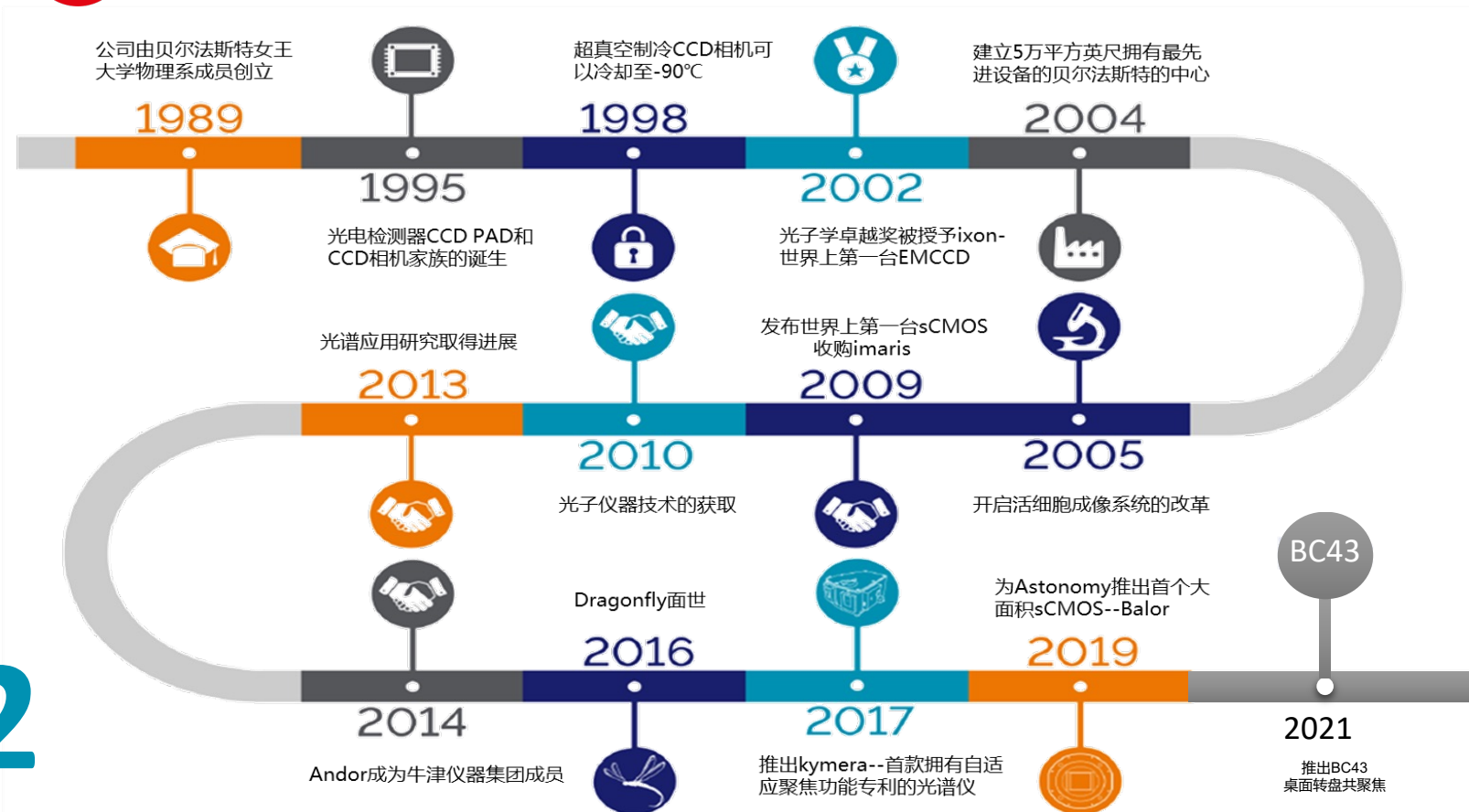
We focus on attractive segments where our key enabling technologies drive long-term growth for customers and where we can maintain leadership positions.



## 28 Offices Worldwide

- Offices in 18 countries, employing over 1600 people worldwide
- Global distribution of technical centres with associated engineers

## 弱光探测、解析 及成像系统 全球制造领跑者



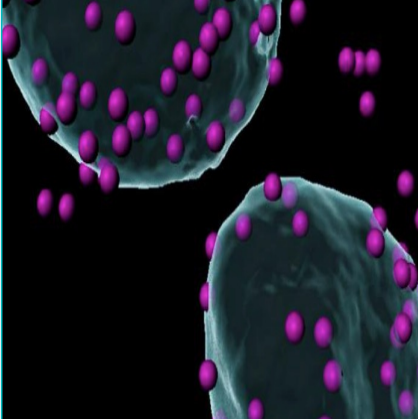
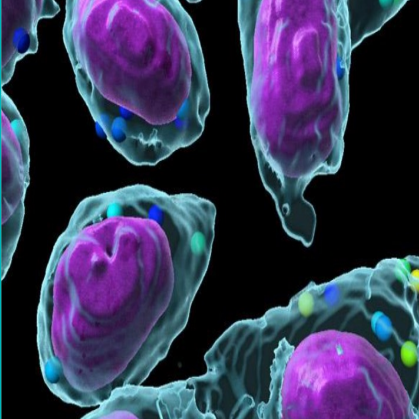
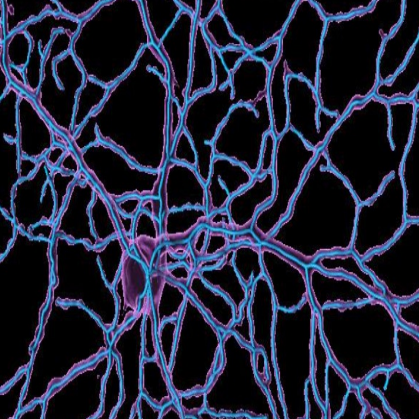
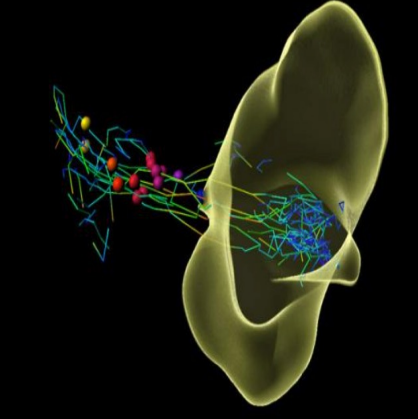
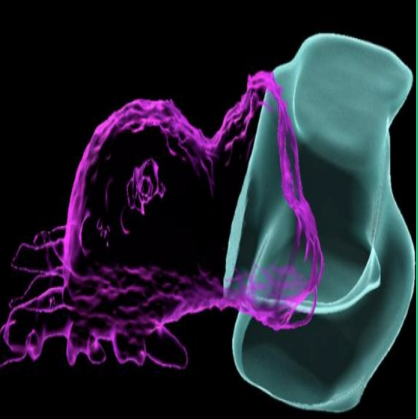
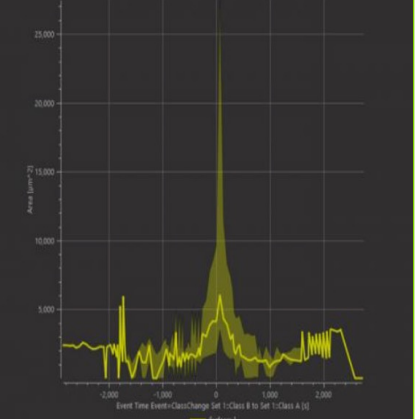
ANDOR  
SINCE

1989

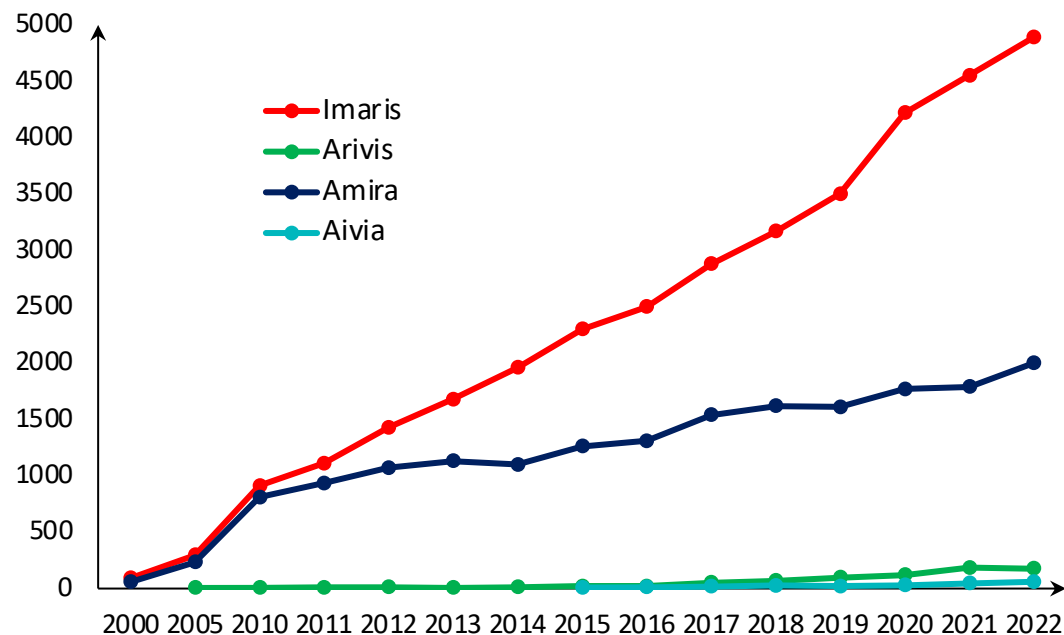
IMARIS  
SINCE

1992

# Quantitative Image Analysis for 3D Microscopy

					
<b>Quantification</b> <ul style="list-style-type: none"><li>•Count of objects</li><li>•Area</li><li>•Volume</li><li>•Intensity</li><li>•Position</li></ul>	<b>Cell</b> <ul style="list-style-type: none"><li>•Volume</li><li>•Vesicles per Cell</li><li>•Distance to Membrane</li><li>•Vesicles per Nucleus</li><li>•Morphology</li></ul>	<b>Filaments/Neurons</b> <ul style="list-style-type: none"><li>•Length, Straightness</li><li>•Mean Diameter</li><li>•Branching Angle</li><li>•Spine Density</li><li>•Spine Shape</li></ul>	<b>Motion Analysis</b> <ul style="list-style-type: none"><li>•Speed</li><li>•Acceleration</li><li>•Cell division tracking</li><li>•Trajectory</li><li>•Event synchronization</li></ul>	<b>Interactions</b> <ul style="list-style-type: none"><li>•Distances between structures</li><li>•Volume overlap, contacts</li><li>•3D intensity profiling</li><li>•Spatial distribution</li><li>•Co-localization</li></ul>	<b>Batch and Plots</b> <ul style="list-style-type: none"><li>•Image processing</li><li>•Measurements</li><li>•Interactions</li><li>•Group comparisons</li><li>•Statistical tests</li></ul>

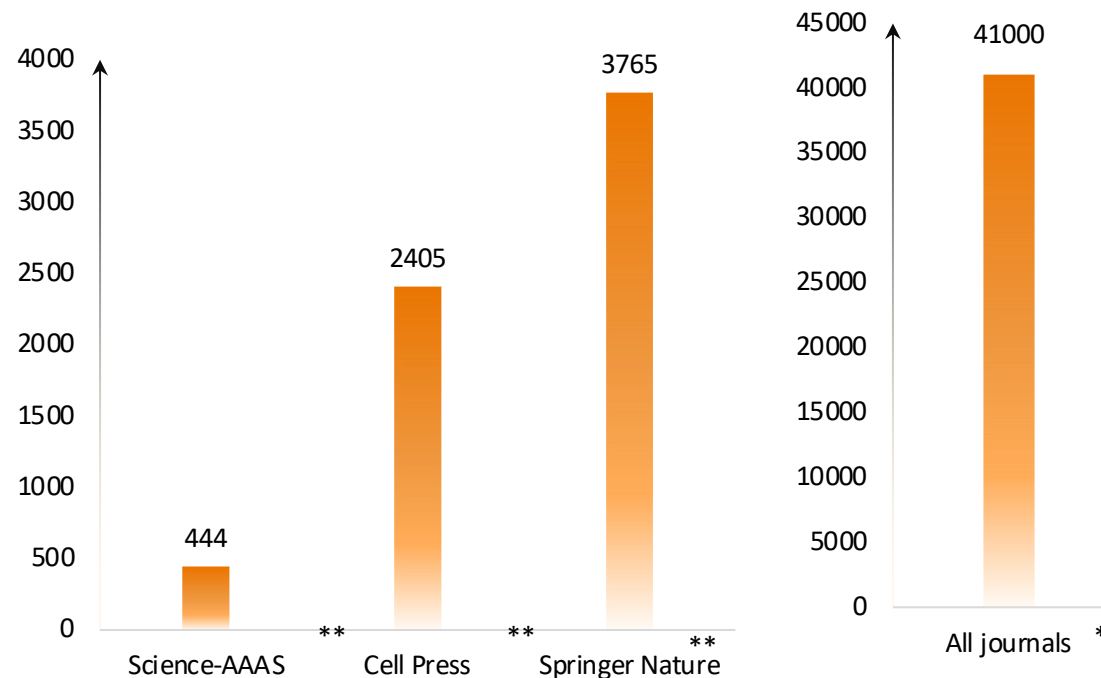
IMARIS and competitors' usage in publications overtime\* (2000 to 2022)



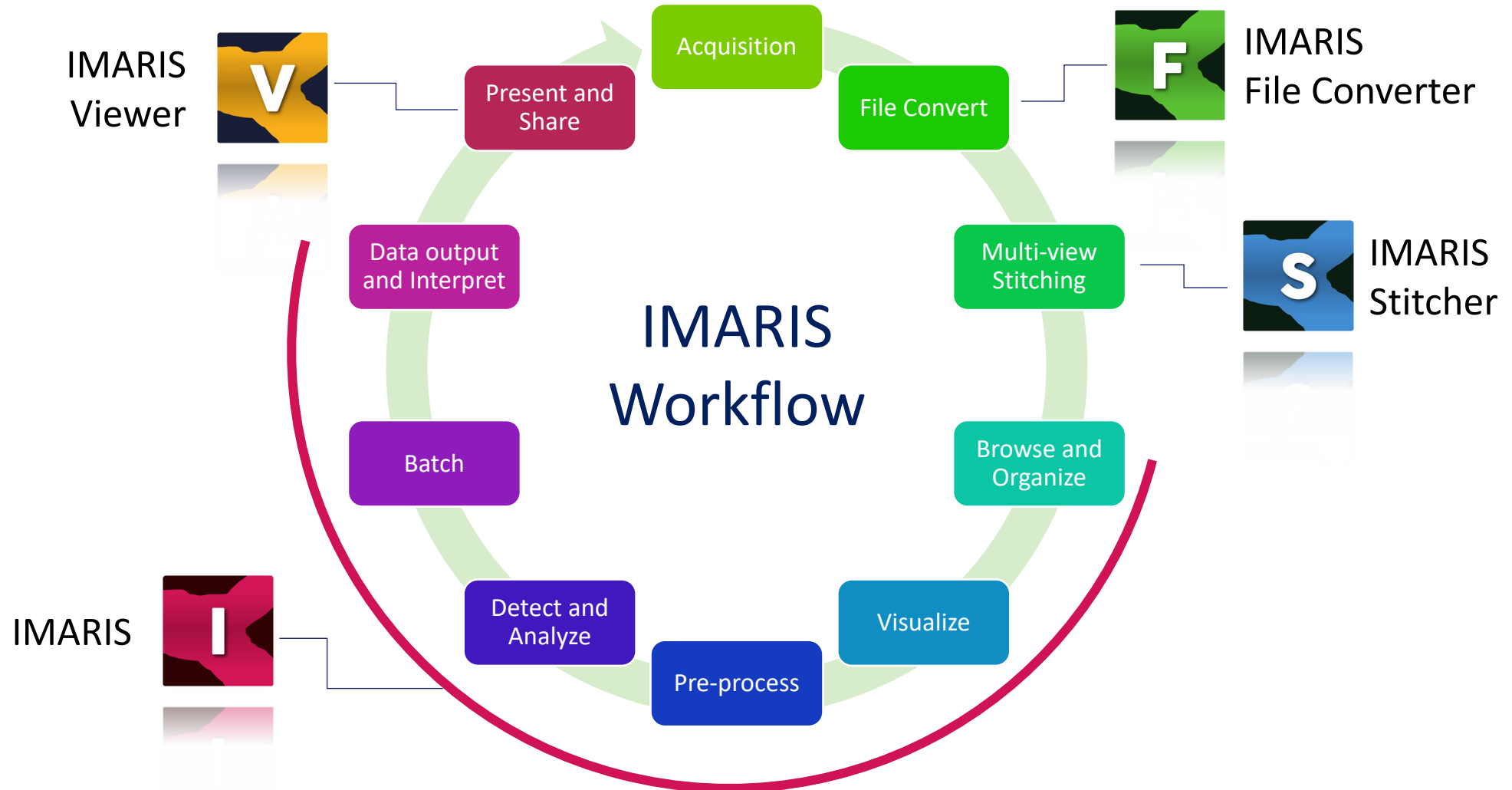
\*Data acquired from Google Scholar

\*\*Data acquired from journal official sites, respectively.

IMARIS usage in publications (2000 to 2023 April)



# Workflow of image analyzing and processing



IMARIS  
File Converter



IMARIS  
Stitcher



IMARIS



IMARIS  
Viewer



## IMARIS File Converter



IMARIS File Converter's redesigned GUI and batch conversion efficiently convert multiple large datasets to save you time.

- Conversion is multithreaded (number of cores selected by the user).
- Files dropped to conversion queue and processed with one click.
- Memory allocation increased to handle big data.
- IMARIS Convert Bio-formats.

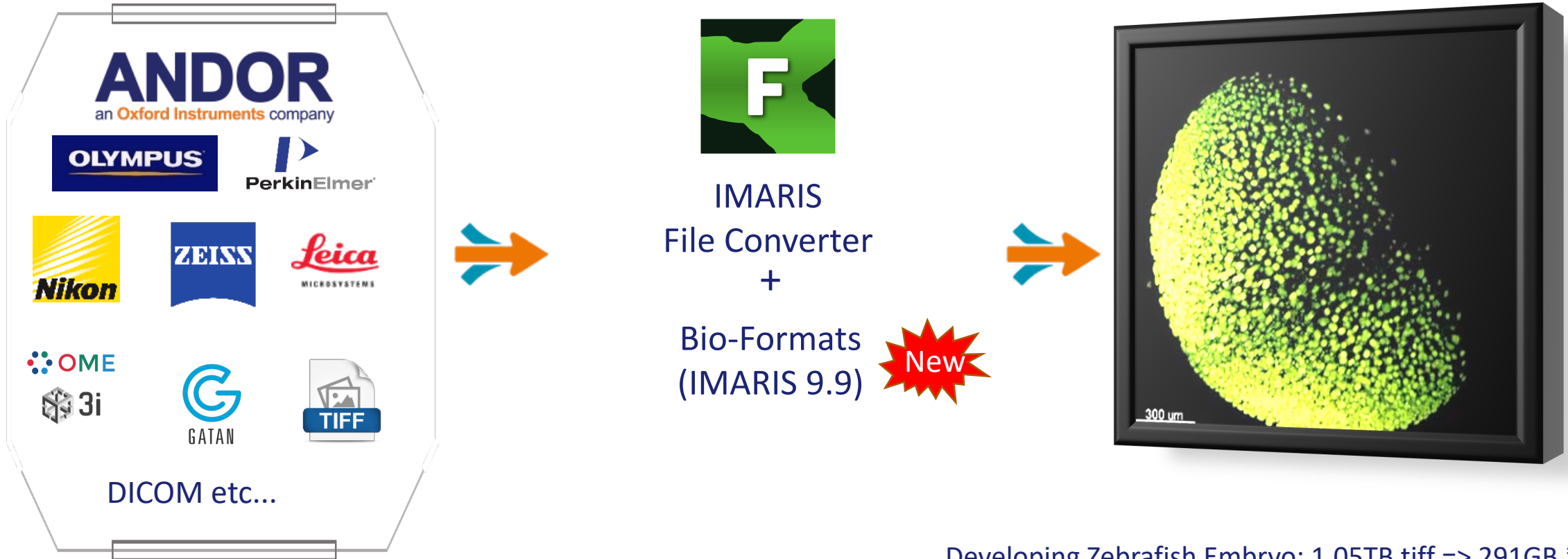
## IMARIS File Converter



IMARIS File Converter's redesigned GUI and **batch** conversion efficiently convert **multiple large datasets** to save you time.

- Conversion is **multithreaded** (number of cores selected by the user).
- Files dropped to conversion queue and processed with **one click**.
- Memory allocation increased to handle **big data**.
- IMARIS Convert **Bio-formats**.



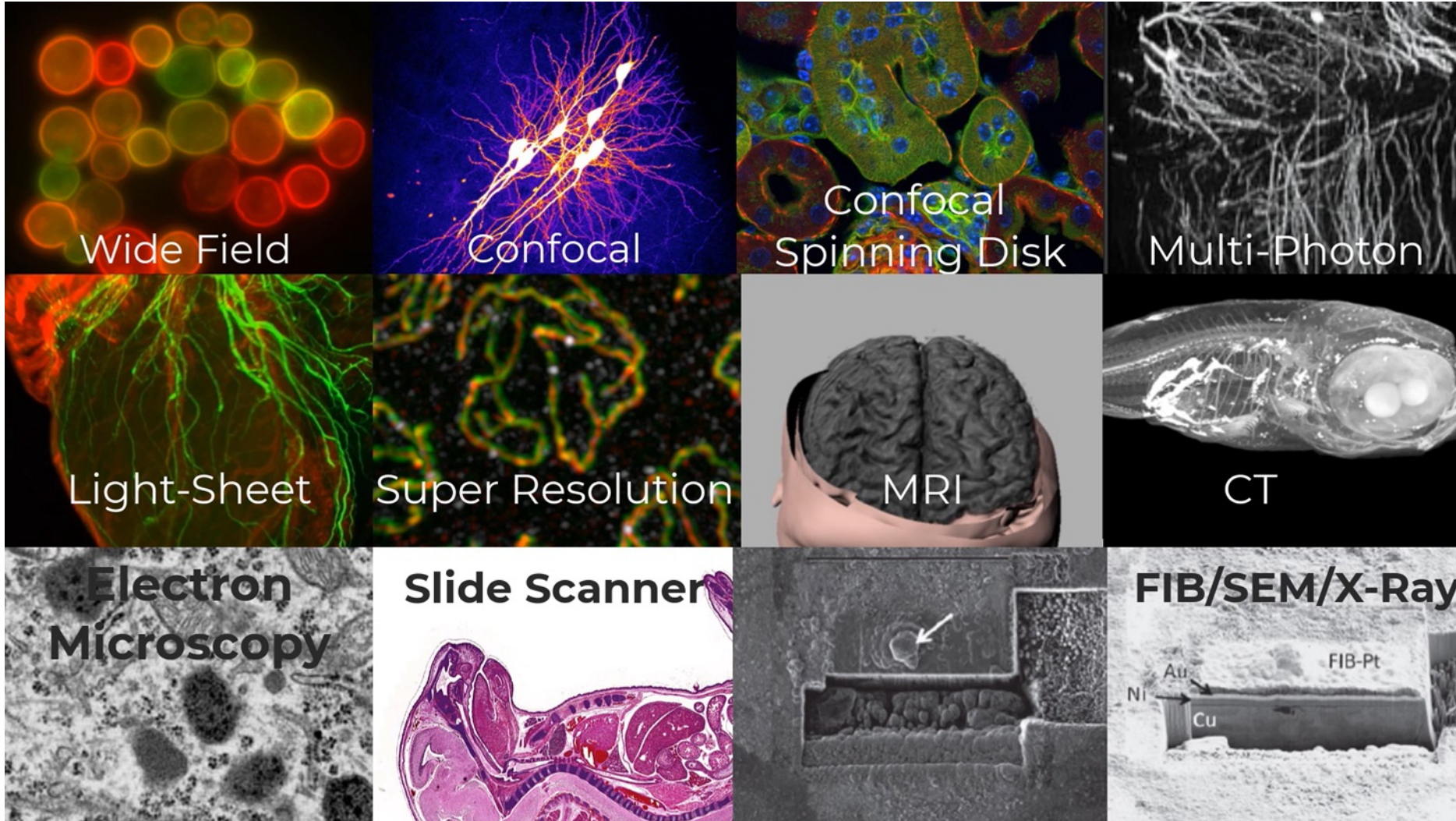


Developing Zebrafish Embryo: 1.05TB tiff => 291GB \*.ims

Courtesy of K. McDole, HHMI Jamelia Farm research Campus,

Ref: Amat *et al.*, 2014, *Nature Methods*

# Hardware Compatibility



IMARIS  
File Converter



IMARIS  
File Converter



IMARIS  
Stitcher



IMARIS



IMARIS  
Viewer



# What is IMARIS – An Overview



IMARIS  
File Converter



IMARIS  
Stitcher



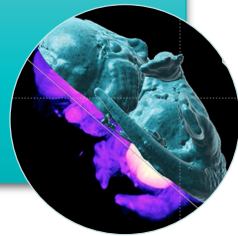
IMARIS



IMARIS  
Viewer

- Stitcher
- Multi-Modalities & Overlays
- Visualization Tools

Visualization



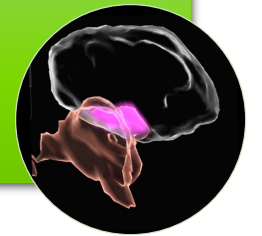
- Spots
- Surfaces
- Cell
- Filament
- Track

Object Detection  
Modules



- Colocalization
- Classification
- Affinity
- XTension

Analysis

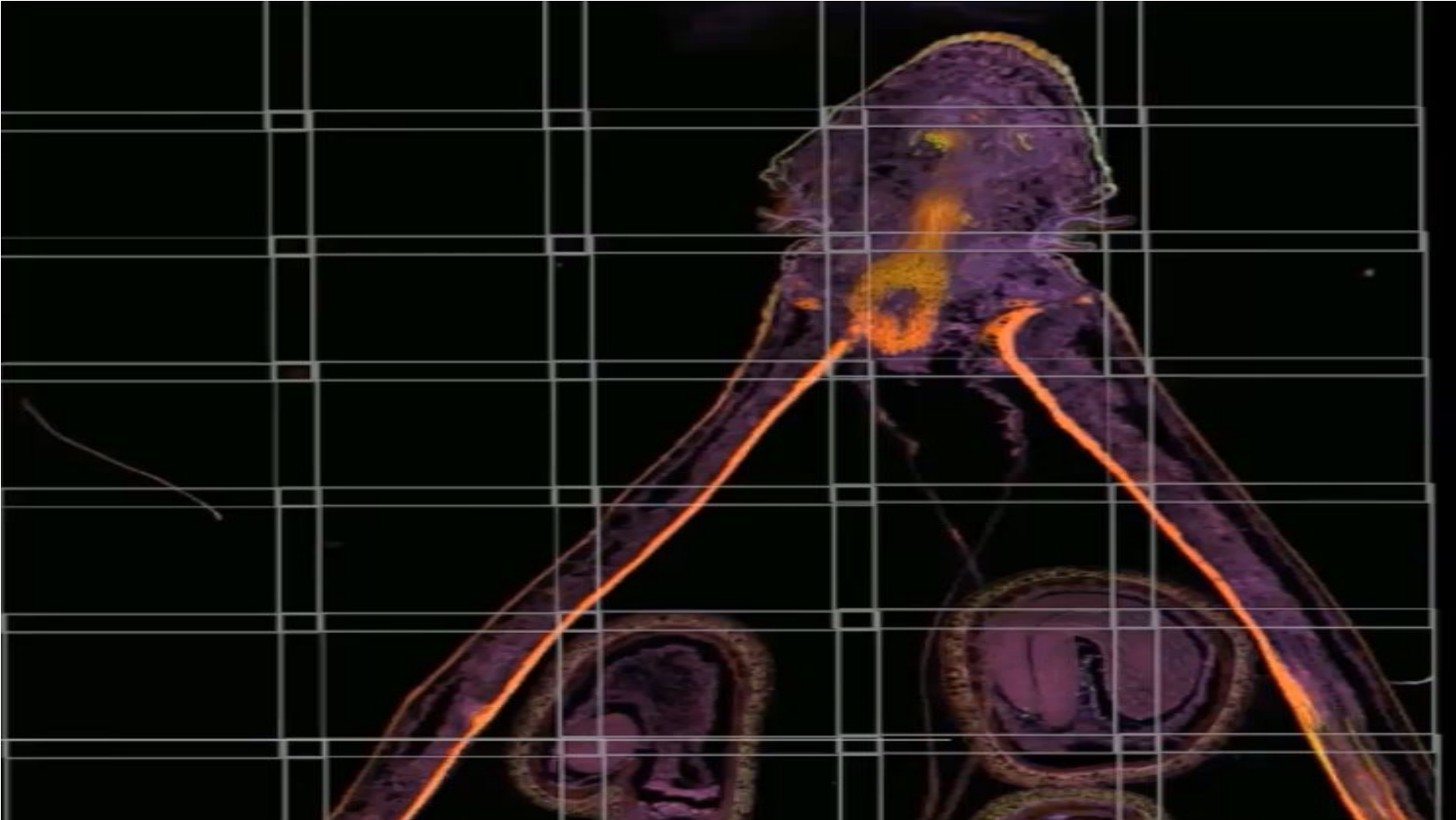


# Stitcher

Capable of Stitching Large 2D, 3D and 4D files



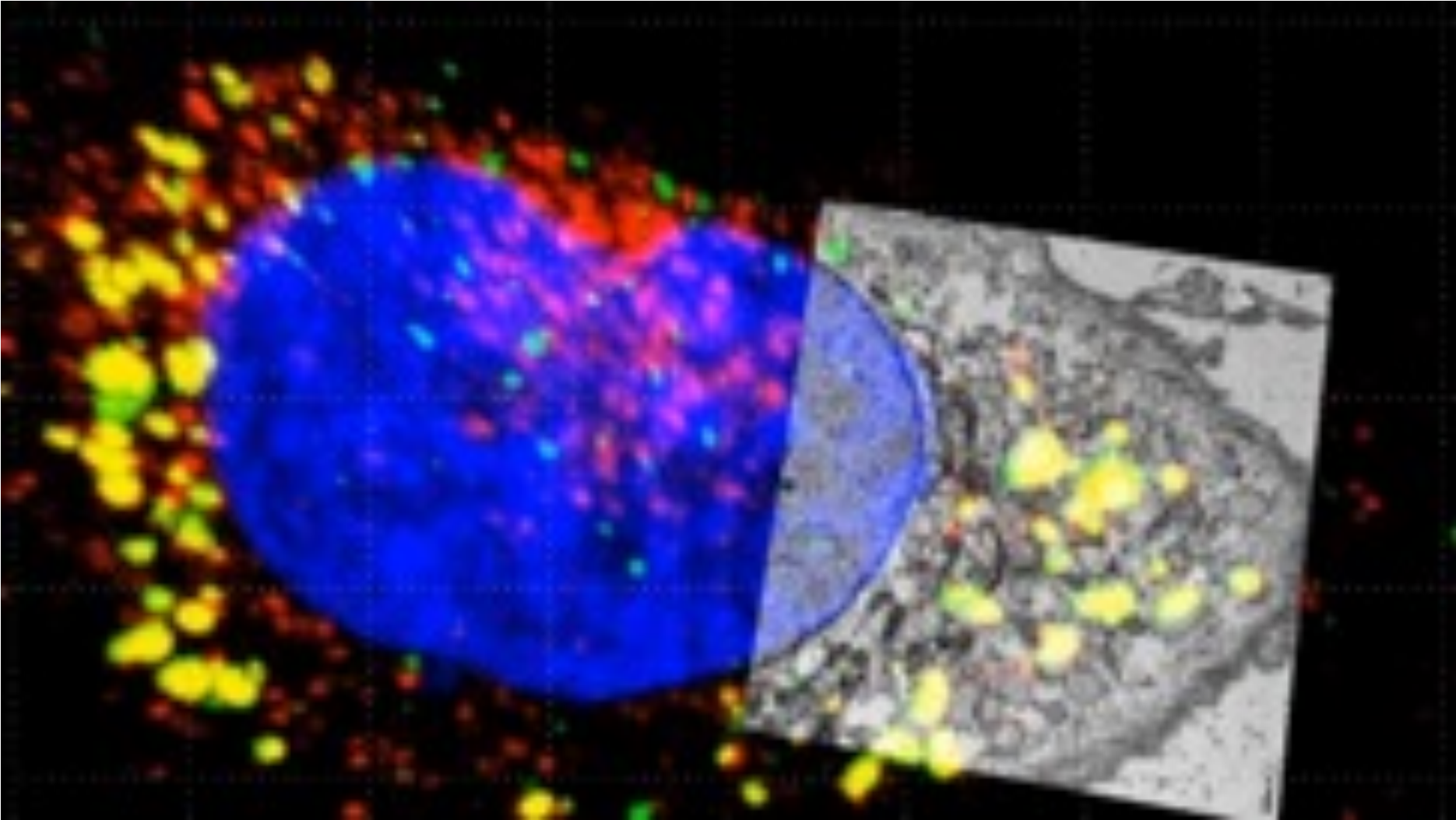
IMARIS



IMARIS  
Stitcher



# Visualize Multi-Modalities & Overlays



IMARIS

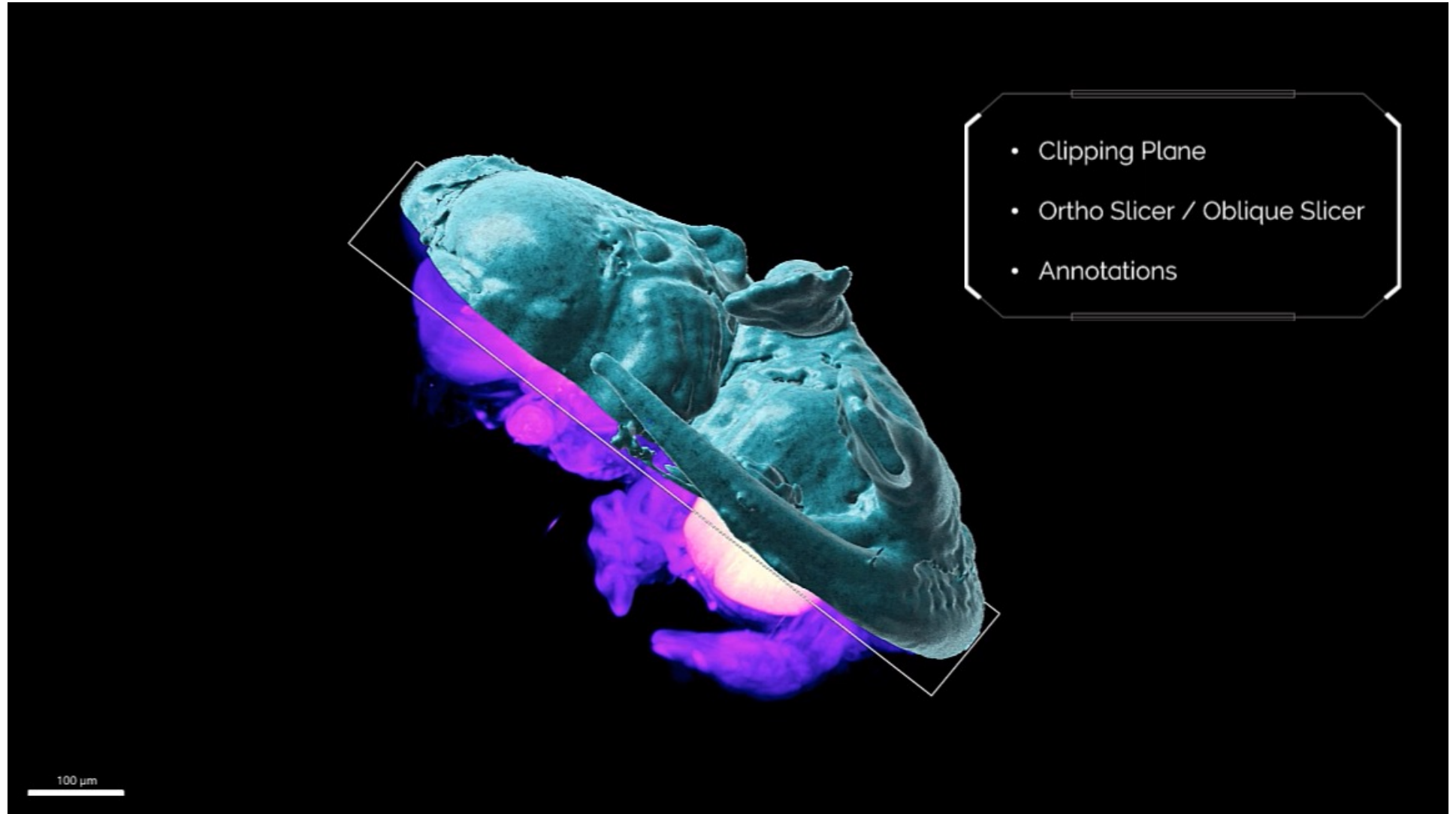




IMARIS



IMARIS  
Viewer



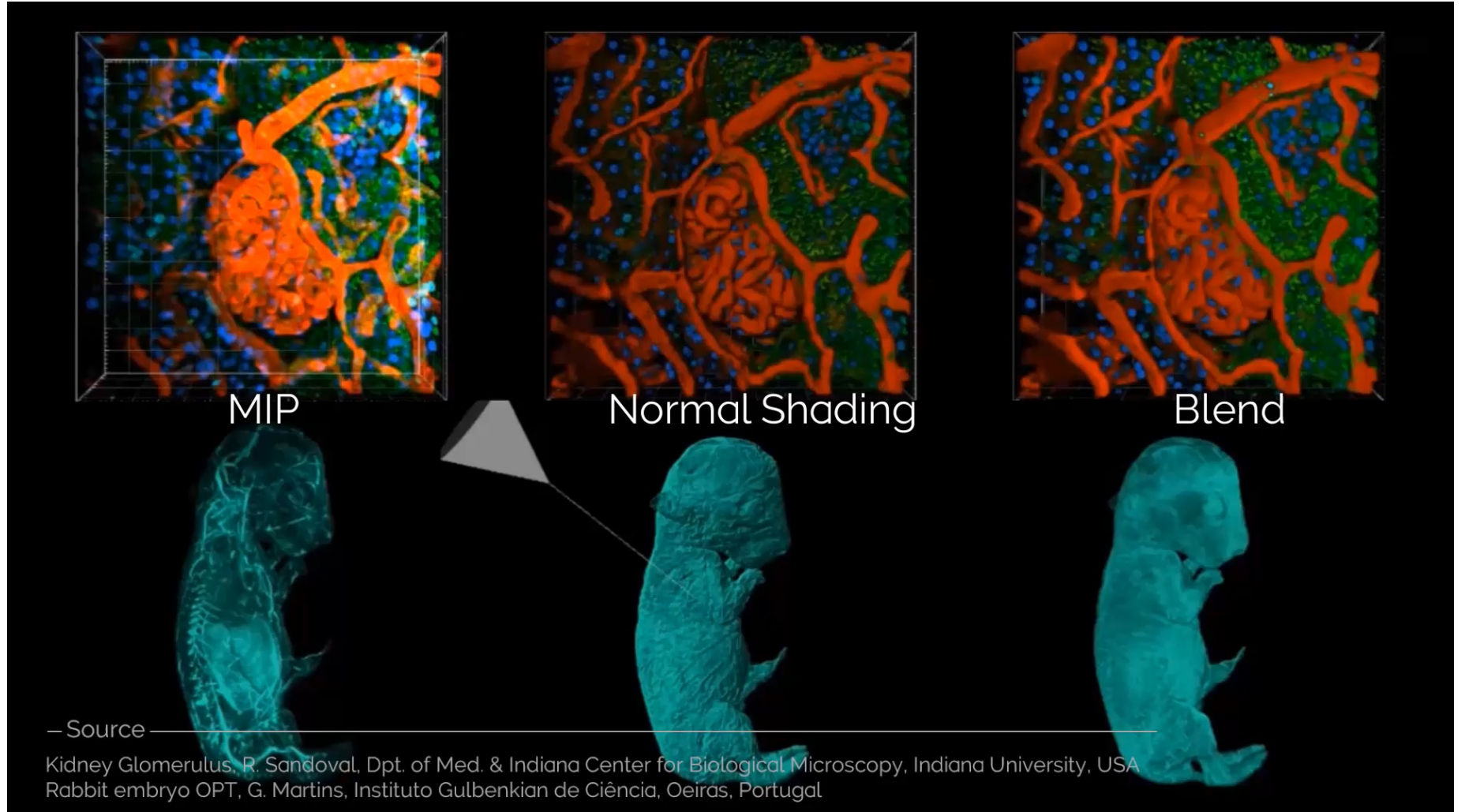
- Clipping Plane
- Ortho Slicer / Oblique Slicer
- Annotations



IMARIS



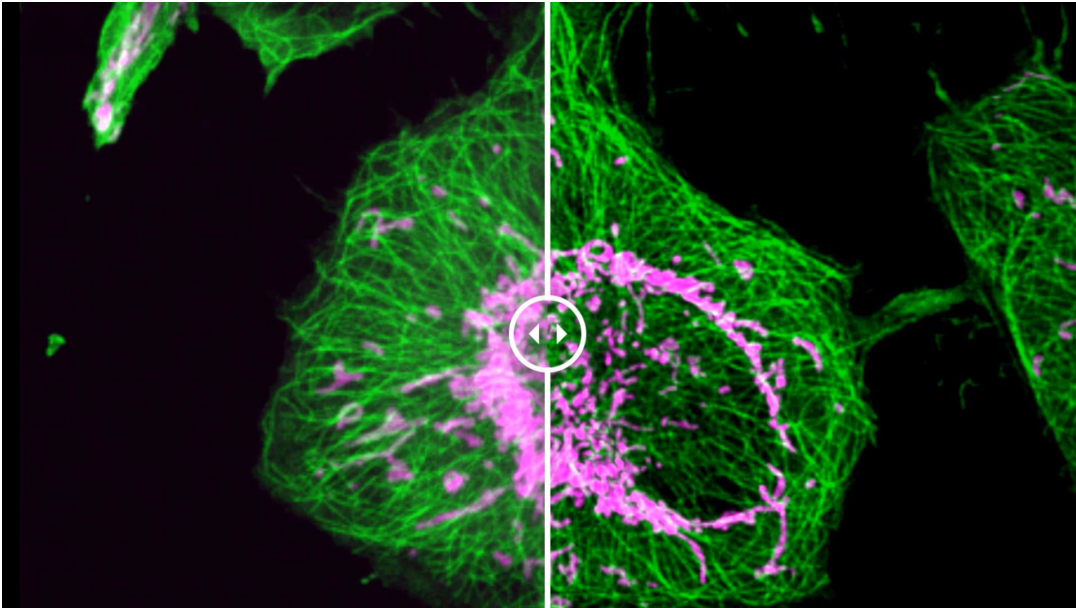
IMARIS  
Viewer





IMARIS

# Deconvolution

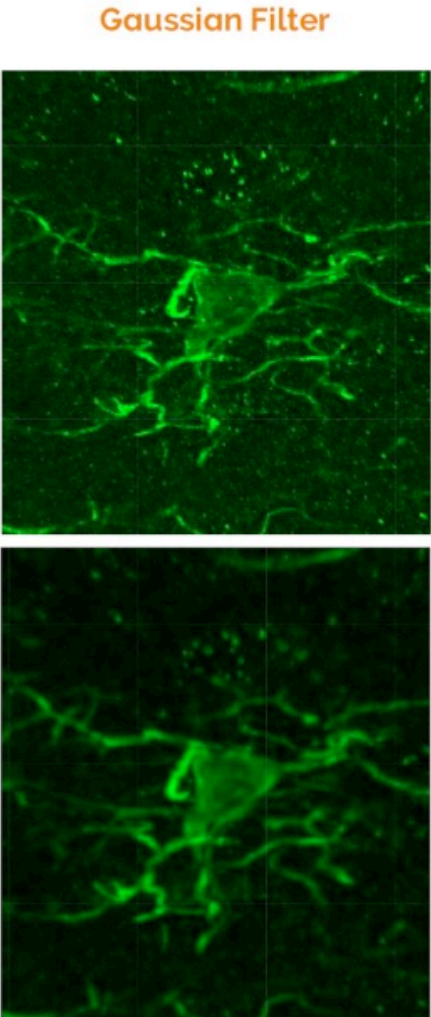
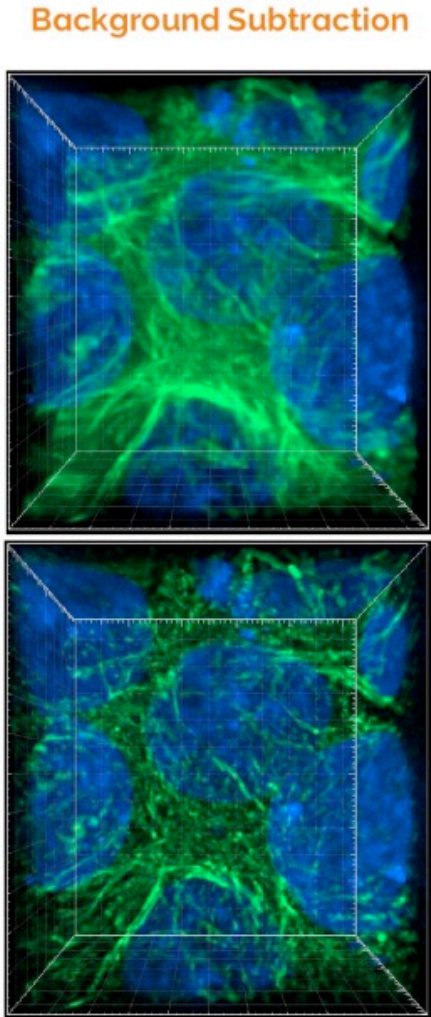
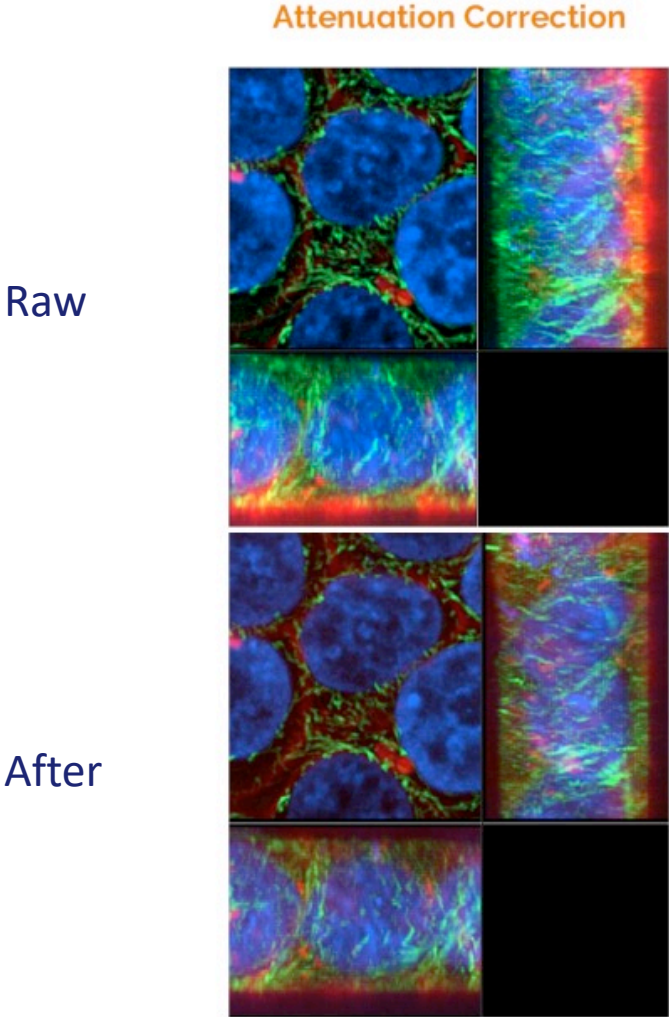


Supported Modalities: WideField, Confocal, Confocal spinning disk, Brightfield, TIRF

Algorithms:

- Qualitative Subtractive : No Neighbour (Fastest)
- Quantitative: Iterative (Robust)

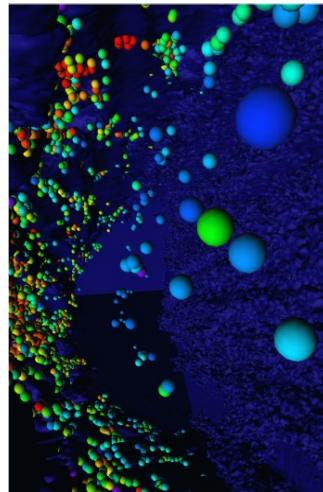




IMARIS



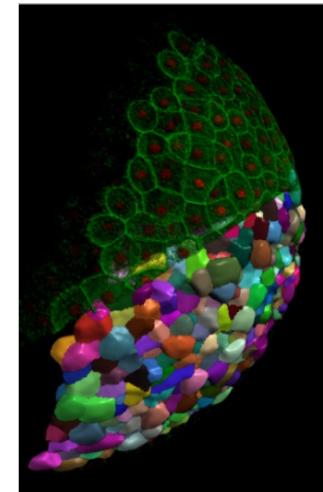
Spot



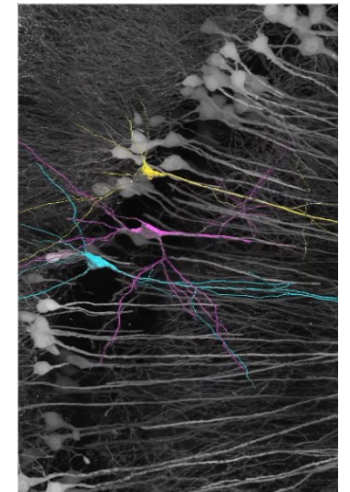
Surface

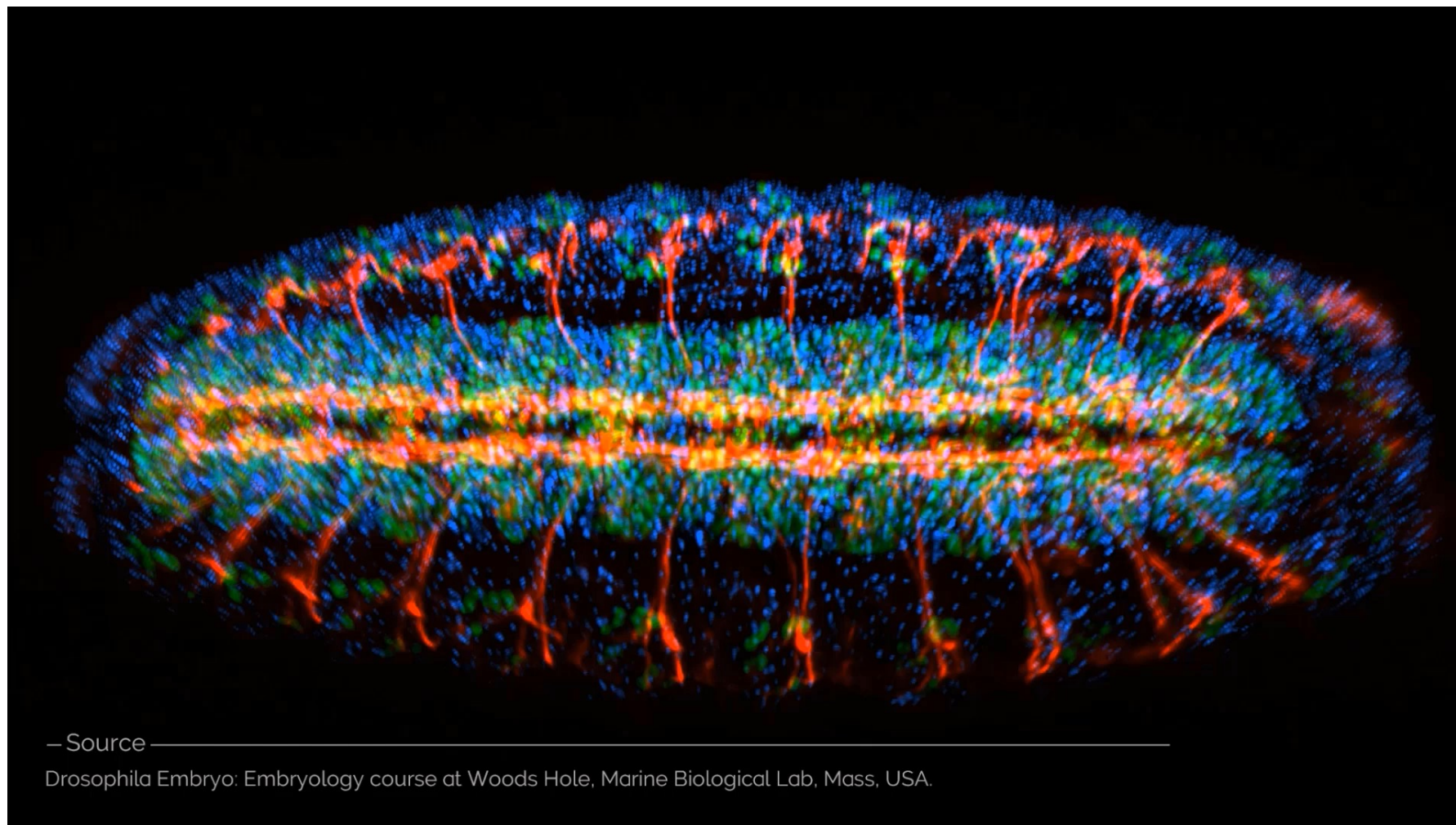


Cell



Filament

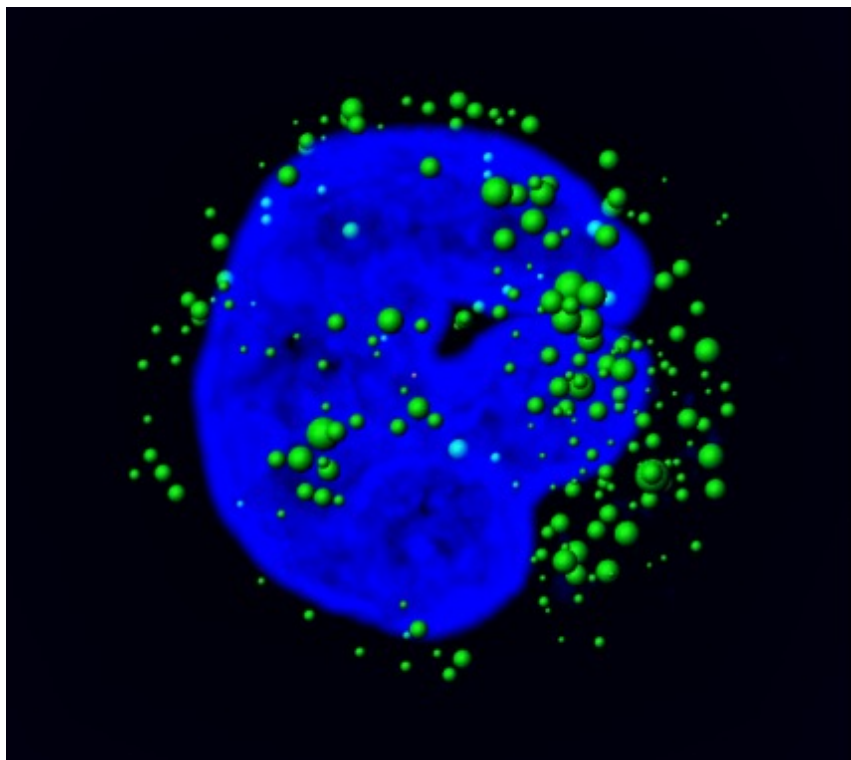
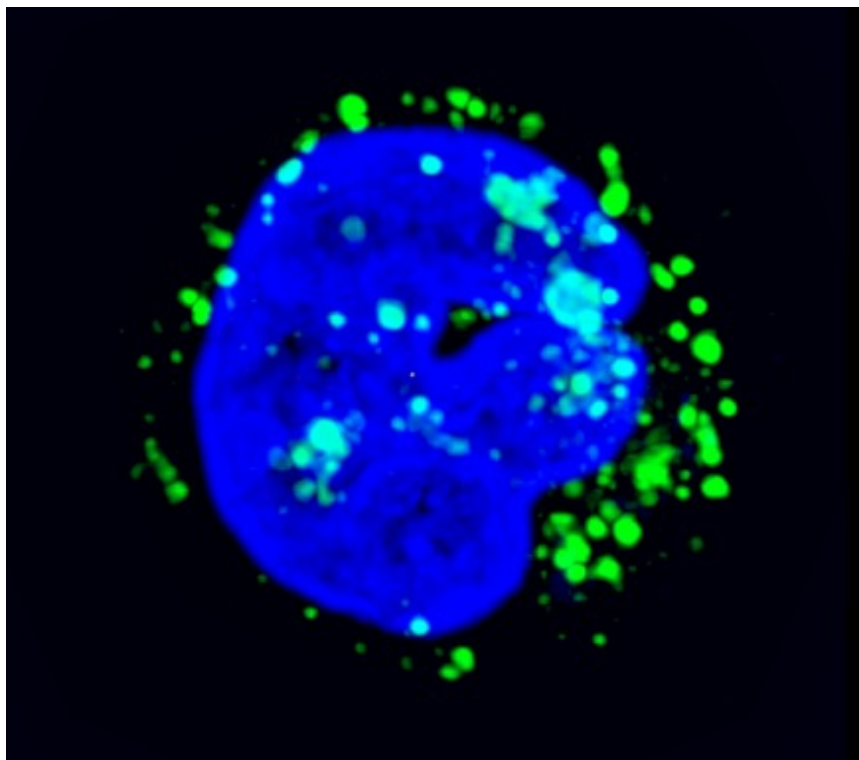


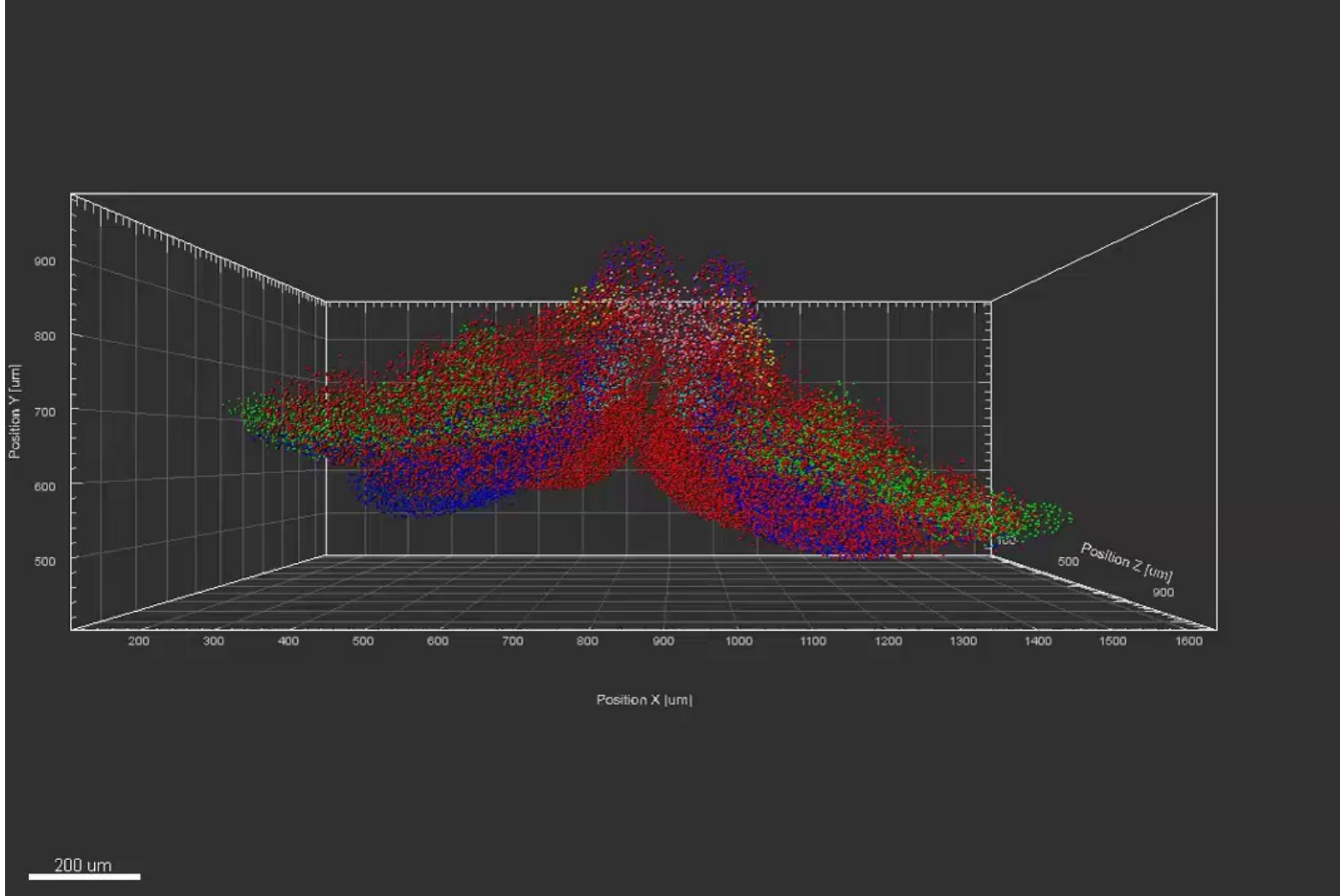


— Source —

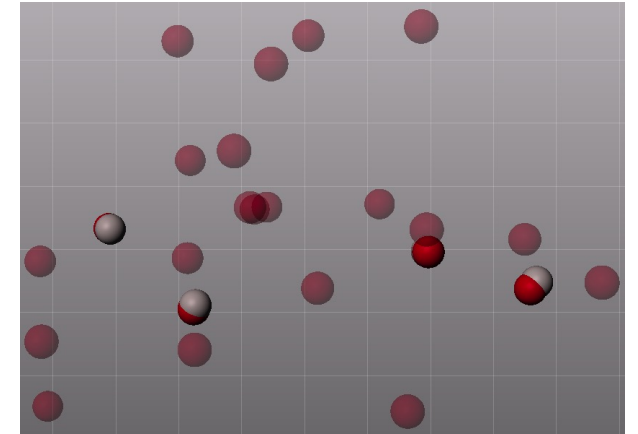
Drosophila Embryo: Embryology course at Woods Hole, Marine Biological Lab, Mass, USA.



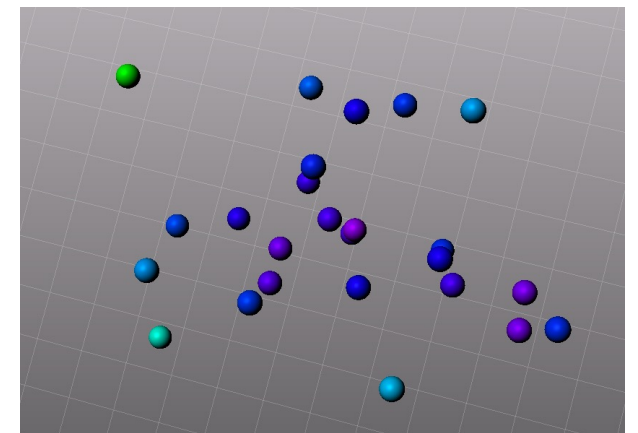




### Colocalized Spots



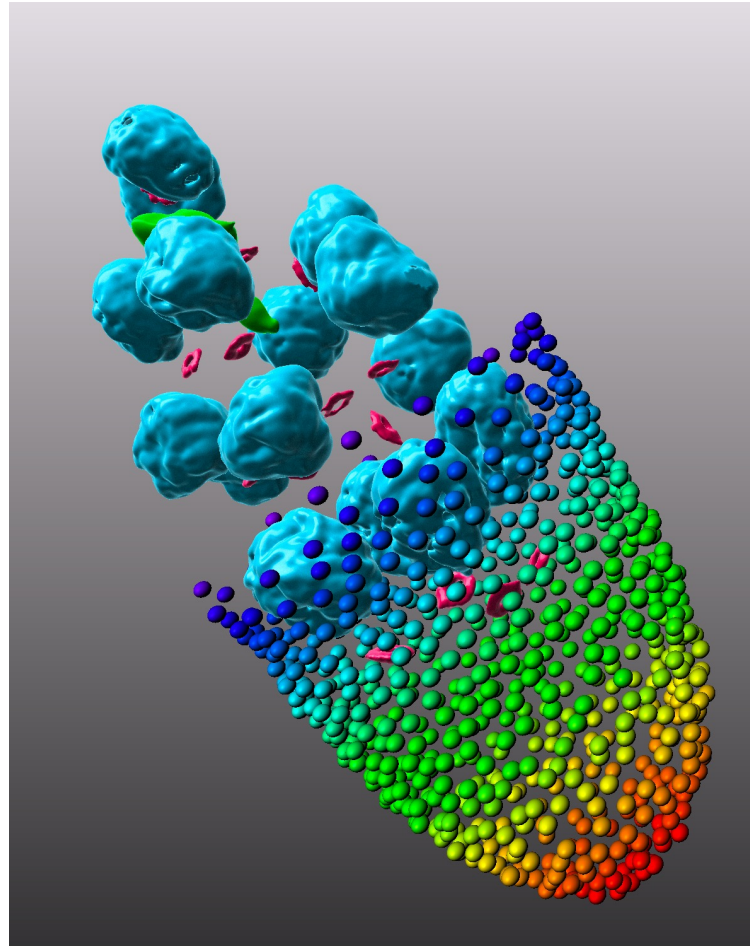
### Average Distance to Neighbour





— Source —

Wei. Dai, Montell's lab, Department of Molecular, Cellular and Developmental Biology, UCSB





Merz, S.F. et al., Nat Commun. (2019)



# Machine Learning Pixel Classification – IMARIS 9.9



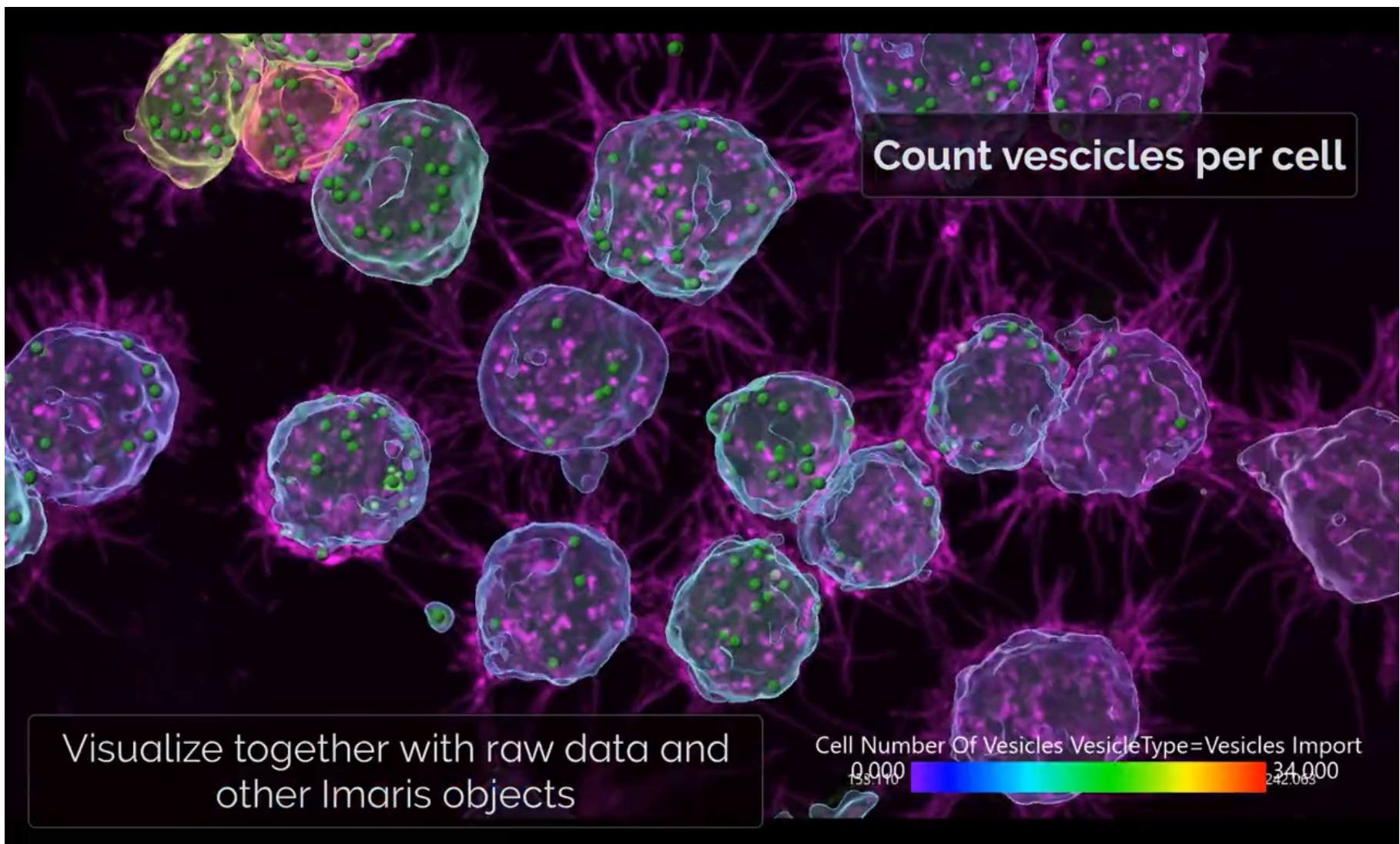
Use colors and materials

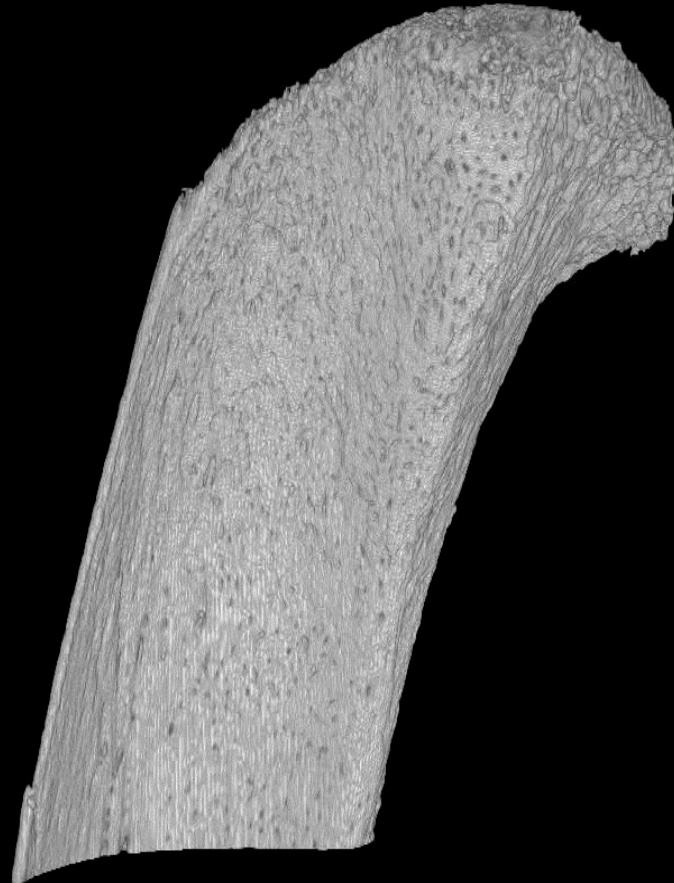
Visualize together with raw data and other Imaris objects





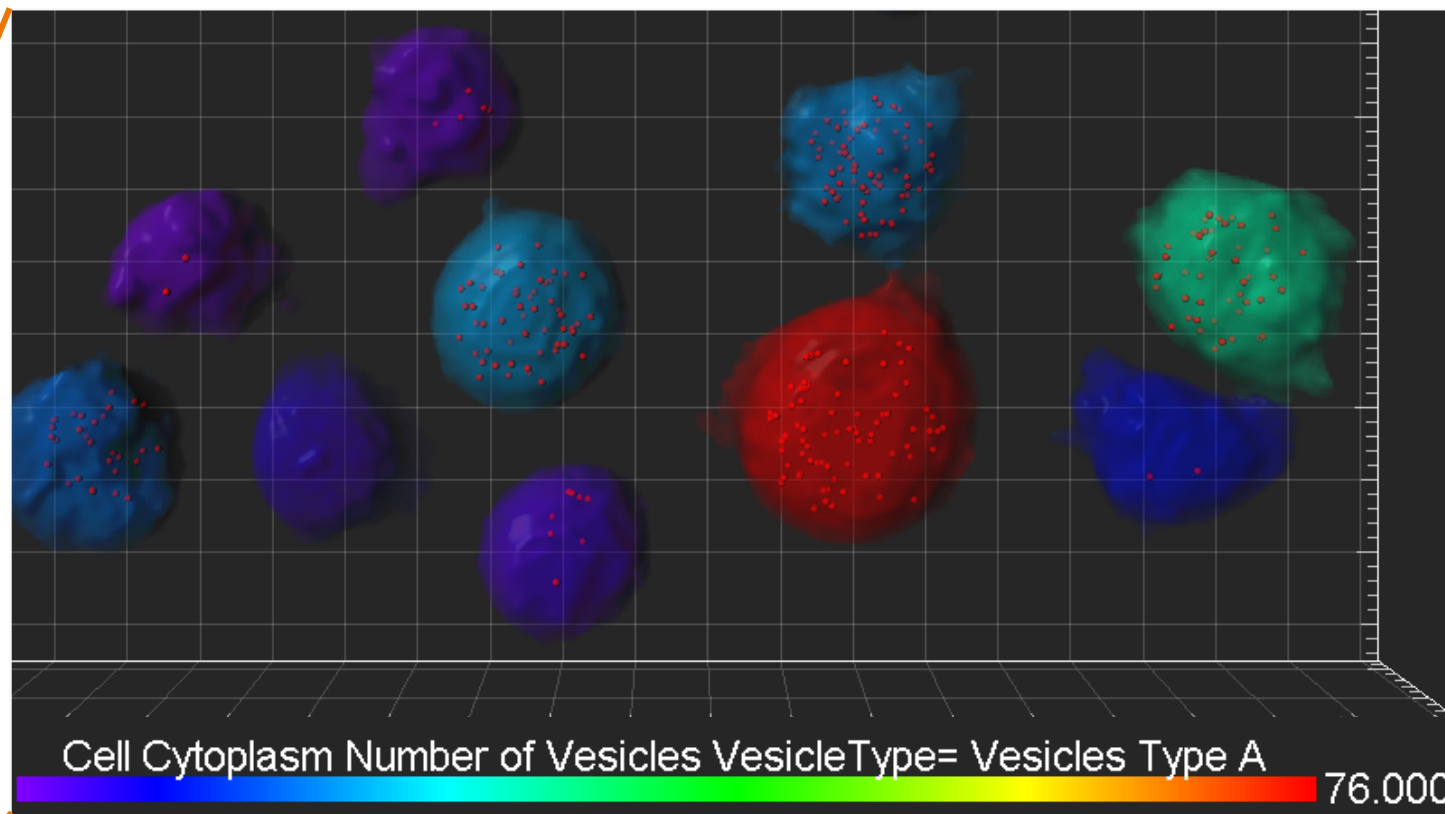
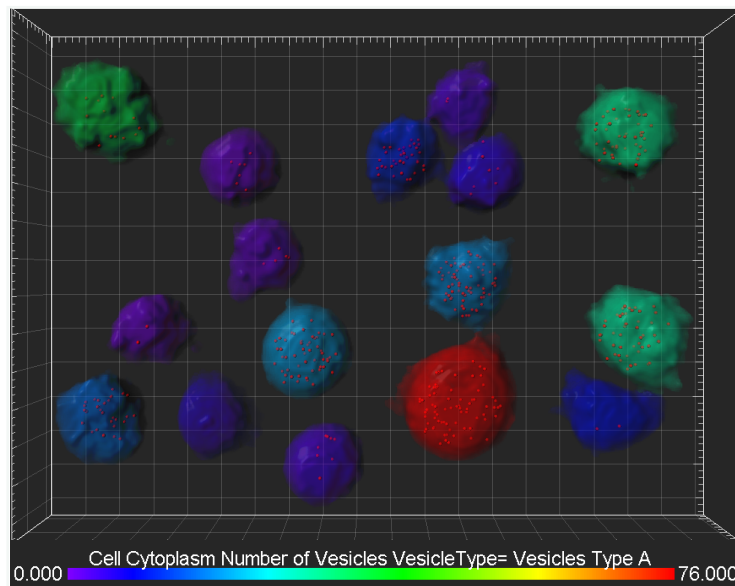
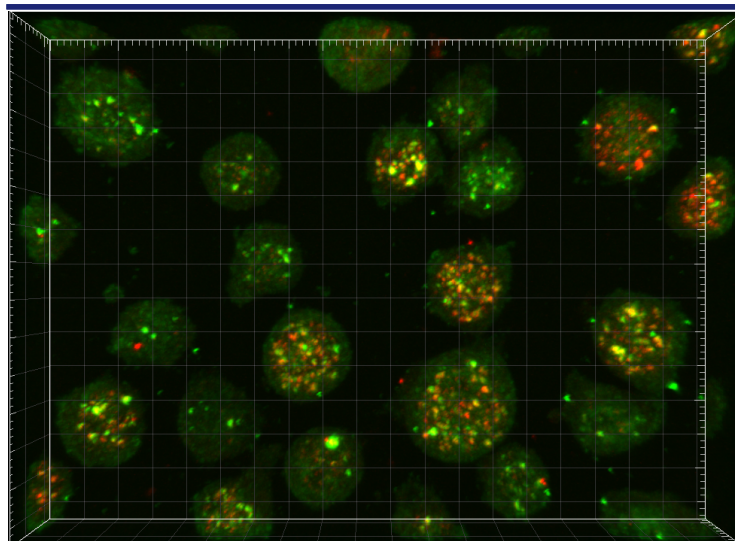
# Machine Learning Pixel Classification – IMARIS 9.9

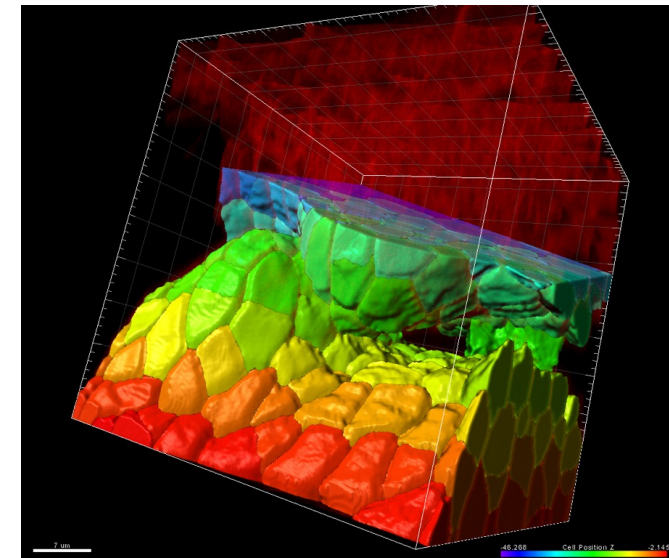
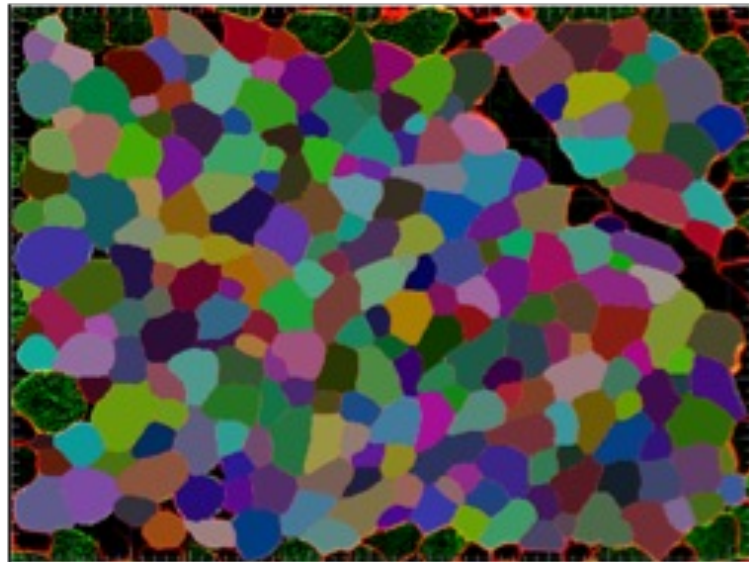
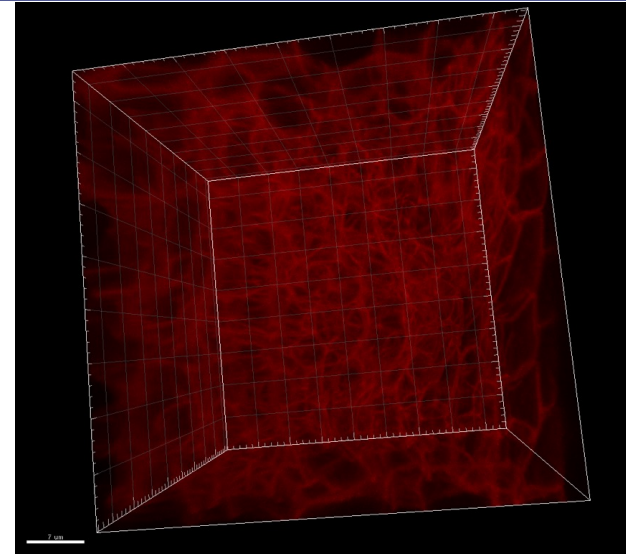
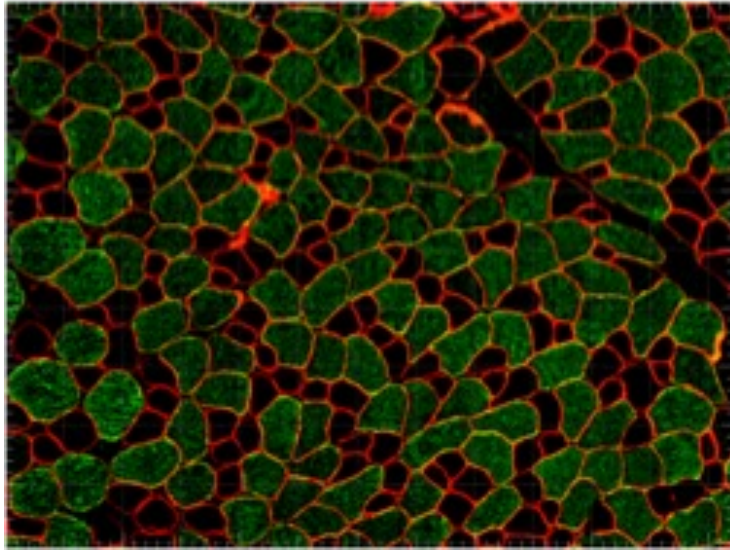


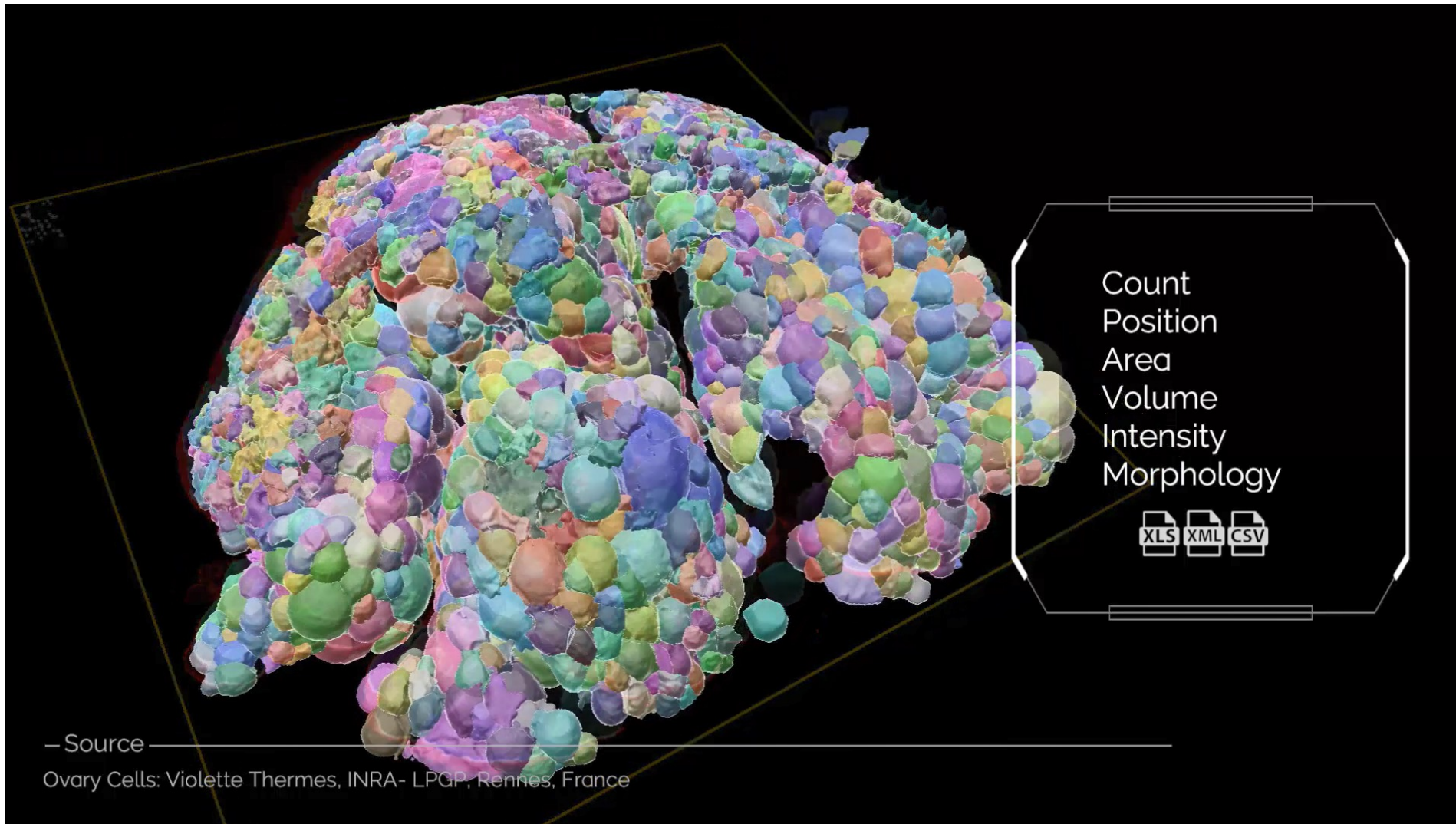


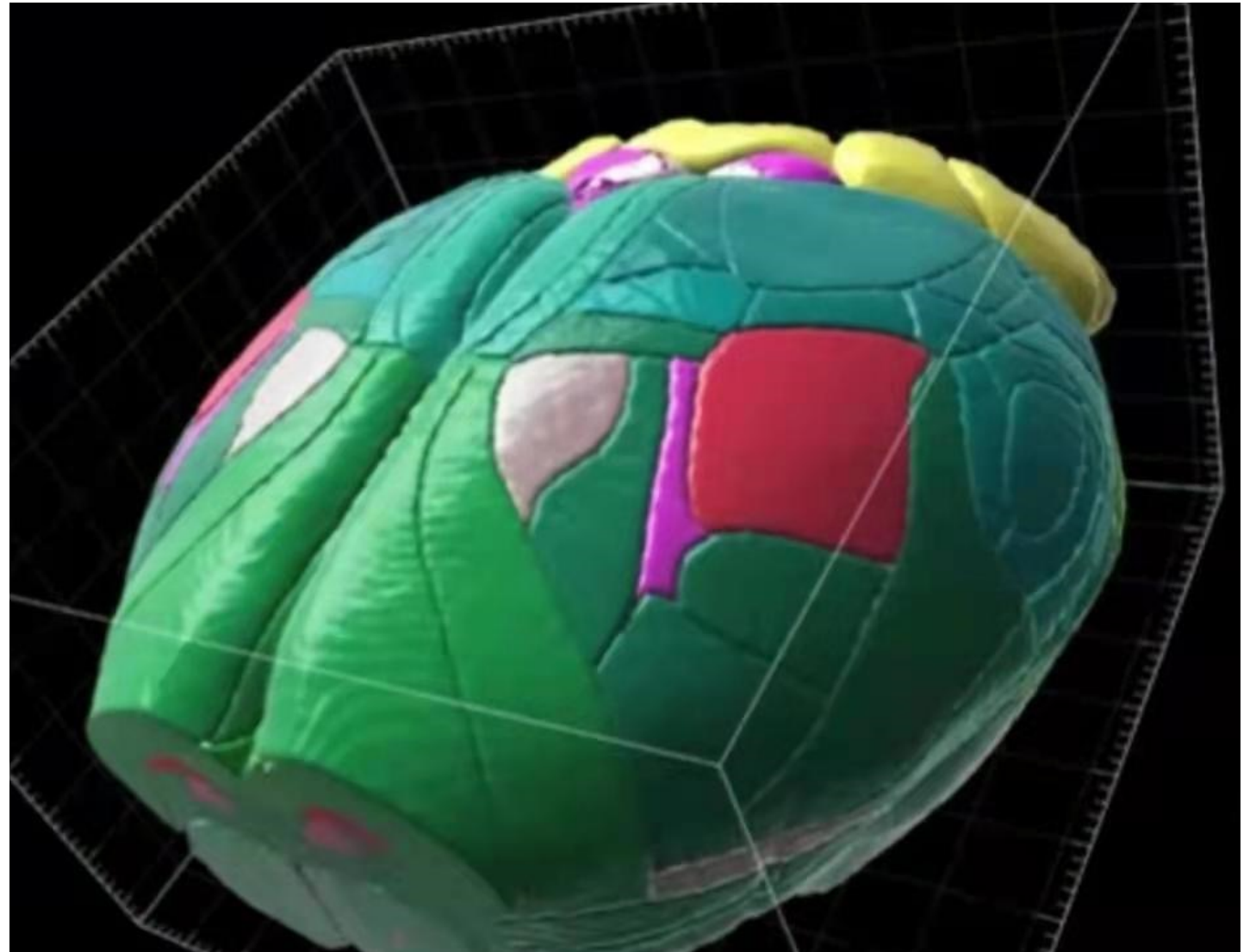
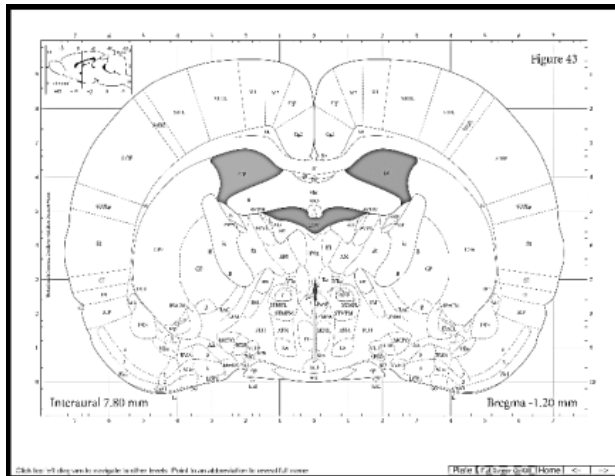
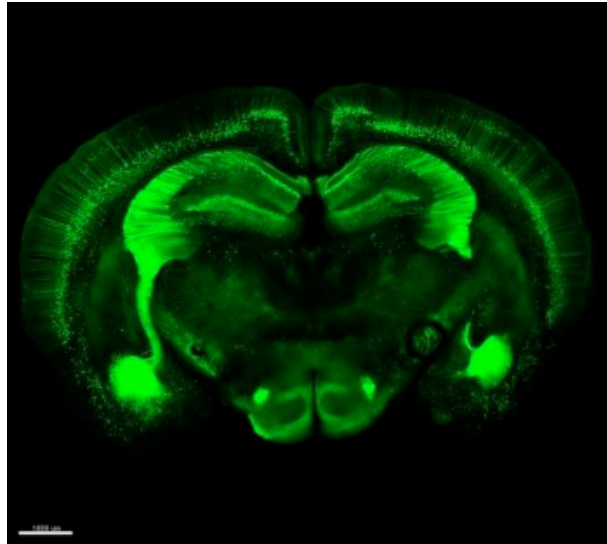
500  $\mu$ m

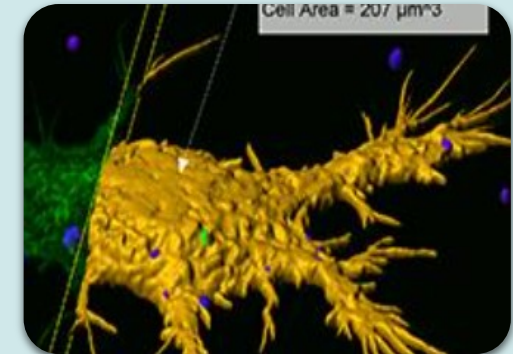
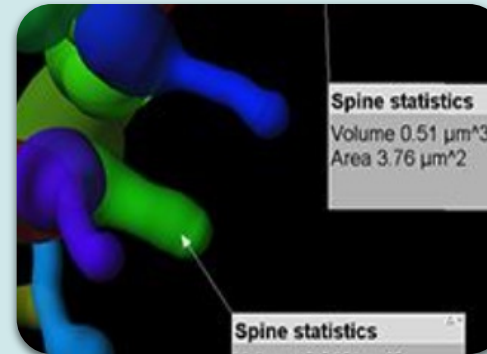
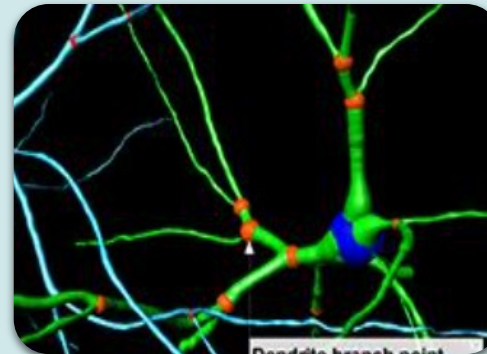
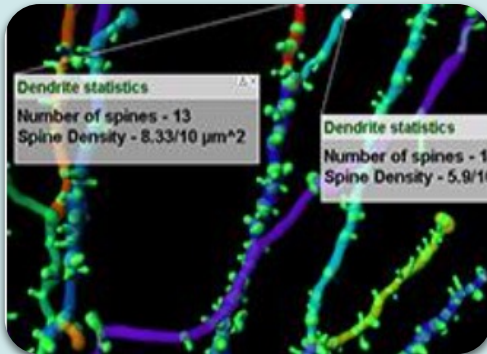
Grüneboom, et al.. Nat Metab (2019)











## Dendrites

- Length
- Mean Diameter
- Branching Angle
- Spine Density
- Resistance

## Filaments

- Dendrite Branch Points
- Dendrite Terminal Points
- Sholl Intersections
- Spine Terminal Points
- Dendrite Branch Level

## Spines

- Length
- Volume
- Mean Diameter
- Area
- Terminal Point Diameter

## Surfaces

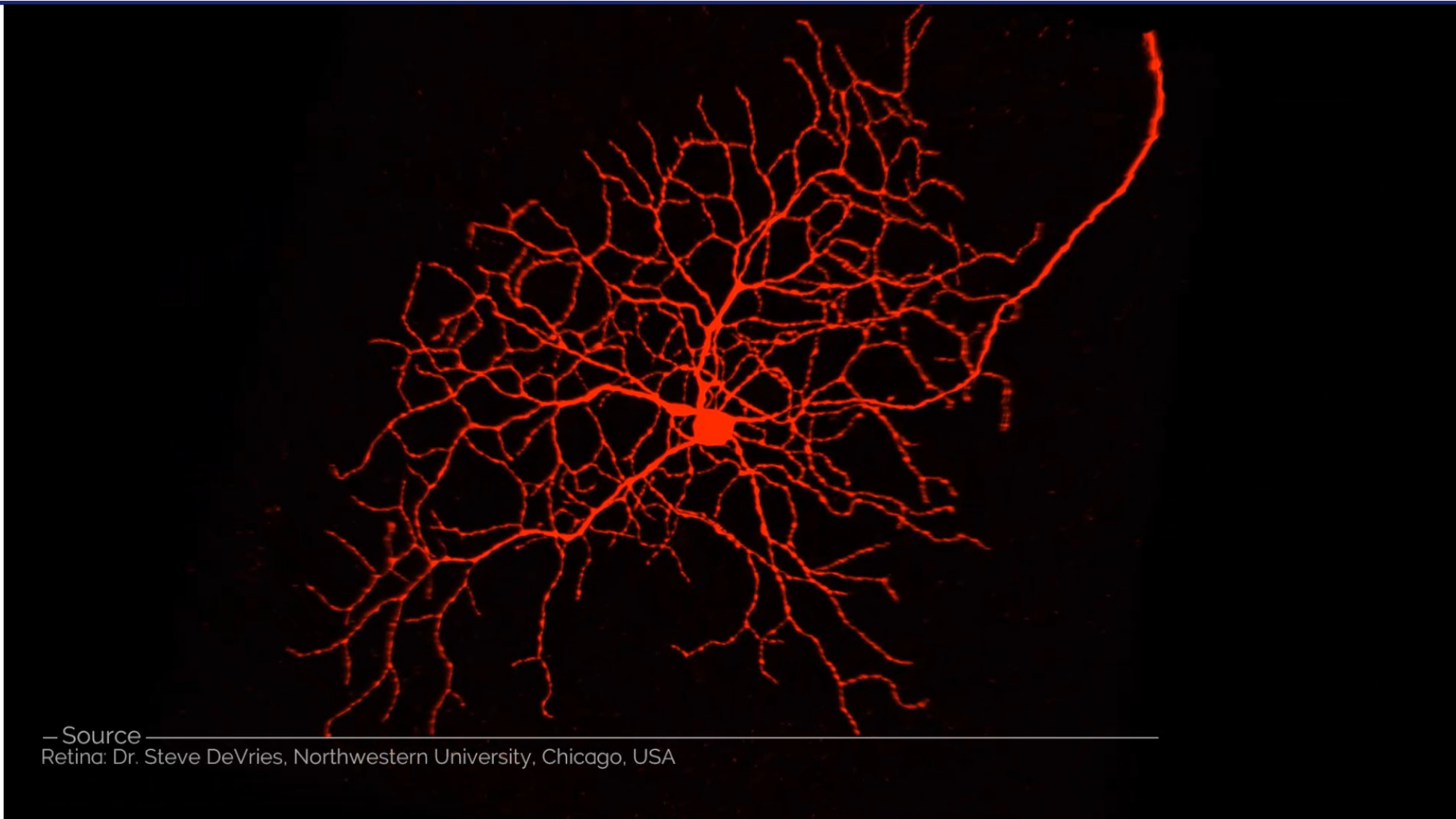
- Area
- Volume
- Intensity
- Position (x, y, z)
- Number (counting objects)



## Spines Stats:

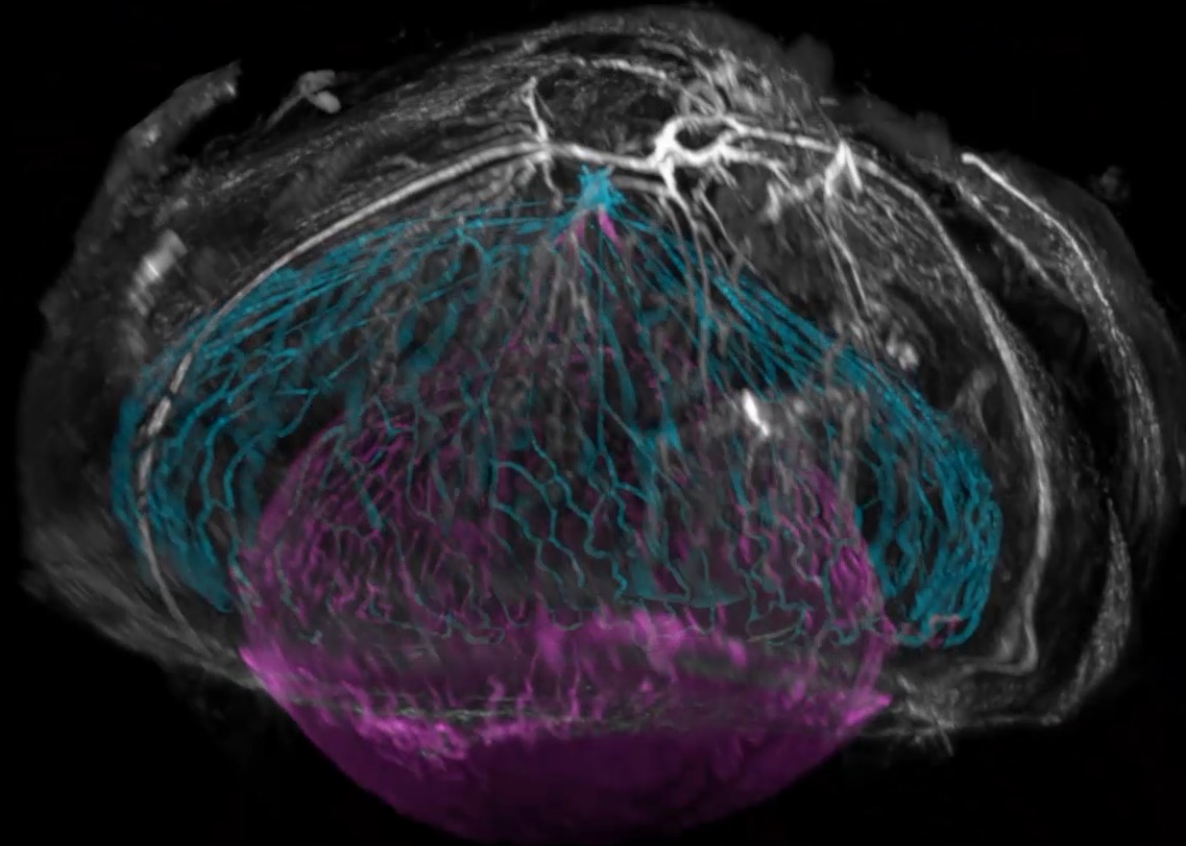
- Counts
- Volume, Area, Diameters,
- Positions
- Morphology: Neck, Head, branching...





— Source —  
Retina: Dr. Steve DeVries, Northwestern University, Chicago, USA

# Filament



— Source —

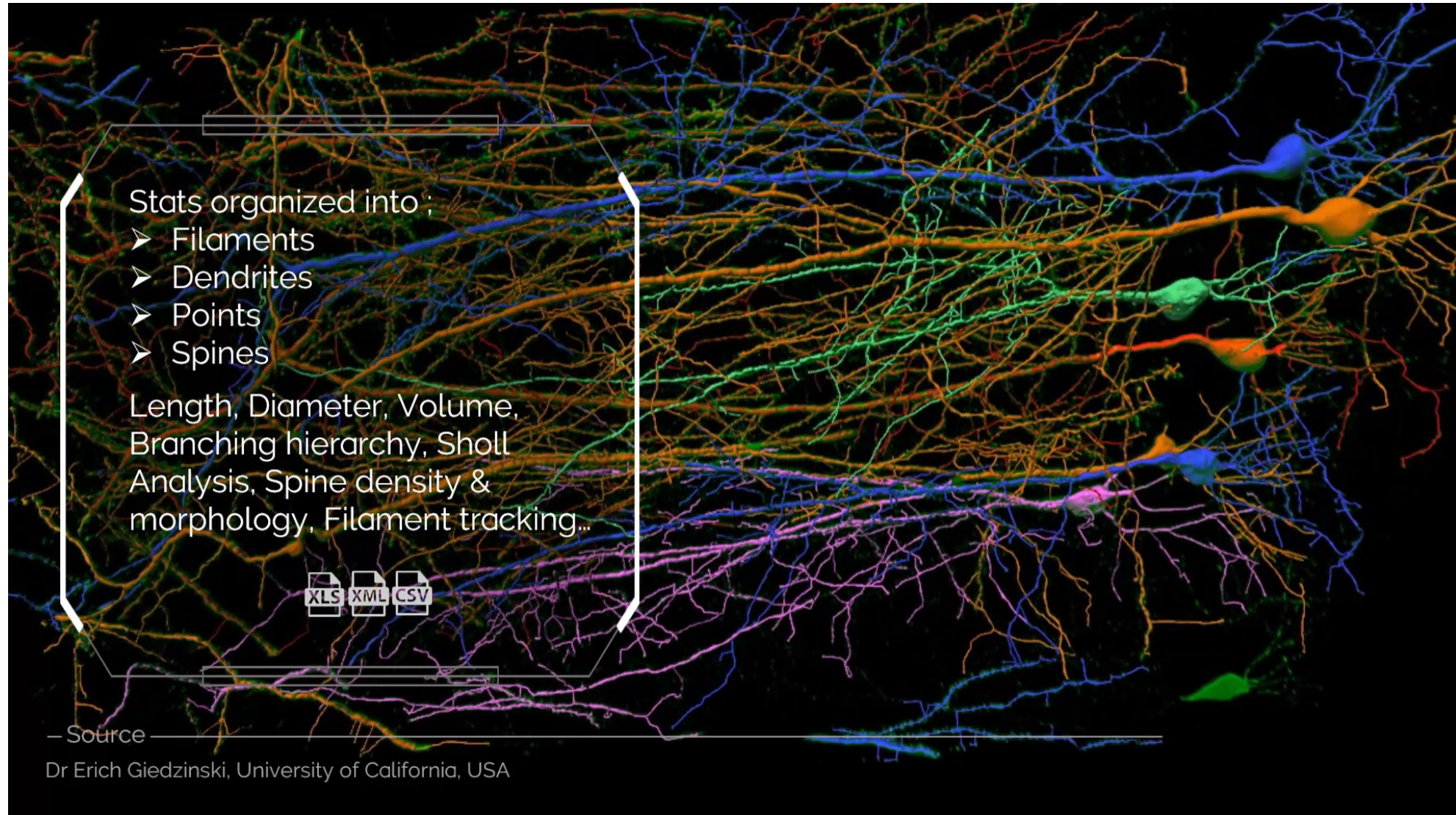
Mouse eye - Retinal Vessels: Marie Darche, Morgane Belle, Michel Pâques Ilaria Cascone Alain Chédotal  
Institut de la Vision & XV-XX Hospital, Paris, France

# Filament



— Source —

Shany Peled-Hajaj and Pablo Blinder, Tel Aviv University, Israel



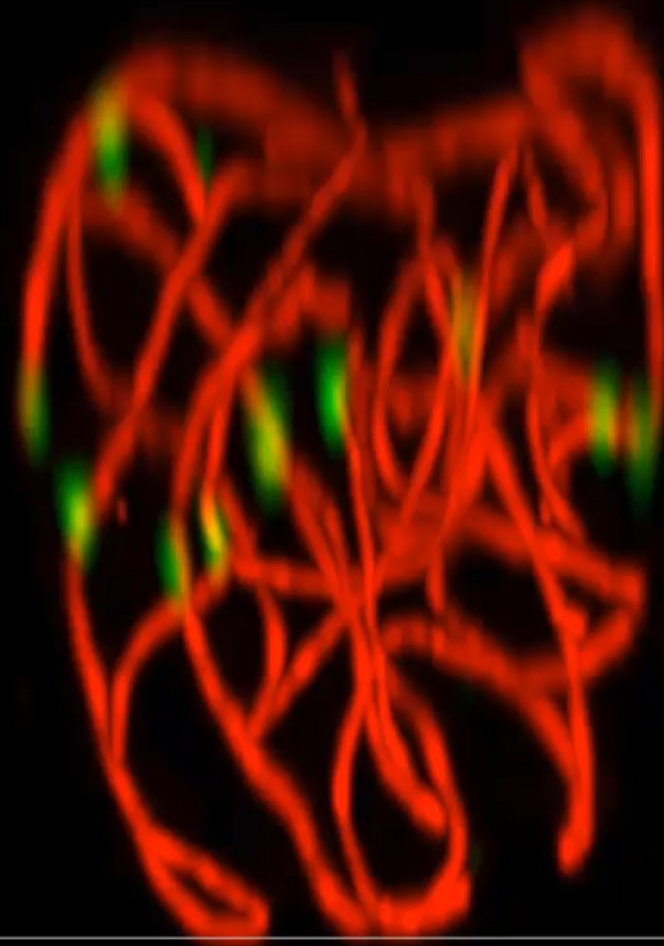
Stats organized into :

- Filaments
- Dendrites
- Points
- Spines

Length, Diameter, Volume,  
Branching hierarchy, Sholl  
Analysis, Spine density &  
morphology, Filament tracking...

XLS XML CSV

— Source —  
Dr Erich Giedzinski, University of California, USA

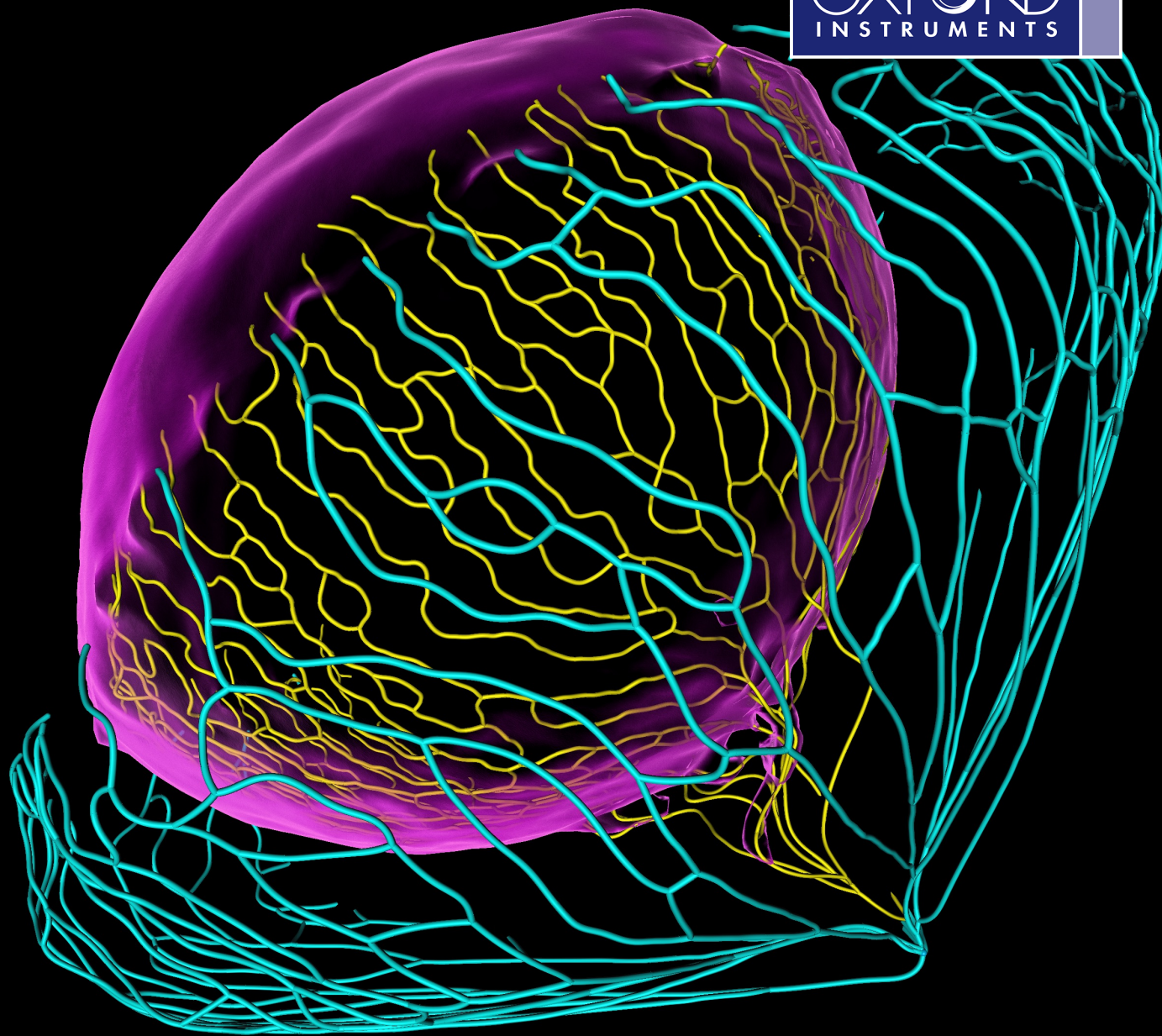


— Source —

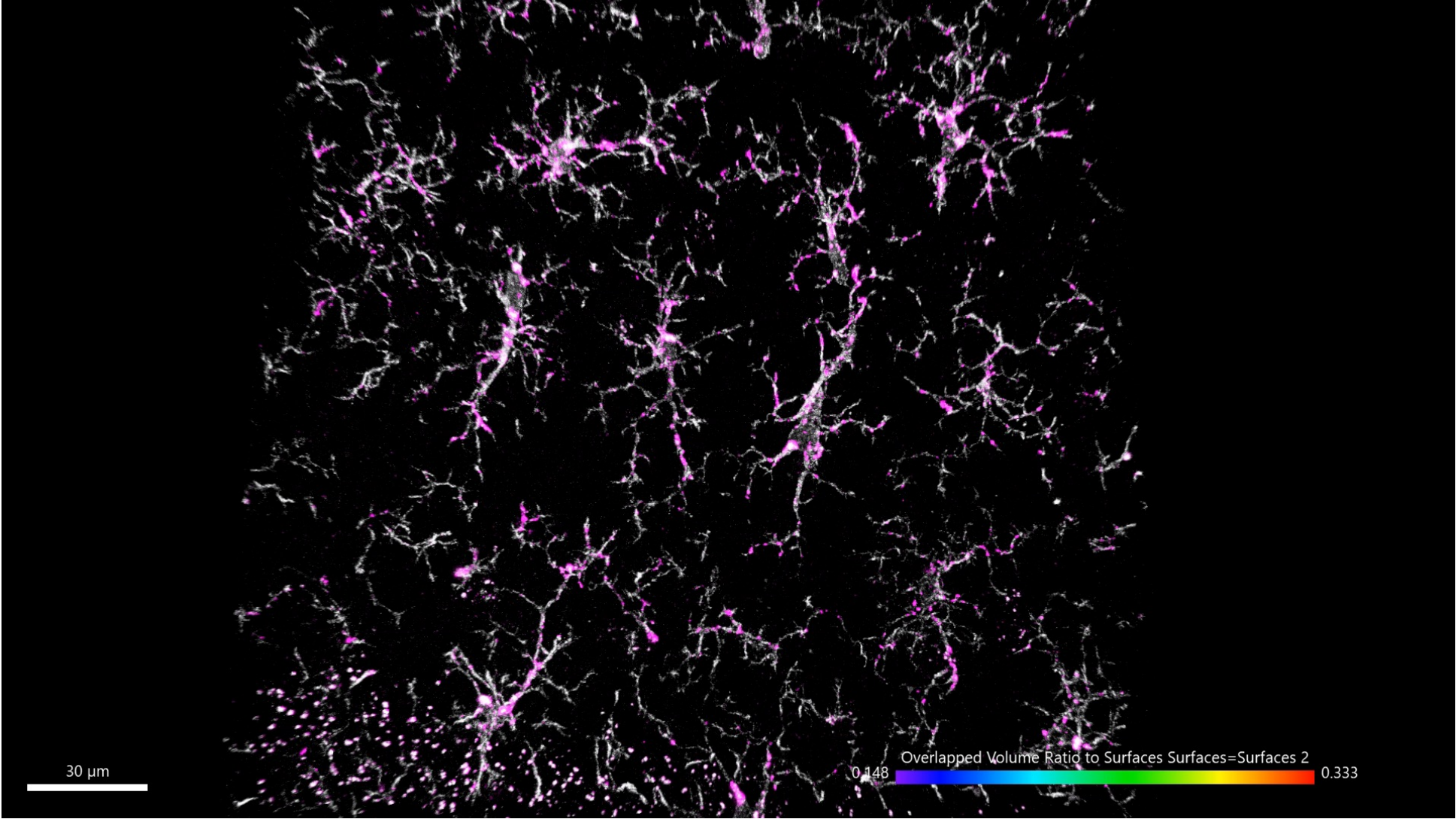
A. Thaliana's Chromosomes: Dr. Mathilde Grelon, INRA Centre de Versailles-Grignon, IJPB, France.

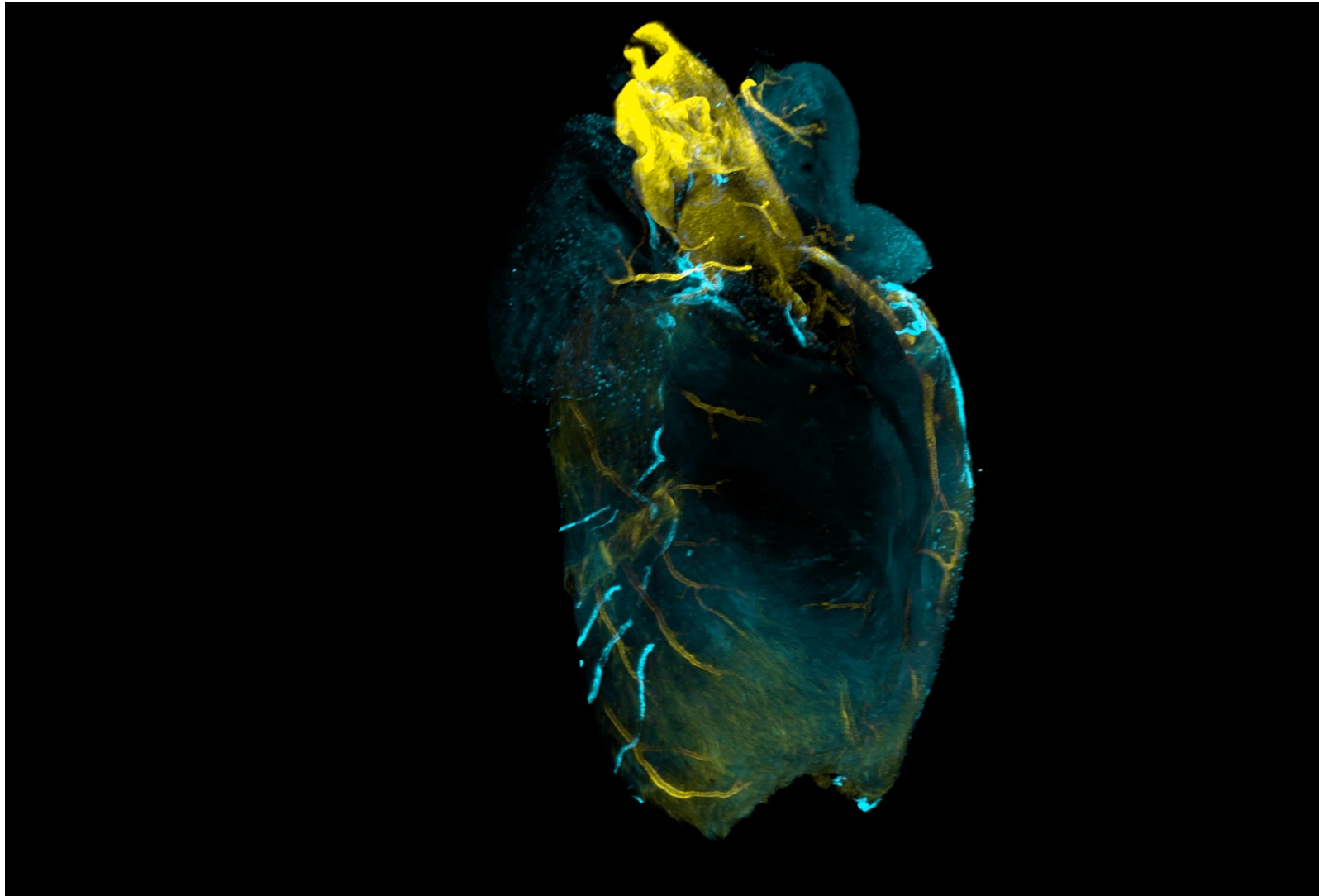
# Imaris 10

AI Powered  
Filament Tracing



# Imaris 10.0 – AI Powered Filament Tracer





- Higher Throughput
  - Blockwise Calculation
  - Improved Rendering
  - AI Powered Creation
  - Usability tools
- Flexibility in sample
  - Multi-scale spots
  - New network model
- Easier to Learn
  - Less training
  - Less Support

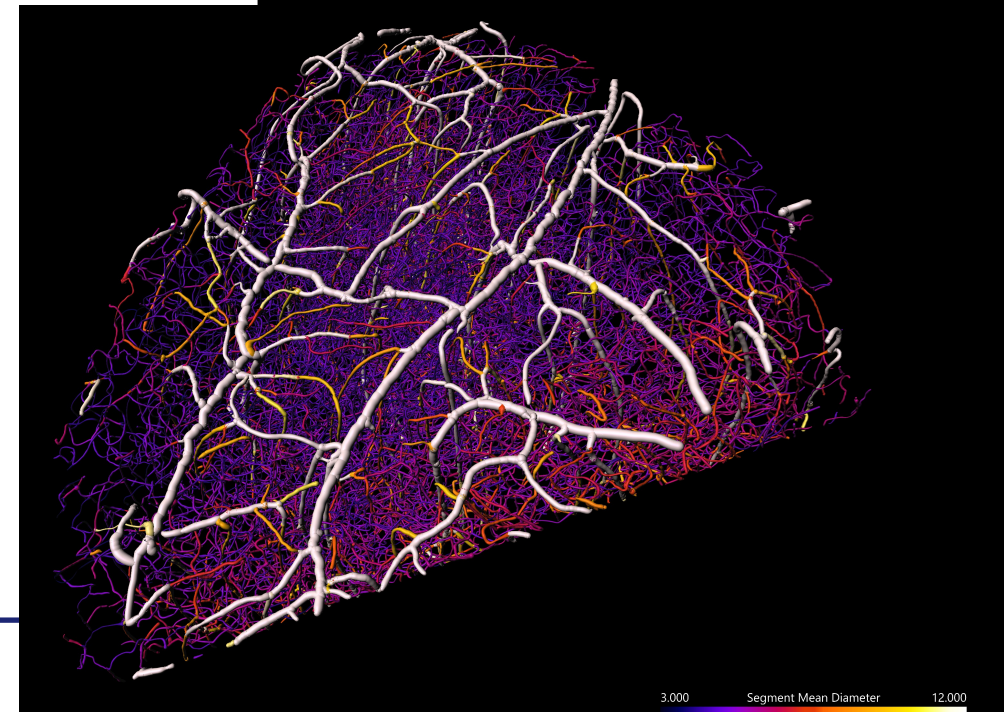
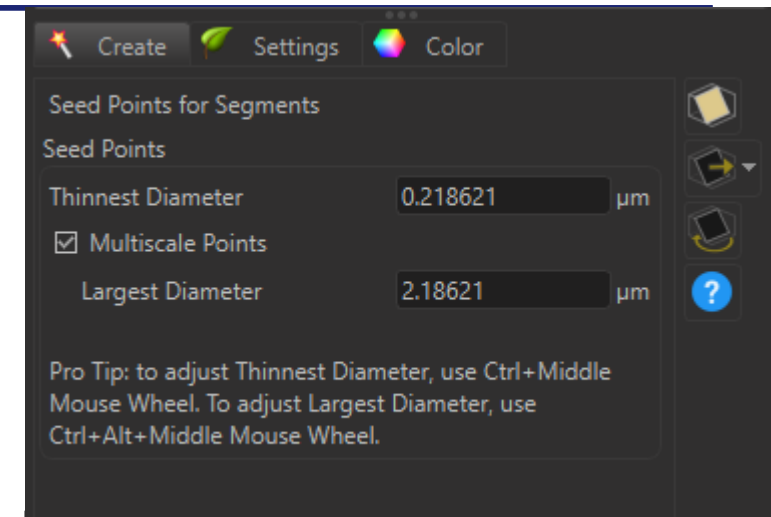
# New Features of Imaris 10.0

## Filament Feature

1. Blockwise calculation of images
2. Faster Filament object rendering
3. Machine Learning point classification
4. Multiscale Seedpoints

## Benefit

1. Trace images greater than 2GB and faster
2. Smooth interaction (rotation, selection, etc.)
3. Improves quality of results for poor quality images
4. Improves quality of results and throughput



# New Features of Imaris 10.0

## Filament Feature

1. Blockwise calculation of images
2. Faster Filament object rendering
3. Machine Learning point classification
4. Multiscale Seedpoints
5. Visual Aides for detection type
6. Dynamic 3D measurement of somas and seed points linked to wizard input boxes
7. Pro Tips for keyboard shortcuts
8. ? Button for Reference Manual
9. Machine Learning point classification
10. Swiping selection tool
11. \*\*HDF5 "position" reader

## Benefit

1. Trace images greater than 2GB and faster
2. Smooth interaction (rotation, selection, etc.)
3. Improves quality of results for poor quality images
4. Improves quality of results and throughput
5. Users pick the correct path every time
6. Stay in wizard for all steps
7. Potentially overlooked EoU features are prominent
8. Easy Reference Manual Link
9. Training data can be reused
10. Faster and easier editing
11. Load Picasso localizations as Spots

The screenshot shows the 'Seed Points Classification' wizard in Imaris. At the top, there are buttons for 'Create', 'Settings', and 'Color'. Below this, the text reads: 'Imaris will use the Seed Points to generate Segments and then Filaments.' It then instructs the user to 'Teach Imaris which seed points to keep and which to discard by adding them to the appropriate class. Click "Train and Predict" to see the results of the classification from your training set. Iterate these steps to achieve a good result.'

Below the text is a table with columns for 'Training', 'Predicted', and 'Model'. The table has two rows of data:

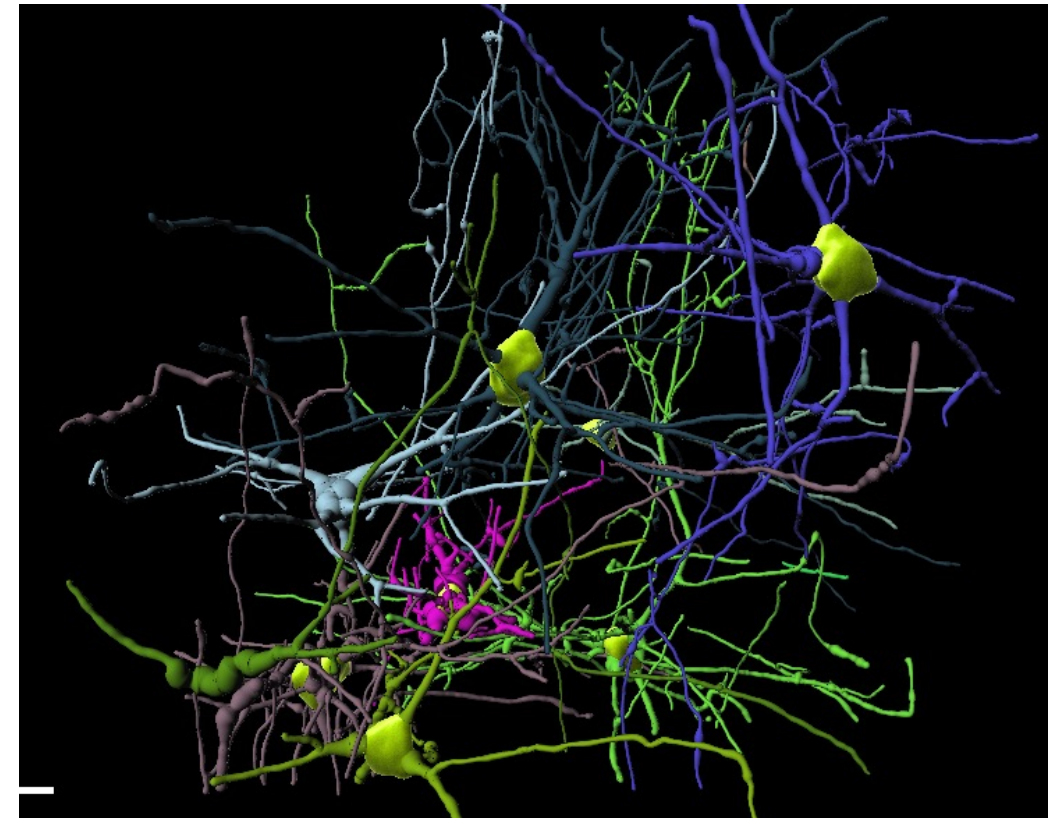
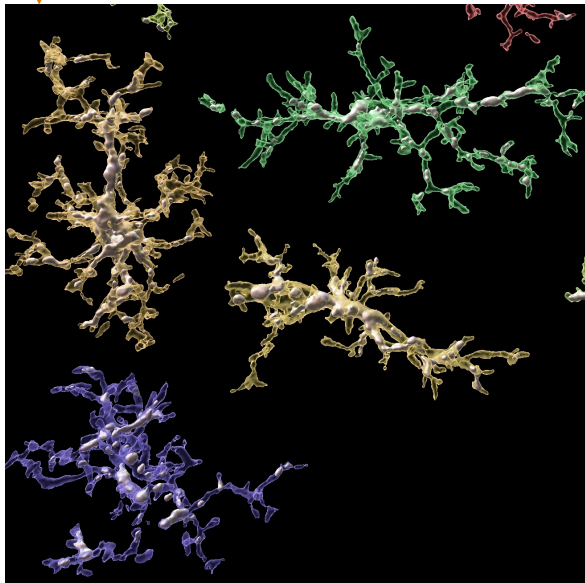
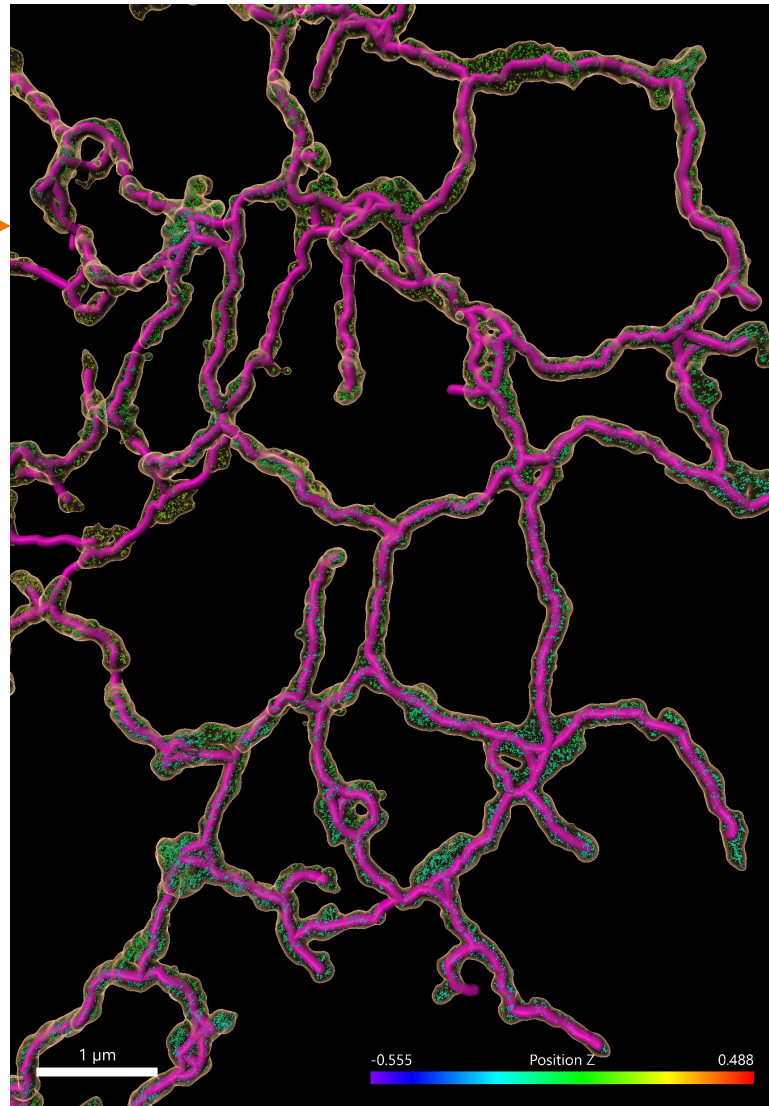
Training	Predicted	Model	
82	1790	Keep	<input checked="" type="checkbox"/>
42	258	Discard	<input checked="" type="checkbox"/>

Below the table are buttons for 'Train and Predict' and 'Clear All'. At the bottom, there are two 'Pro Tip' messages: 'Pro Tip: When in Circle Select Mode hold Ctrl+Left Mouse Button while dragging to select many points in one swipe' and 'Pro Tip : After selecting points click A to add them to the Keep class or D to add them to the Discard class'.

# Imaris 10.0 – Applications

Sub-cellular endoplasmic reticulum network imaged with DF600 super-resolution microscopy and traced with Imaris 10.0

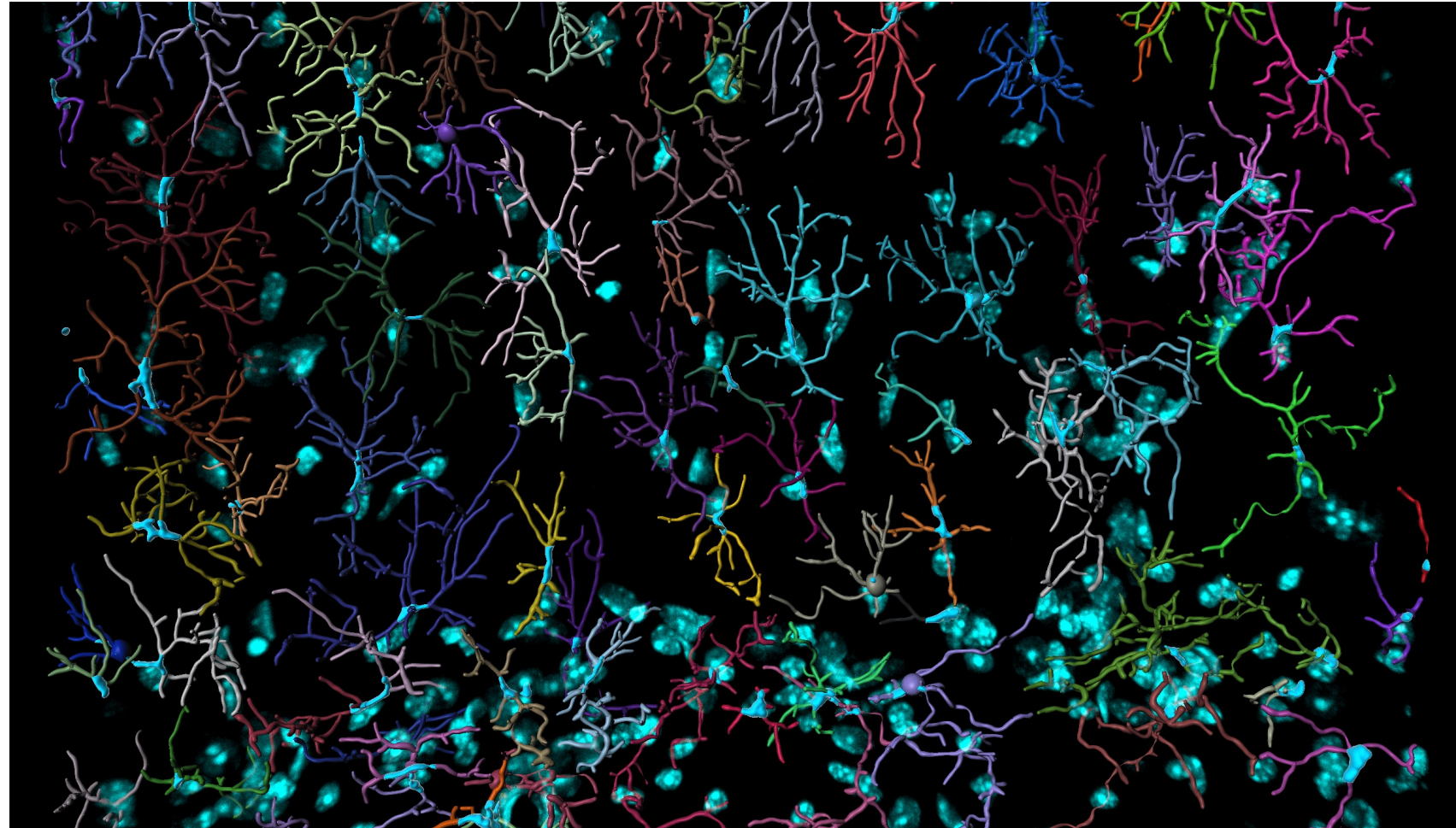
Microglia traced in Imaris 10.0 with additional analysis via Surfaces to determine activation state



Neurons in a cleared mouse brain. Pre-10.0 analysis required ½ day of work by an experienced Imaris user. The above result was completed in 13 minutes.

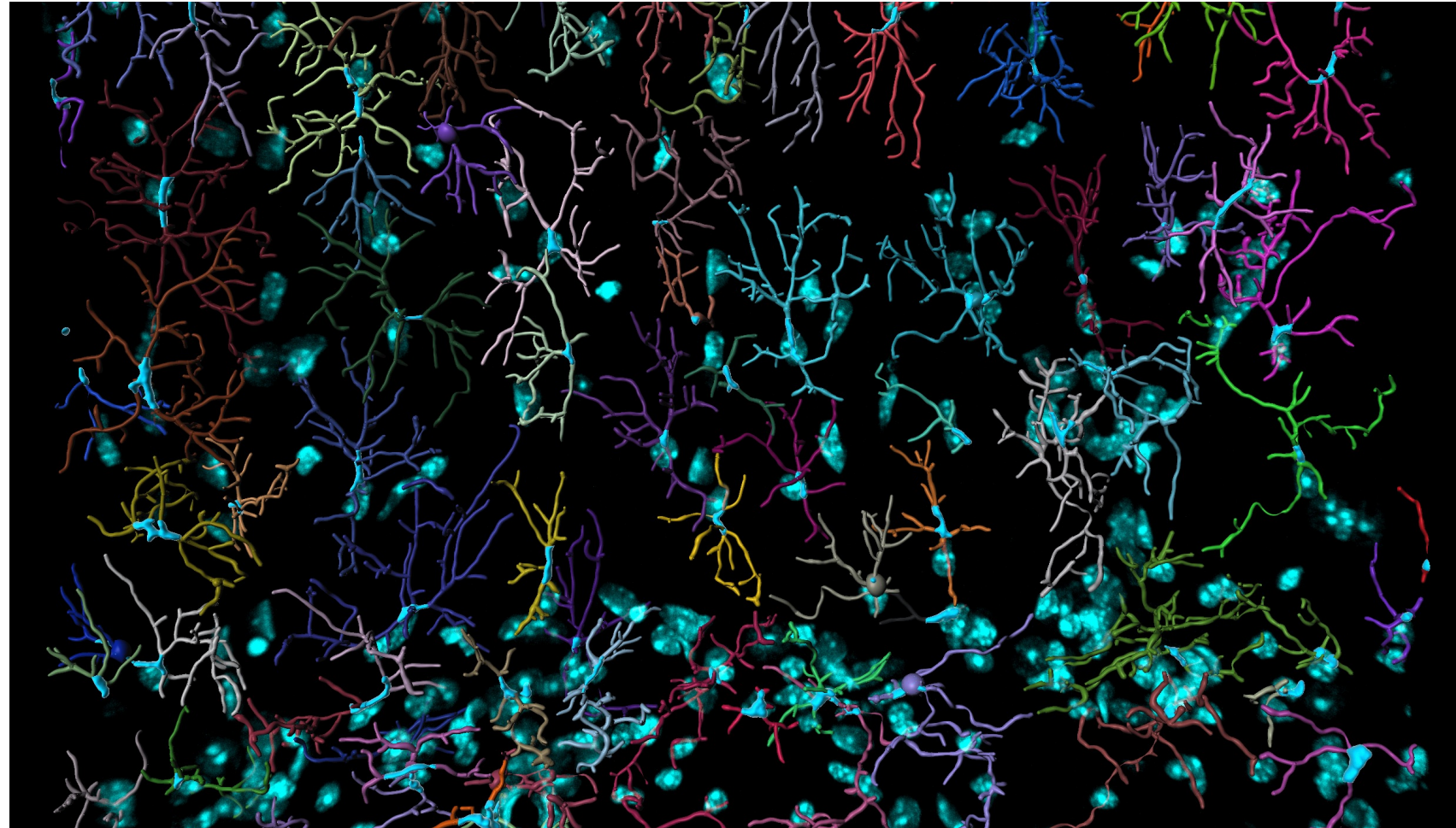
## + Neuroscience

- **Intensity**
- **Distance to Spots**
  - Colocalization
- **ML-based creation**
  - Batchability
- **EoU Improvements**



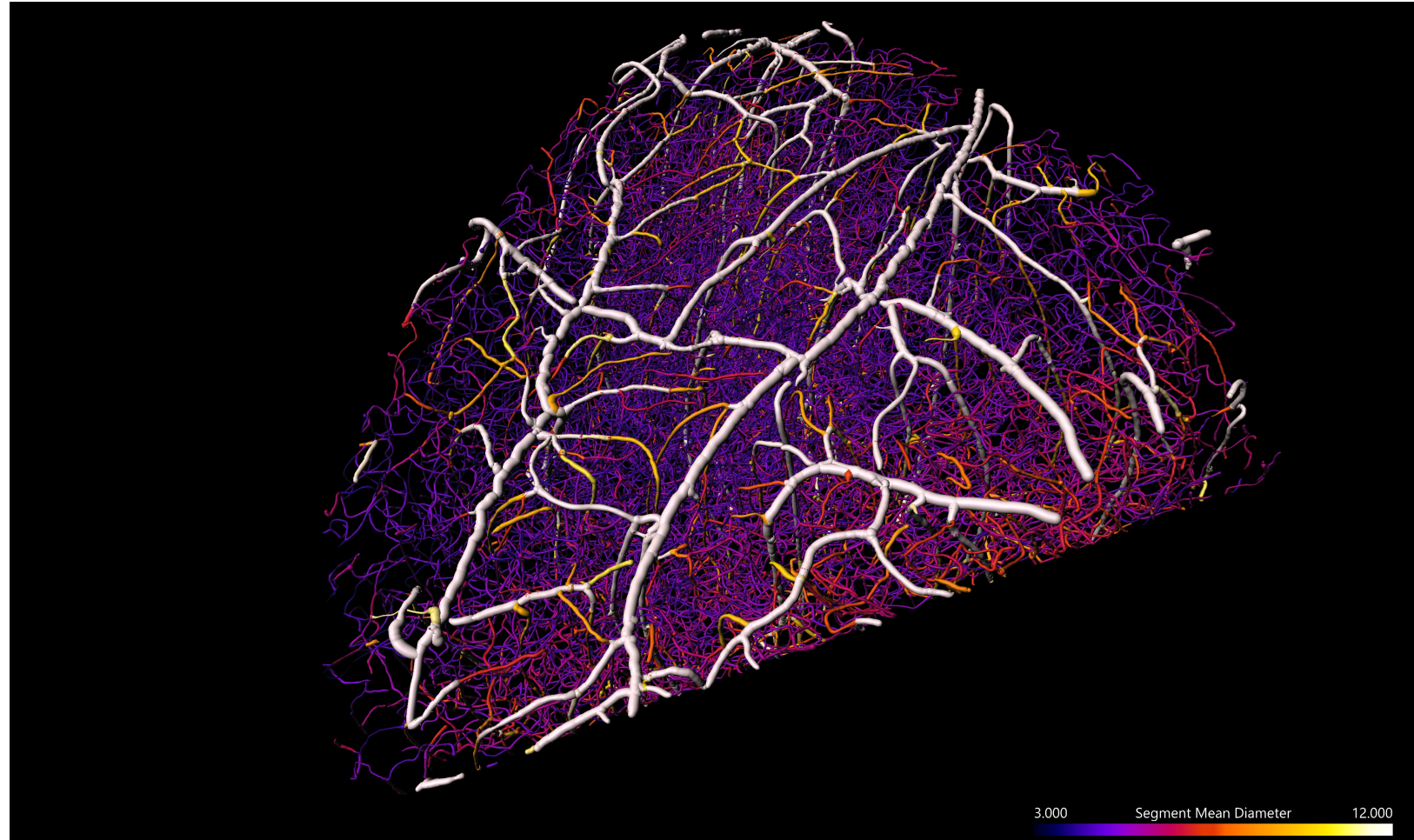
## + Neuroscience

- **Tree Structure for Neurons**
  - Branching
  - Diameter
- **Spine characterization**
- **Microglia**
  - Alzheimer's Disease
- **Astrocytes**
- **Axons**



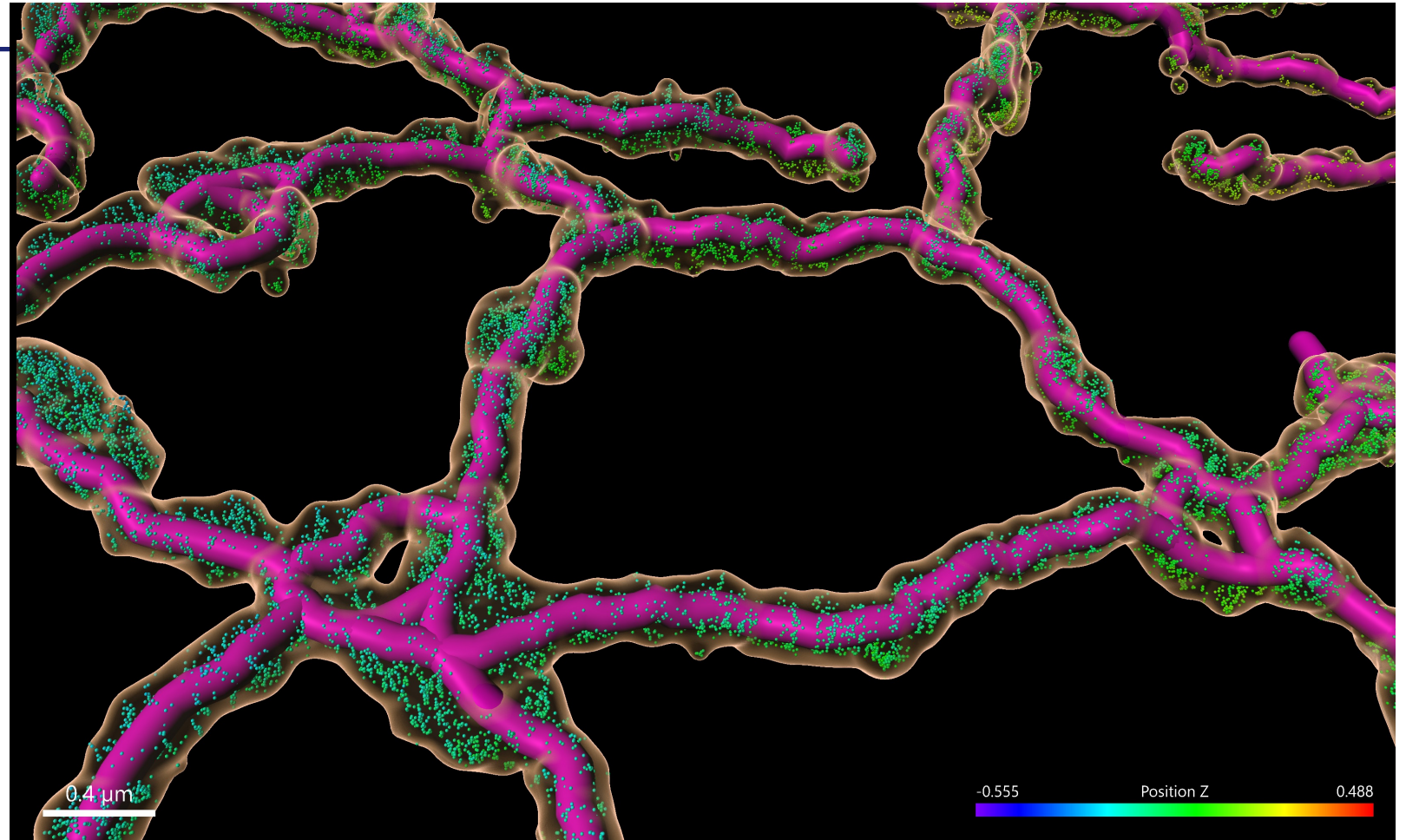
## + Vasculature

- **Network**
  - Multi-scale diameter
- **Vast speed increase**
- **Distance to Spots**
  - Colocalization
- **ML-based creation**
  - Batchable
- **EoU Improvements**



## + Sub-cellular Organelles

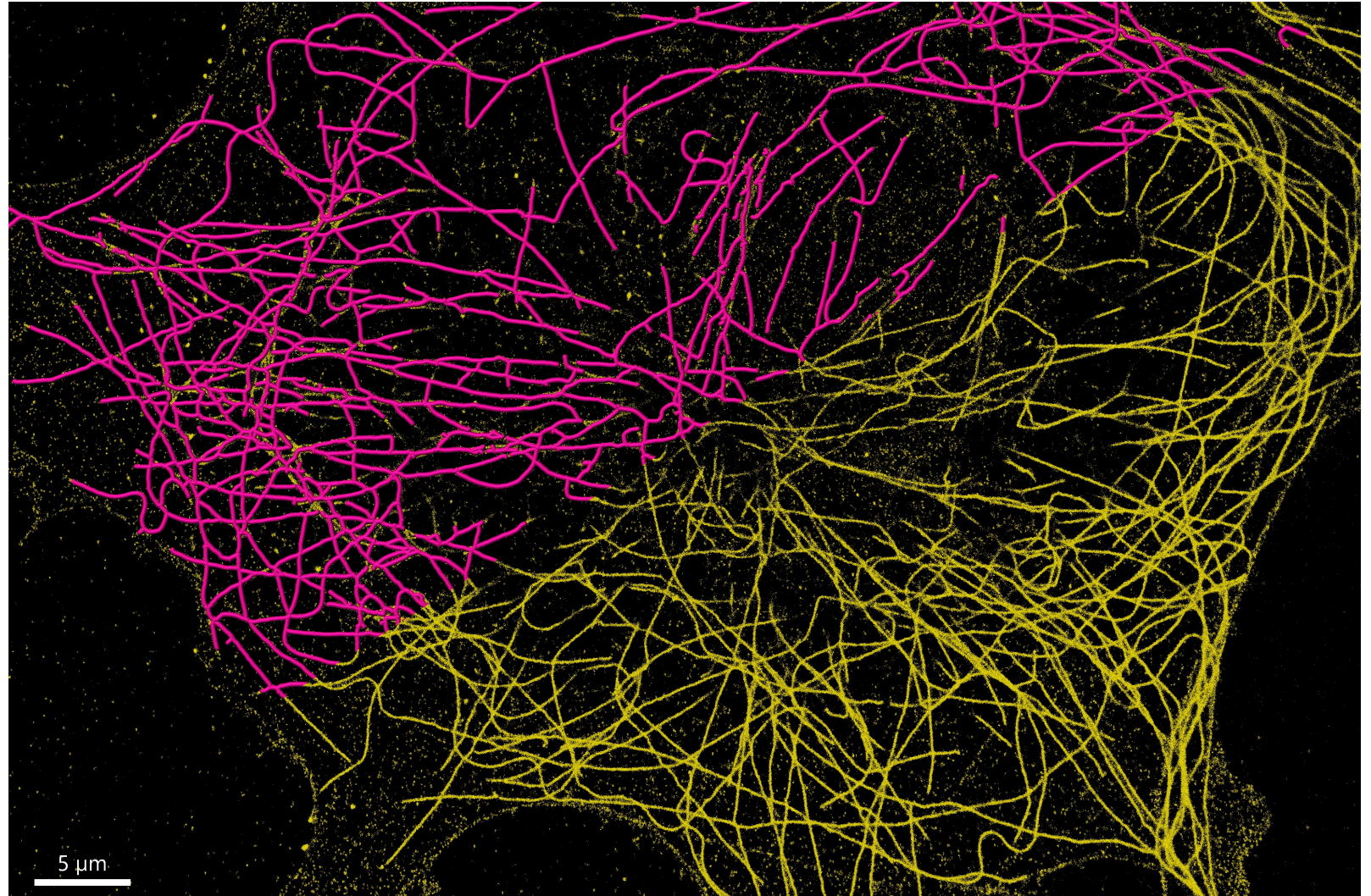
- In harmony with DF600
- Vast speed increase
- Distance to Spots
  - Colocalization
- ML-based creation
  - Batchable
- EoU Improvements



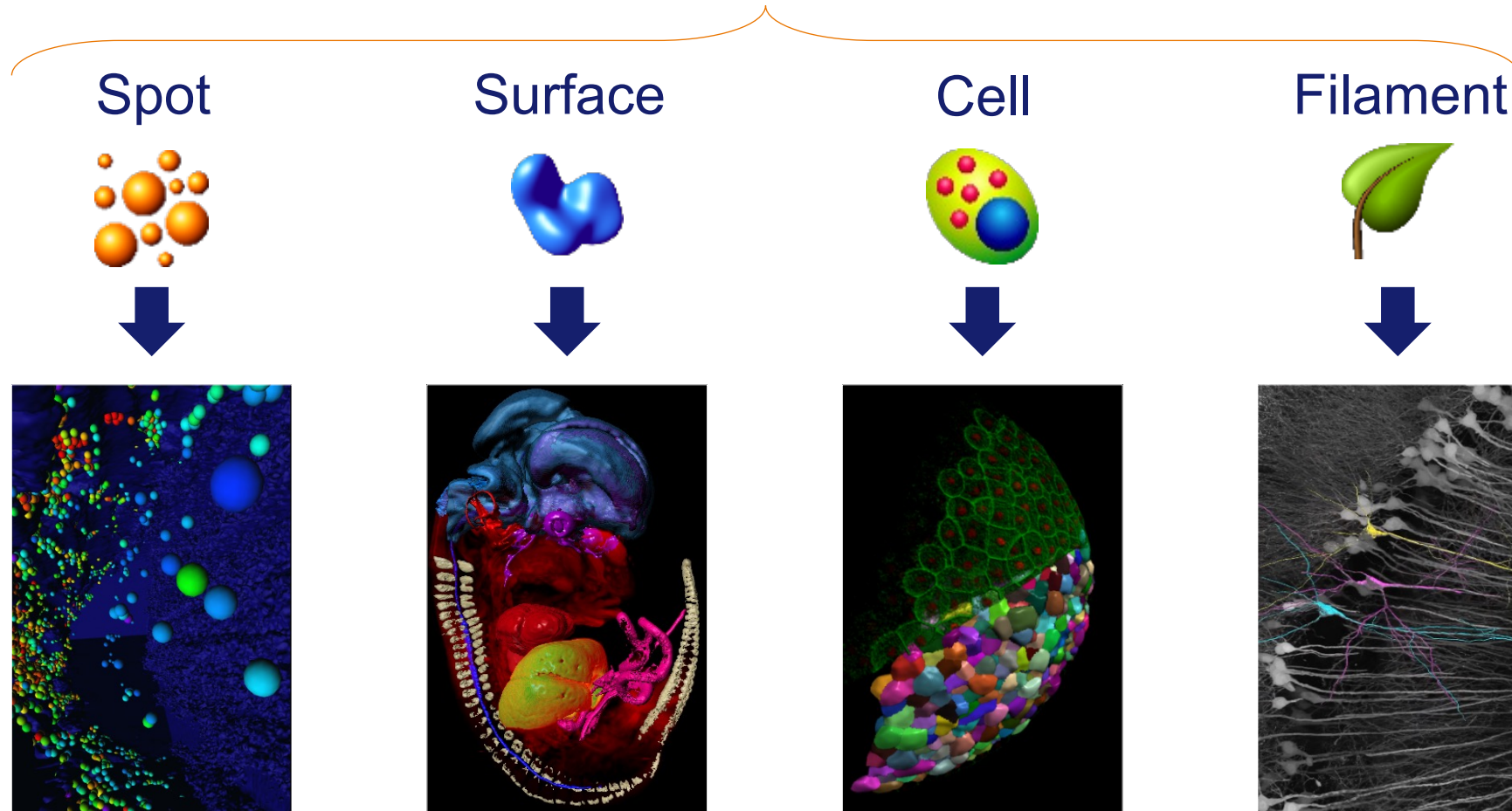


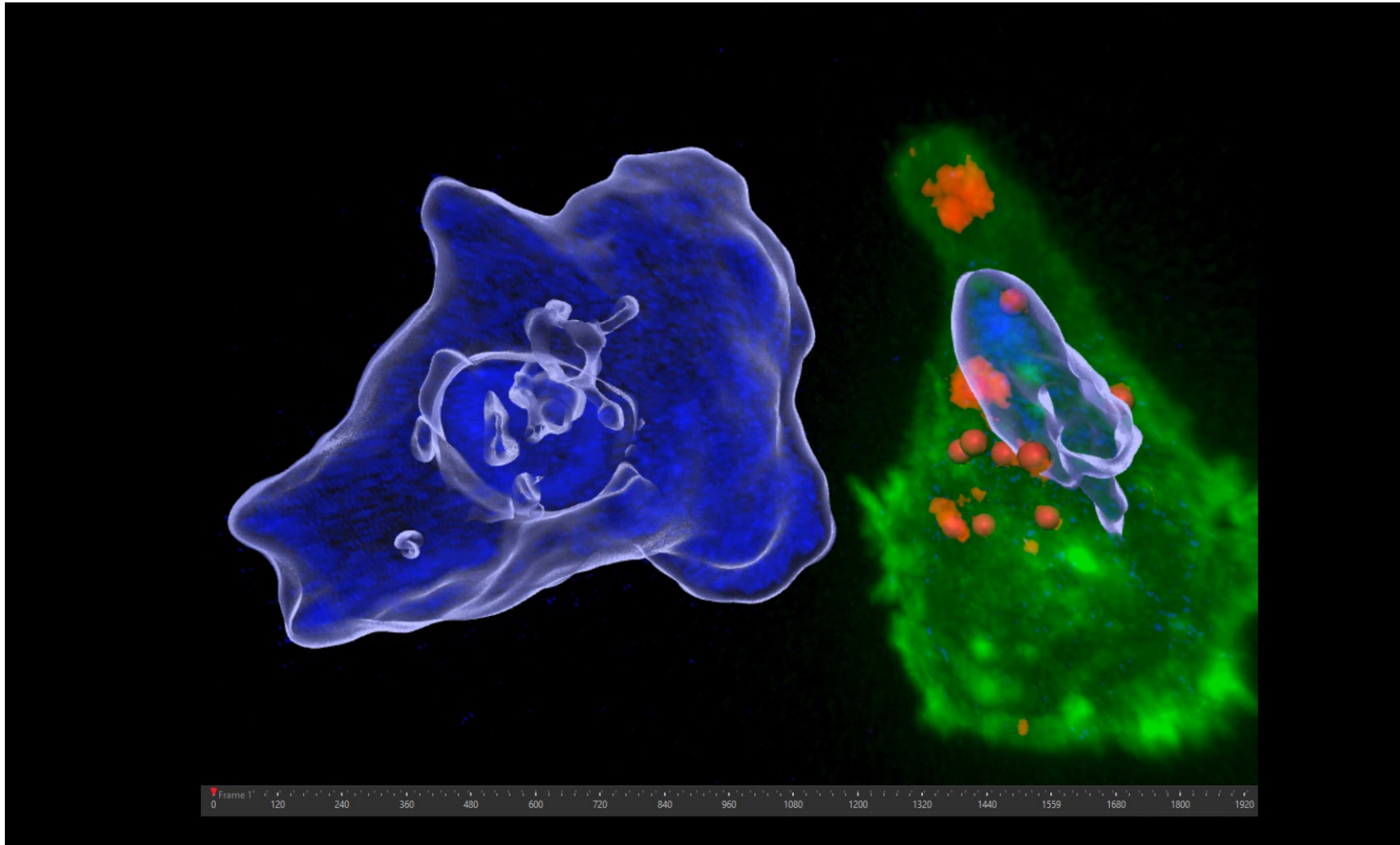
## Resolution, resolution, resolution!

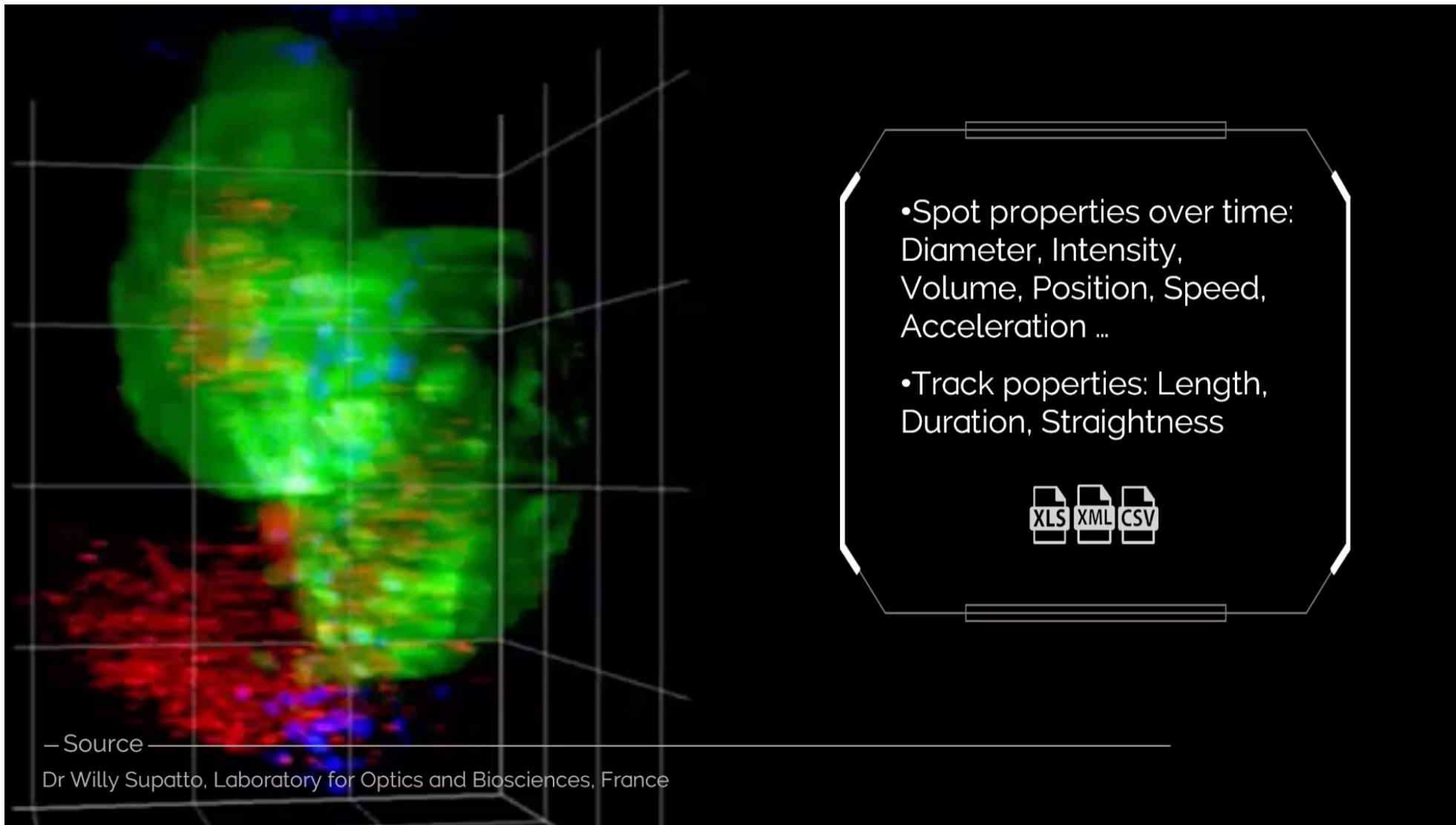
- **Requires acquisition with a super-res technique**
  - DF600 with SMLM
  - SIM



## Track





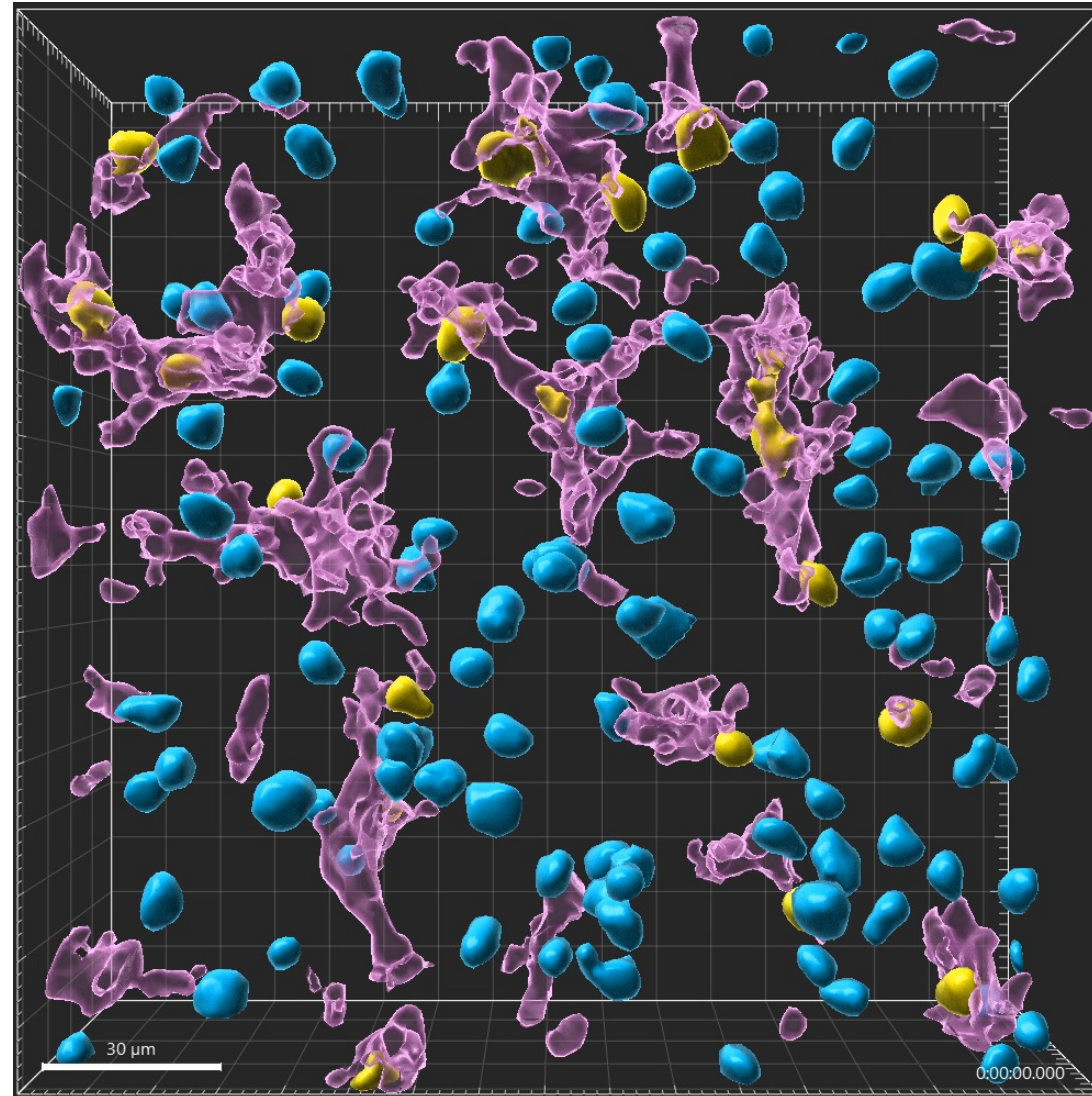


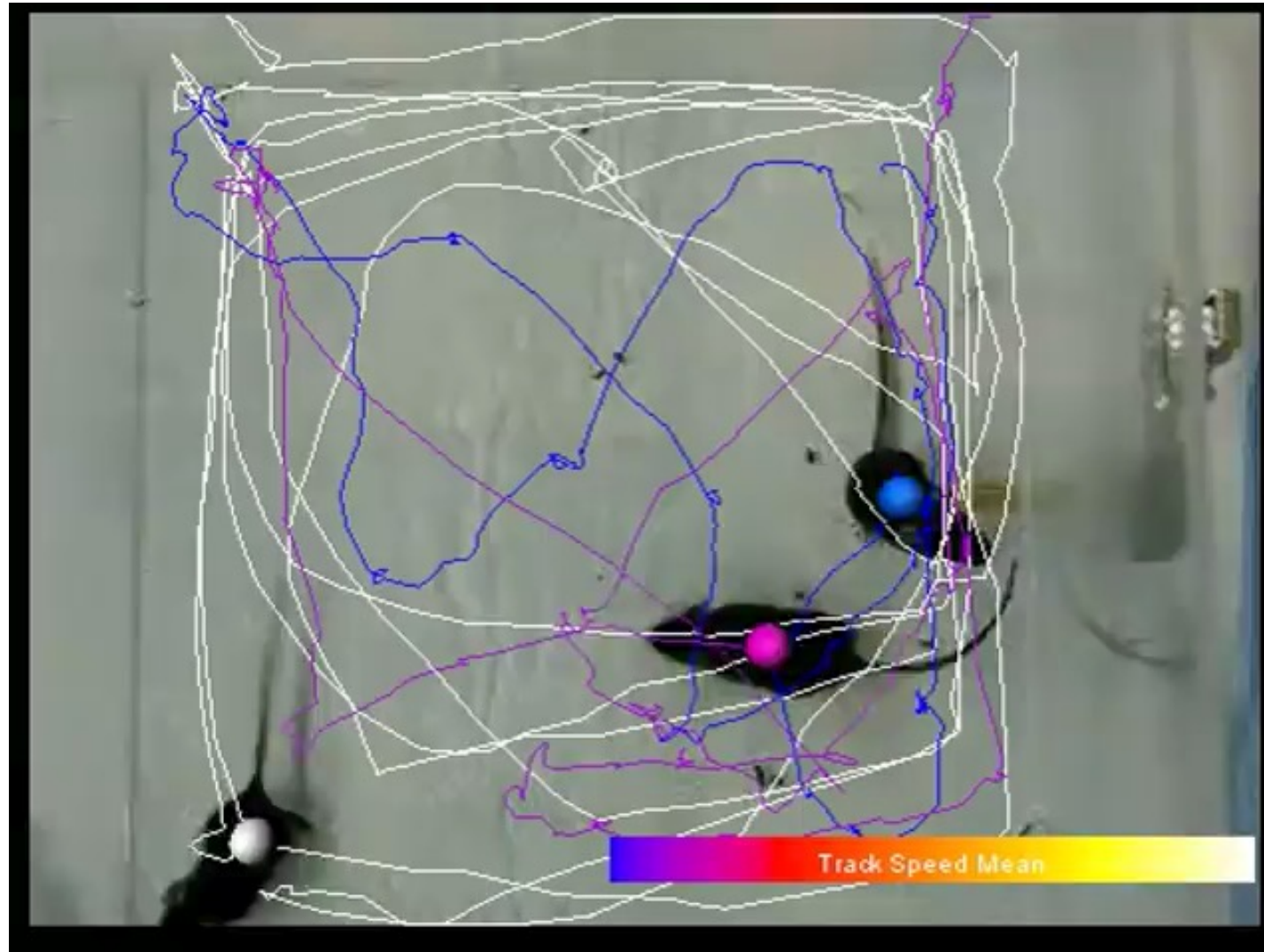
•Spot properties over time:  
Diameter, Intensity,  
Volume, Position, Speed,  
Acceleration ...

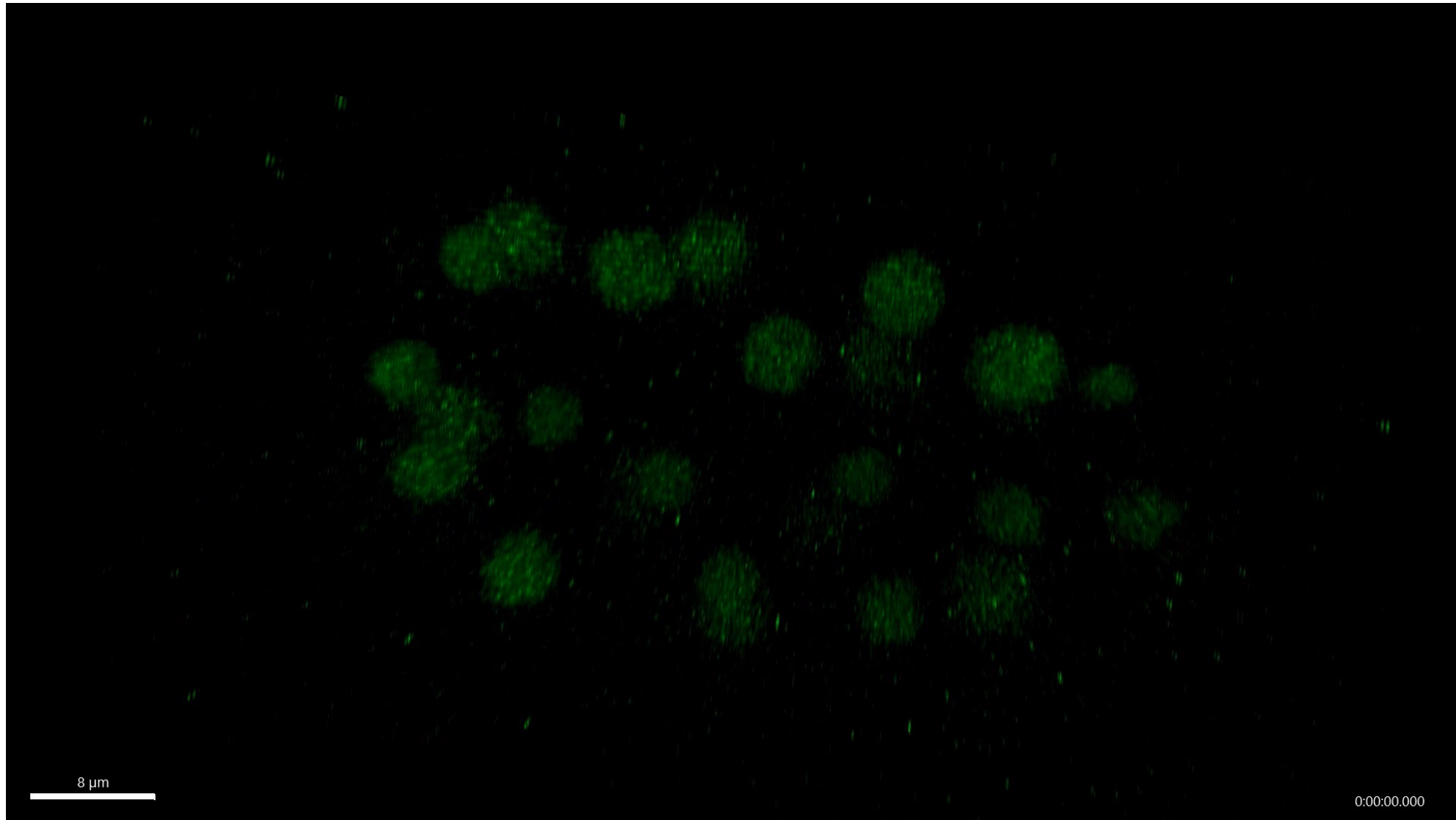
•Track properties: Length,  
Duration, Straightness

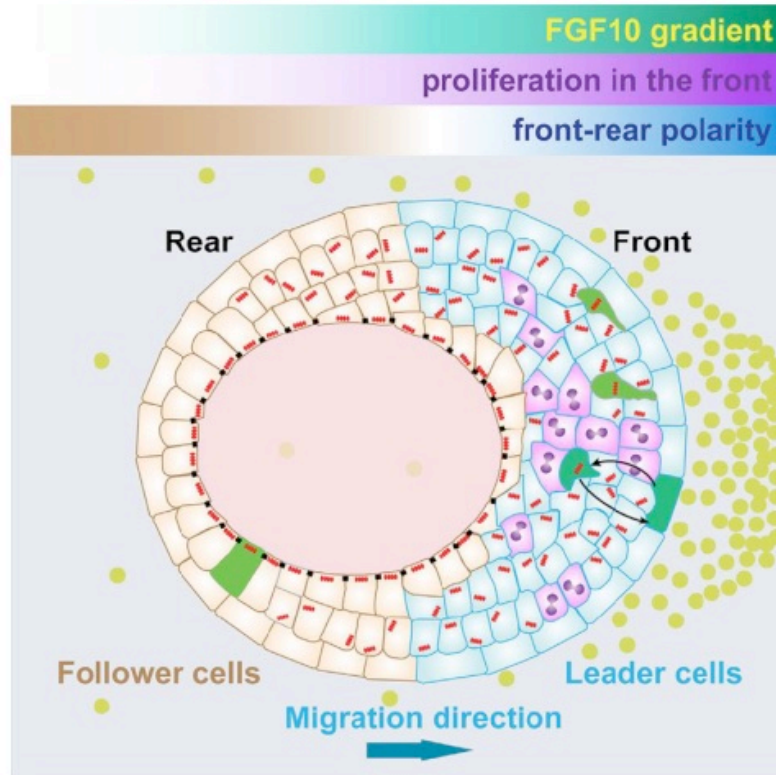
XLS XML CSV

— Source —  
Dr Willy Supatto, Laboratory for Optics and Biosciences, France

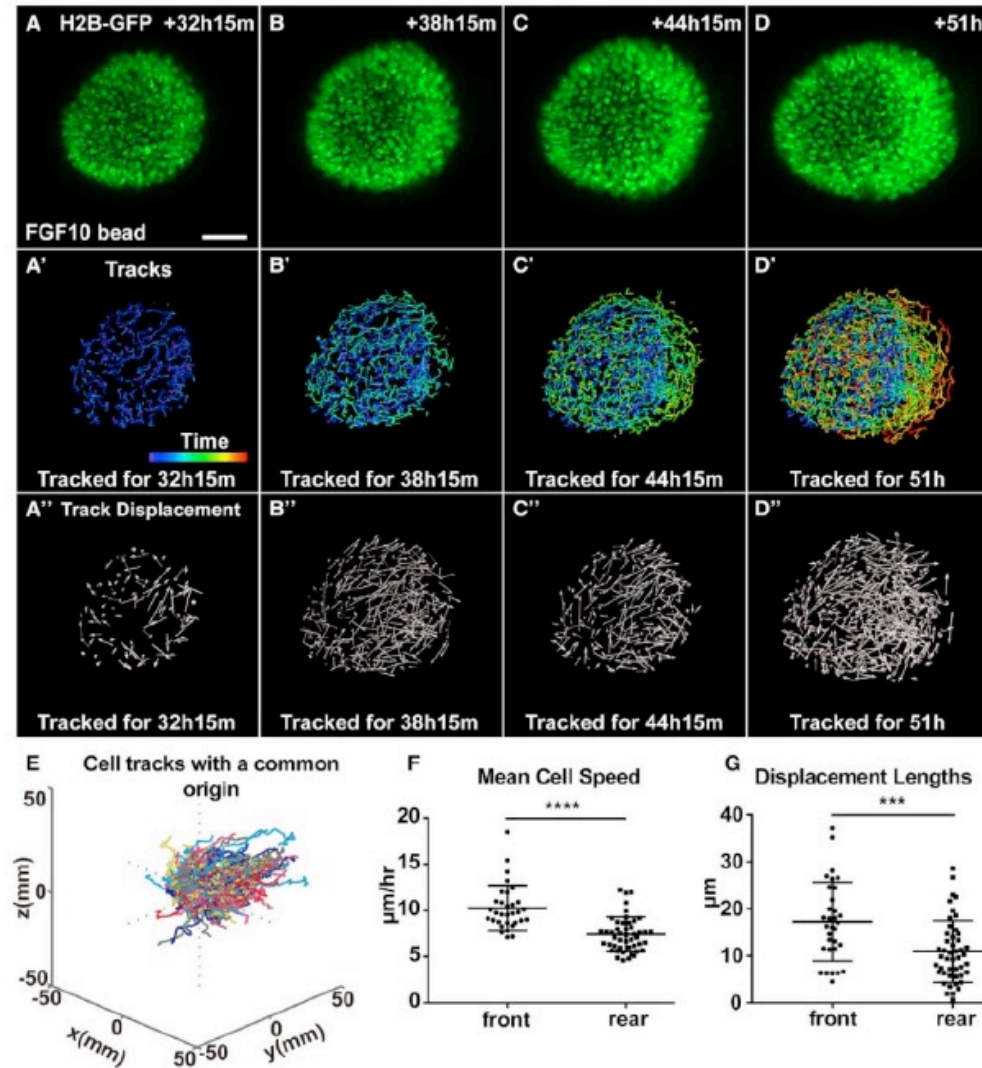












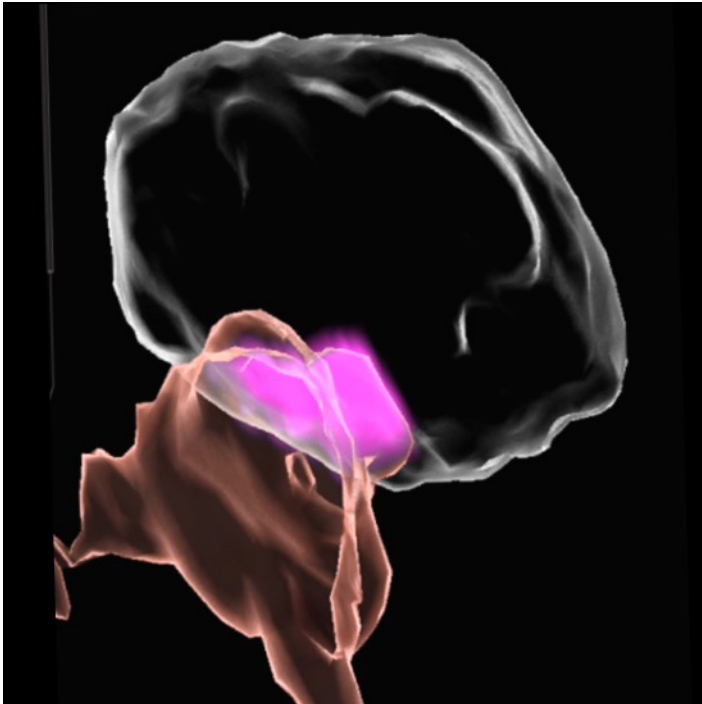
Lu et al. Cell Reports. 2020



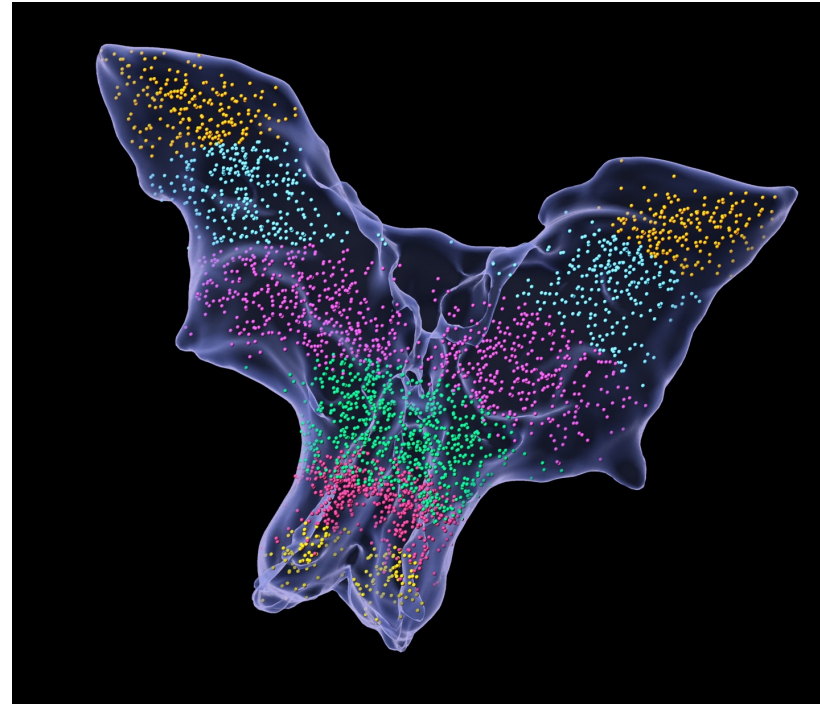
# Detect Summary

	 <b>Spot</b>	 <b>Surface</b>	 <b>Cell</b>	 <b>Filament</b>
Intensity	✓	✓	✓	X
Counts. Positions	✓	✓	✓	✓
Diameters	✓	X	✓	✓
Volume, Area & Morphology	X Est. Volume	✓	✓	X Est. Volume
Intercellular Component Analysis: Num. Vesicles/Cell&Nucleus Num. Nuclei/Cell	X	X	✓	X
Membrane Staining	X	X	✓	X
Network Complexity: Lengths, Branches, Scholl, Straightness, Orientation, Spines...	X	X	X	✓
<b>Track</b>	✓	✓	✓	✓

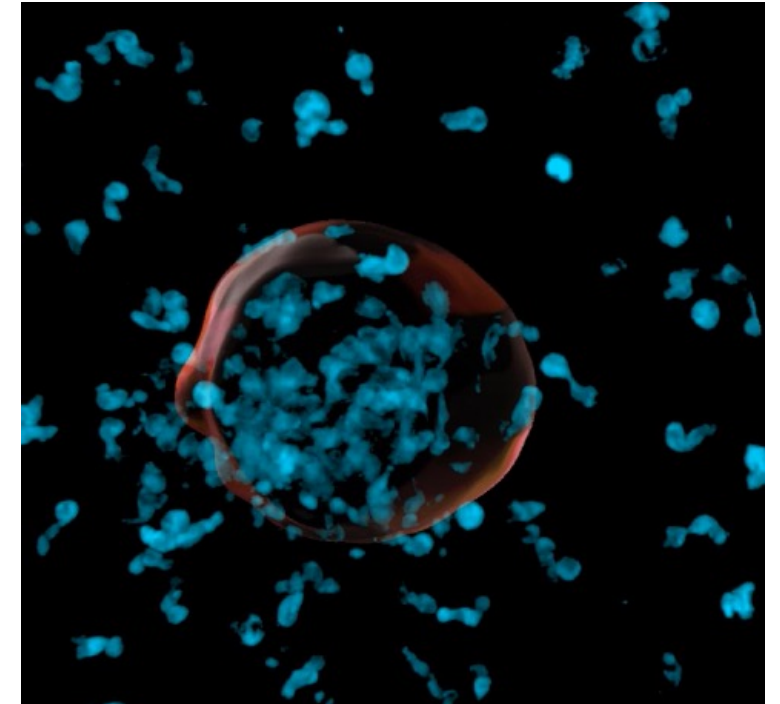
## Colocalization

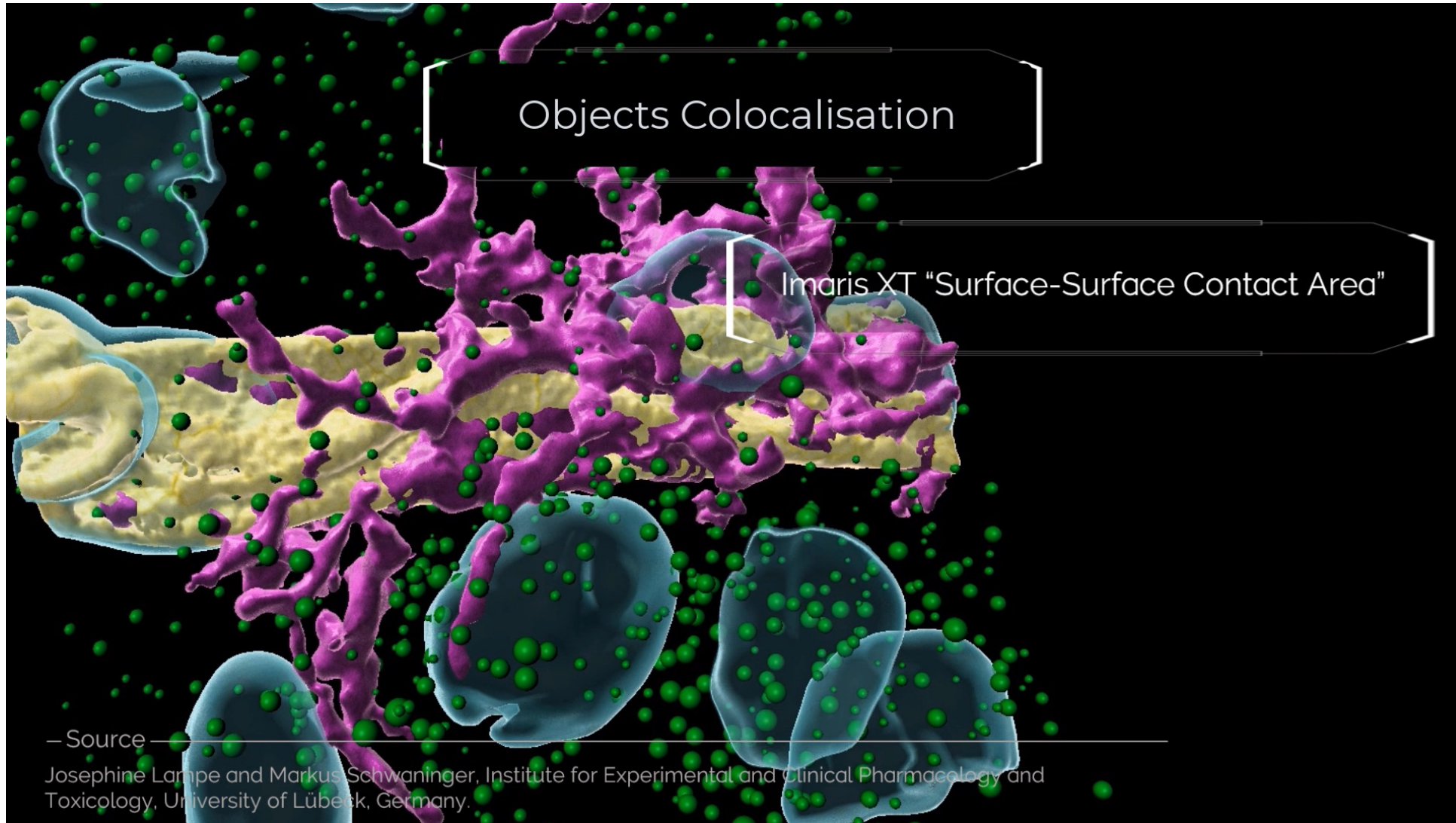


## Object Classification



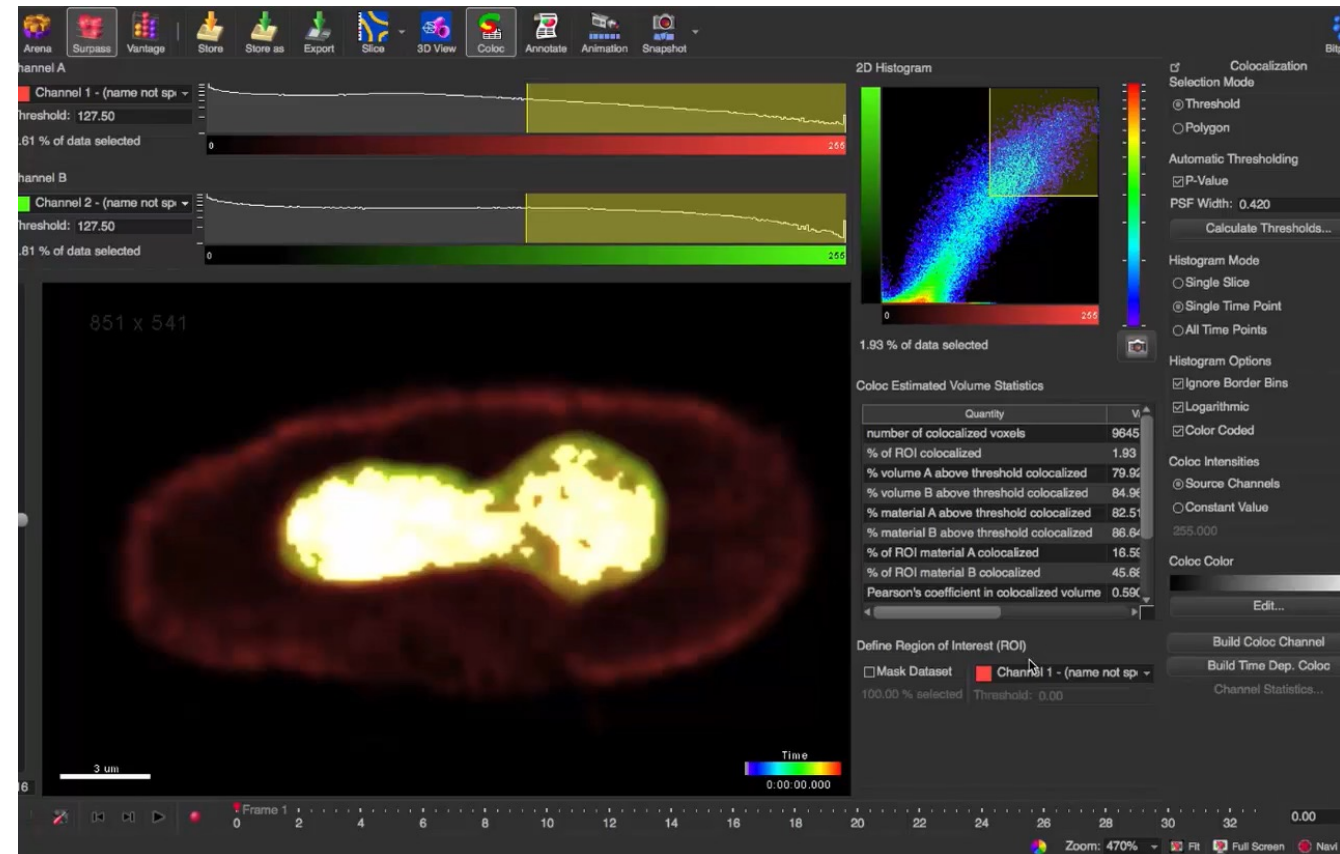
## Affinities





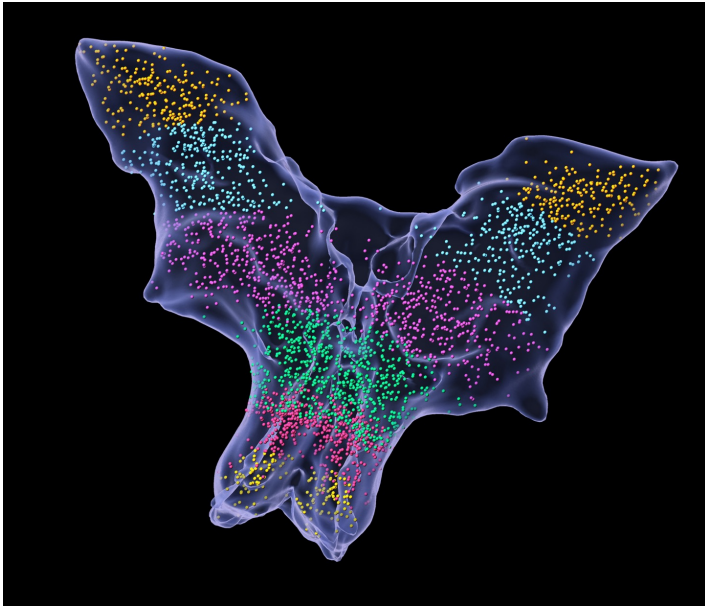
# Colocalization – ImarisColoc

- ImarisColoc is the most powerful colocalization analysis tool to quantify and document codistribution of multiple stained biological components.
  - Co-localization available for 2D, 3D data and time series
  - Co-localized regions can be presented as new 3D or 4D color channel
  - Users can expand or narrow the region from which histograms for colocalization are computed
  - Automatic calculations: **Pearson's coefficient**, **Mander's coefficient**, co-localized voxels, co-localized percentages



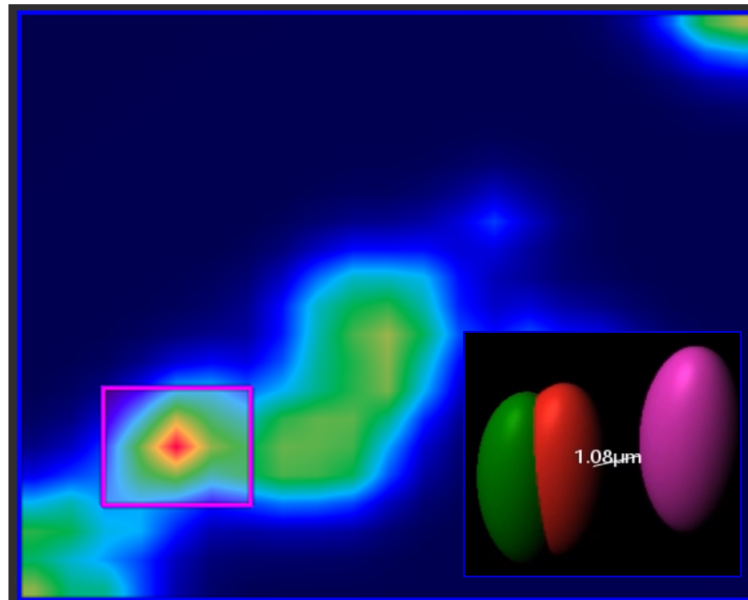
## 1 Parameter

*Ex: Cell migration*



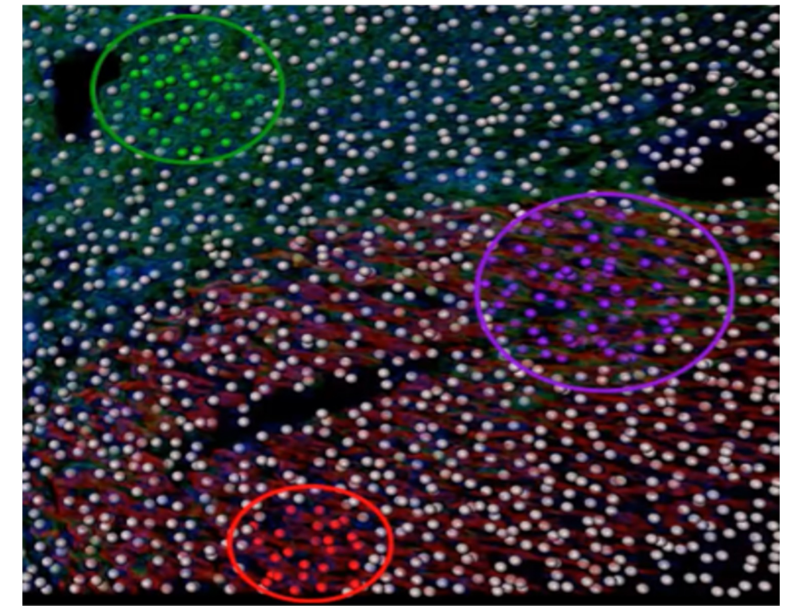
## 2 Parameters

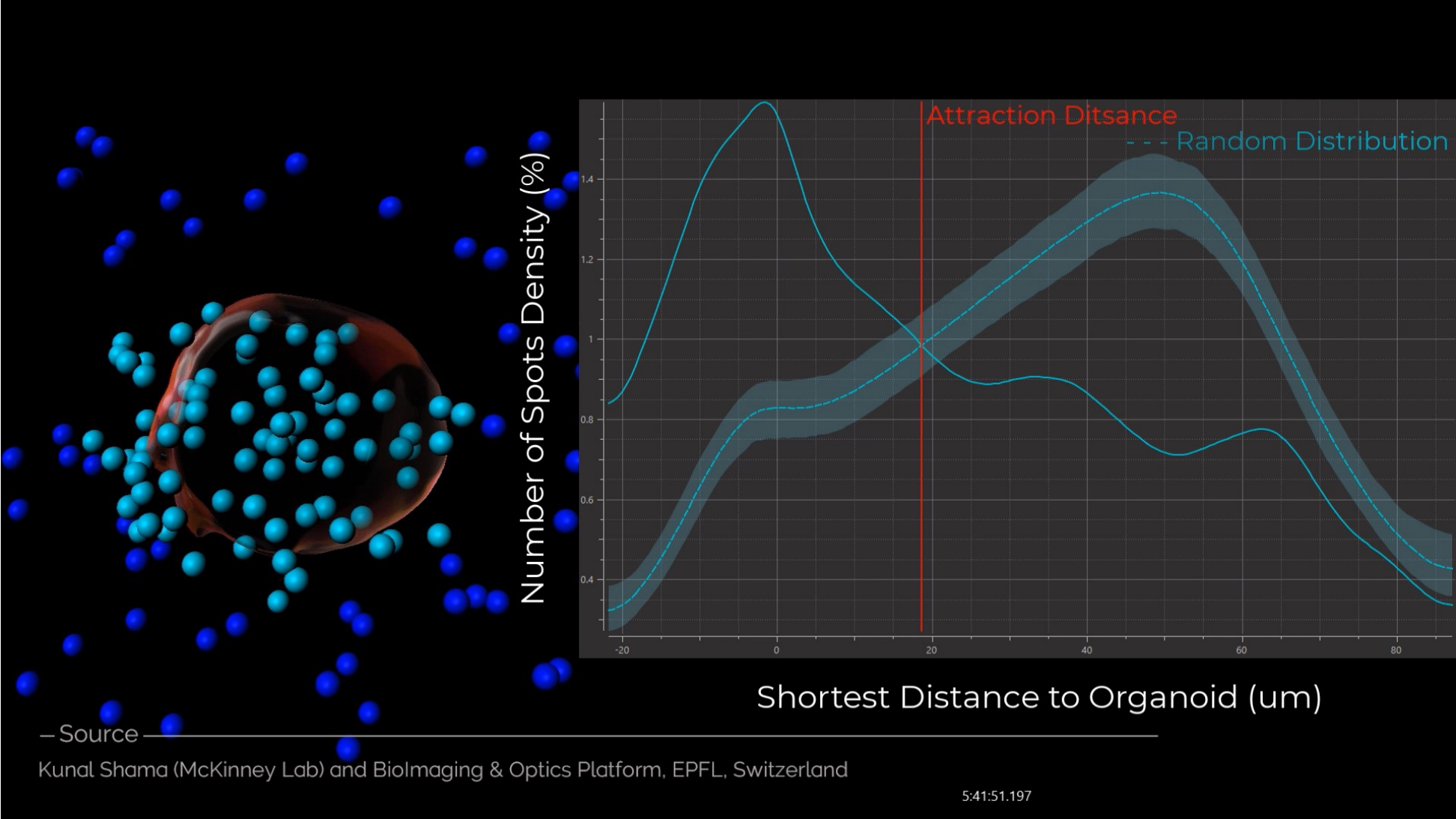
*Ex: Triplets colocalization*



## Machine Learning

*Ex: Identification of regions*



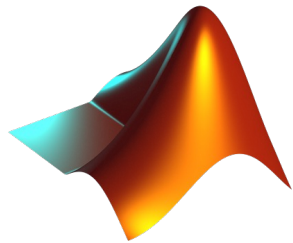


## Expand IMARIS power with Imaris XTension (plugins)

Write Your Own XTensions

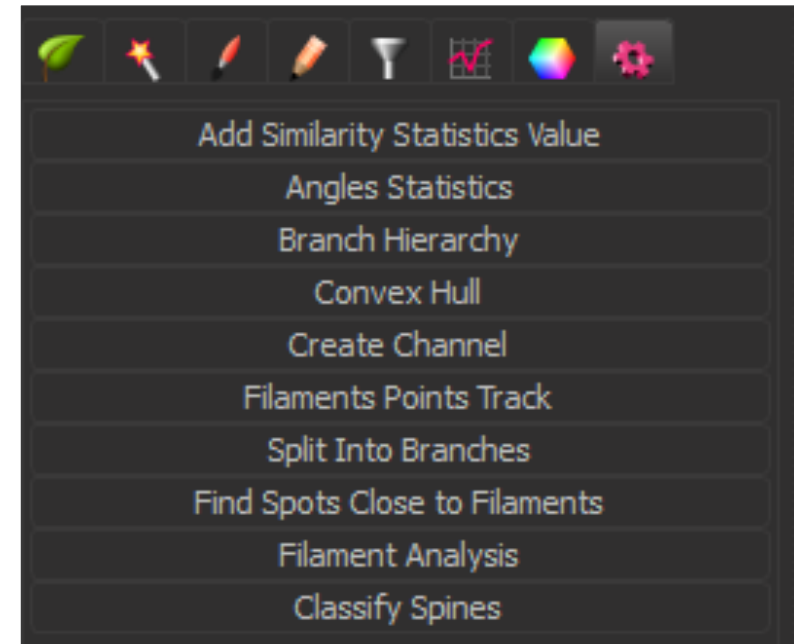


Python



Matlab

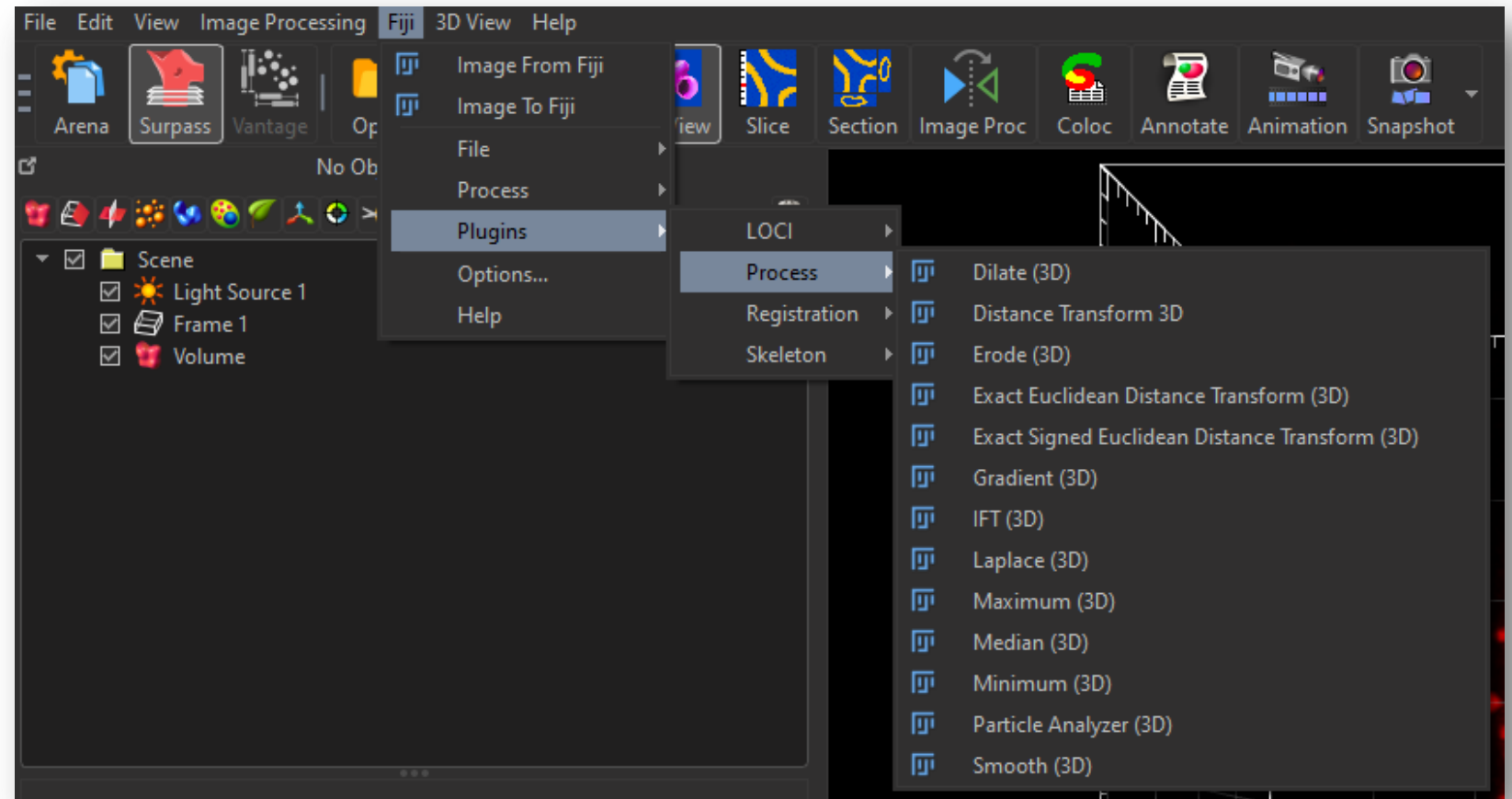
Integrate Xtensions



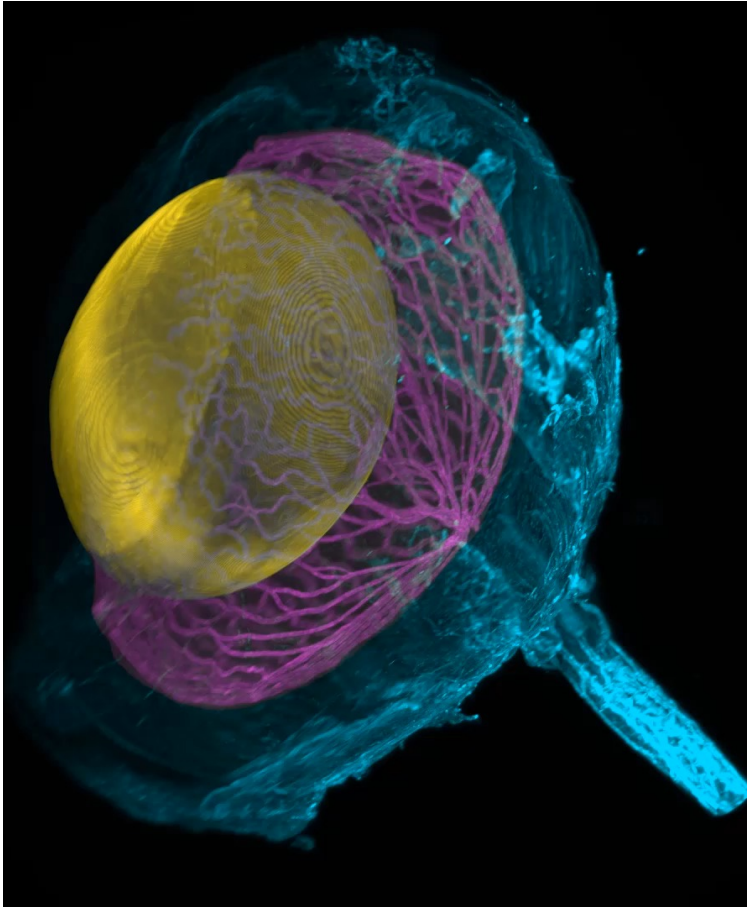
## Connect to Fiji & ImageJ



- Multiple plugins already incorporated
- Direct Bridging



Animation

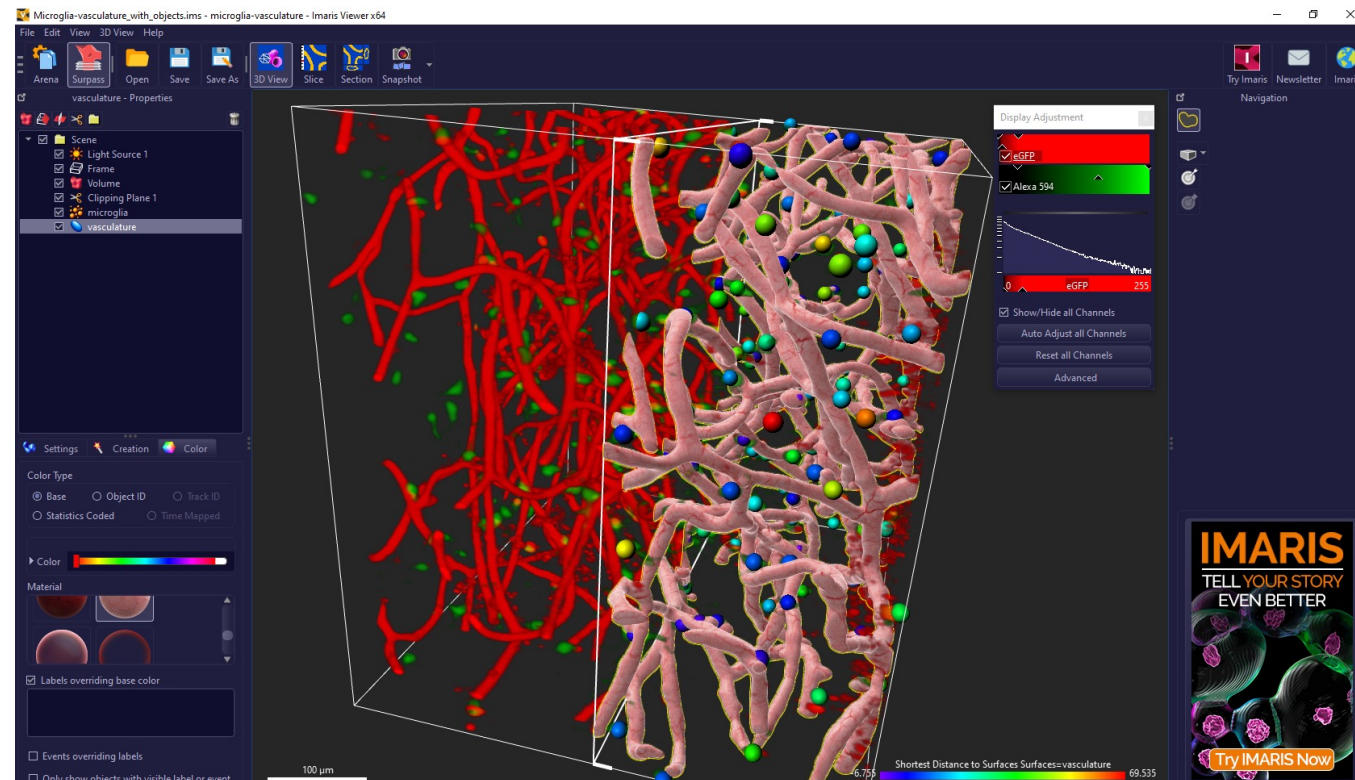


Snapshot





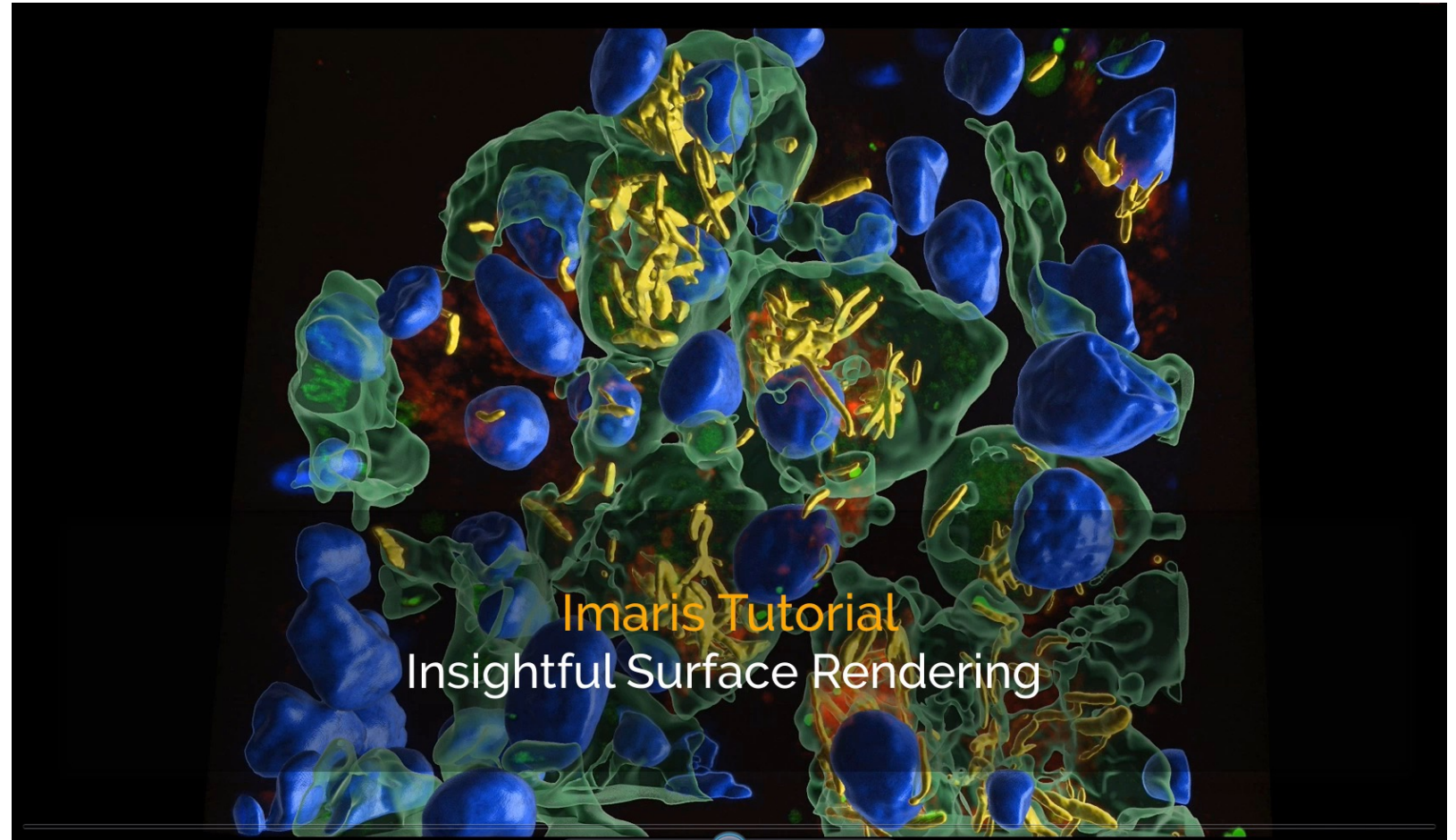
## Imaris viewer



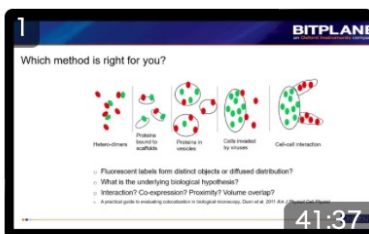
## Learning center

[imaris.oxinst.com/learning/](https://www.oxinst.com/learning/)

- Webinar recordings
- Customer case Study
- Tutorial videos
- IMARIS Homeschools



## 操作教程



Various ways of solving the colocalization problem

1521 2020-5-28



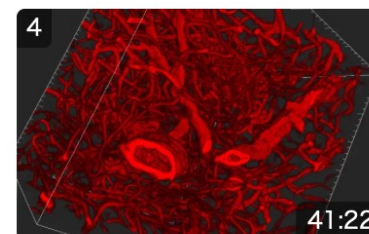
Imaris Plots as an added value of your analysis

685 2020-6-2



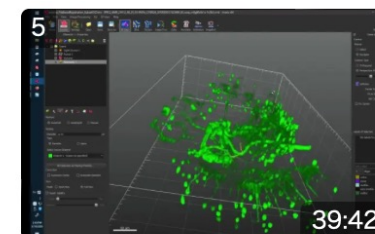
Batch-make your workflows more efficient

666 2020-5-27



Analysis of Vasculature-Combining multiple Imaris

1834 2020-5-21



Filament Tracer manual

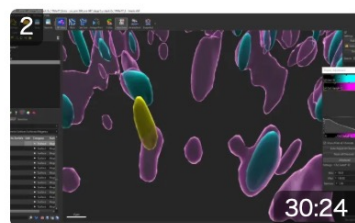
1651 2020-5-19

## 新版本发布



Imaris 9.8 | I can see clearly now!

1006 2021-11-9



Imaris 9.7 Diving into Structure and Dynamics

922 2021-3-3



[合集] Imaris9.6 新功能介绍

2809 2020-8-21

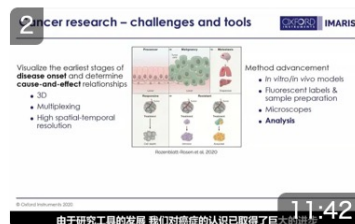


## 前沿应用分享



Imaris for Immunology Research

734 2021-10-19



Imaris for Cancer Research

242 2021-10-19



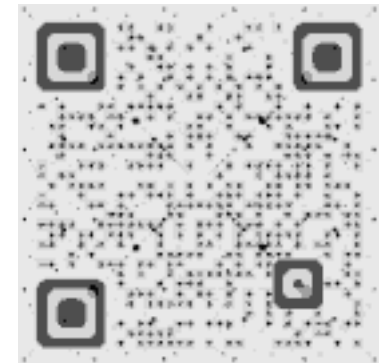
Bone Analysis with Surface Tool~~

734 2020-11-20

粉丝数 获赞数 播放数  
3935 1311 11万

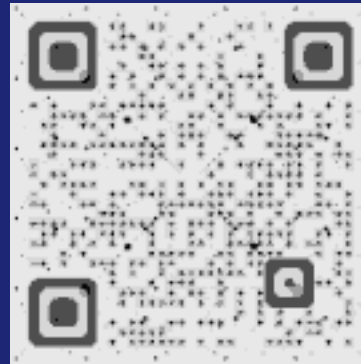


- Free Imaris File Converter:  
<https://imaris.oxinst.com/microscopy-imaging-software-free-trial>
- Free Imaris Viewer:  
<https://imaris.oxinst.com/imaris-viewer>
- Free 10 Days Trail:  
<https://imaris.oxinst.com/microscopy-imaging-software-free-trial>
- System Requirement for Windows and Mac:  
<https://imaris.oxinst.com/support/system-requirements>
- Imaris Home School  
<https://imaris.oxinst.com/homeschool>
- Bilibili, Account: 牛津仪器-Imaris  
<https://space.bilibili.com/512602011/video>



欢迎关注  
牛津仪器官方微信公众号

# Thanks for your attention!



欢迎关注  
牛津仪器官方微信公众号



SCIENCE ADVANCES | RESEARCH ARTICLE

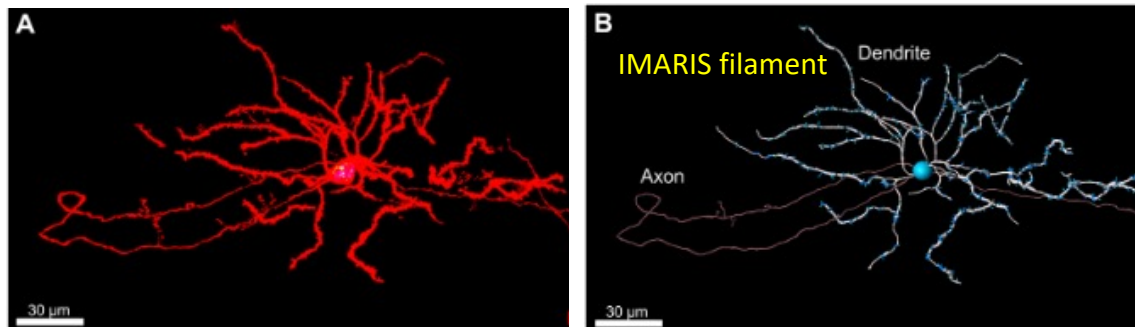
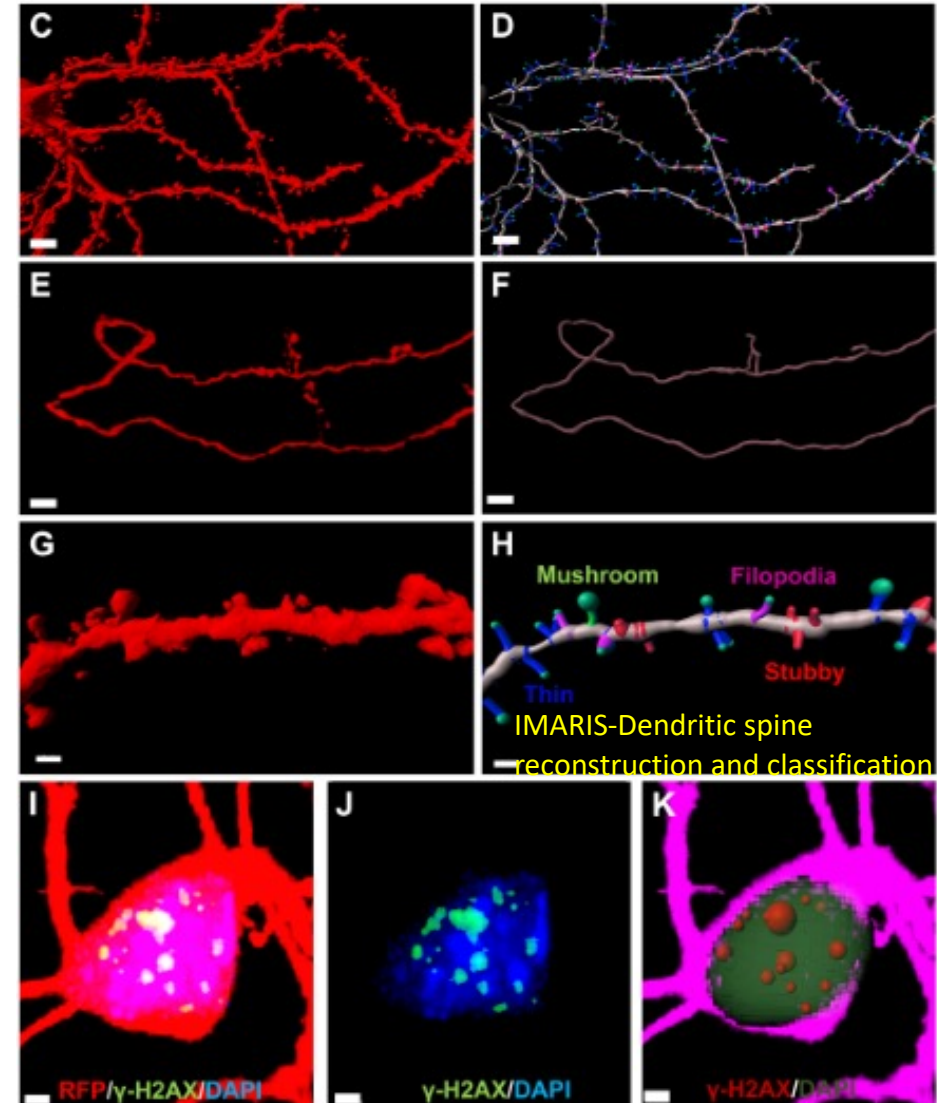
NEUROSCIENCE

## Tracing brain genotoxic stress in Parkinson's disease with a novel single-cell genetic sensor

Madison Wynne El-Saadi<sup>1</sup>, Xinli Tian<sup>1</sup>, Mychal Grames<sup>1</sup>, Michael Ren<sup>1</sup>, Kelsea Keys<sup>1</sup>, Hanna Li<sup>1</sup>, Erika Knott<sup>1</sup>, Hong Yin<sup>2</sup>, Shile Huang<sup>3</sup>, Xiao-Hong Lu<sup>1\*</sup>

To develop an *in vivo* tool to probe brain genotoxic stress, we designed a viral proxy as a single-cell genetic sensor termed PRISM that harnesses the instability of recombinant adeno-associated virus genome processing and a hypermutable repeat sequence-dependent reporter. PRISM exploits the virus-host interaction to probe persistent neuronal DNA damage and overactive DNA damage response. A Parkinson's disease (PD)-associated environmental toxicant, paraquat (PQ), inflicted neuronal genotoxic stress sensitively detected by PRISM. The most affected cell type in PD, dopaminergic (DA) neurons in substantia nigra, was distinguished by a high level of genotoxic stress following PQ exposure. Human alpha-synuclein proteotoxicity and propagation also triggered genotoxic stress in nigral DA neurons in a transgenic mouse model. Genotoxic stress is a prominent feature in PD patient brains. Our results reveal that PD-associated etiological factors precipitated brain genotoxic stress and detail a useful tool for probing the pathogenic significance in aging and neurodegenerative disorders.

El-Saadi, M. W. *et al.* Tracing brain genotoxic stress in Parkinson's disease with a novel single-cell genetic sensor. *Sci. Adv.* **8**, eabd1700 (2022).





ARTICLES

<https://doi.org/10.1038/s41592-020-0792-1>

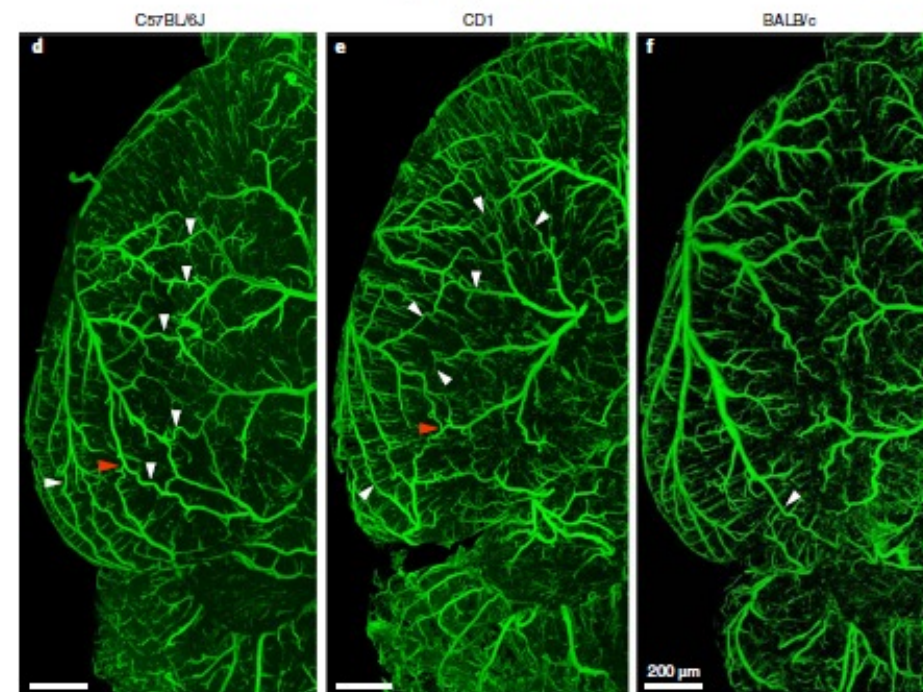
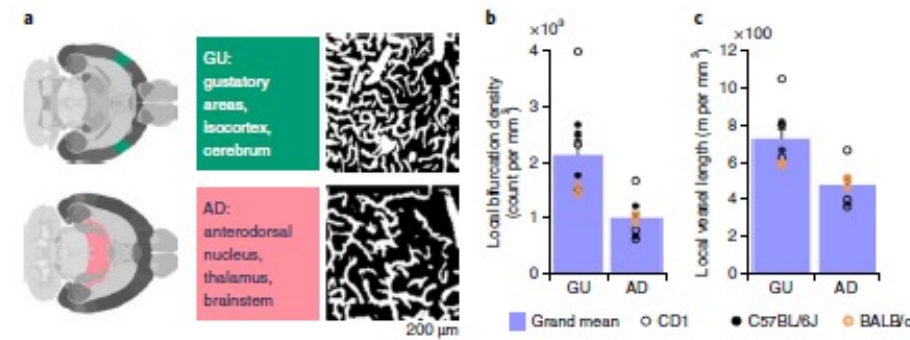
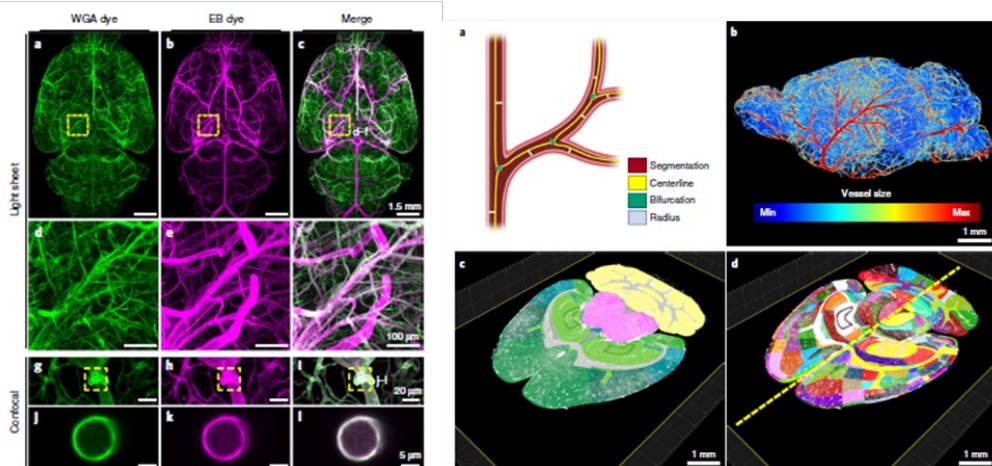
nature methods

Check for updates

## Machine learning analysis of whole mouse brain vasculature

Mihail Ivilinov Todorov<sup>1,2,3,10</sup>, Johannes Christian Paetzold<sup>4,5,6,10</sup>, Oliver Schoppe<sup>4,5</sup>, Giles Tetteh<sup>4</sup>, Suprosanna Shit<sup>4,5,6</sup>, Velizar Efremov<sup>4,7</sup>, Katalin Todorov-Völgyi<sup>2</sup>, Marco Düring<sup>2,8</sup>, Martin Dichgans<sup>2,8,9</sup>, Marie Piraud<sup>4</sup>, Bjoern Menze<sup>4,5,6,11</sup> and Ali Ertürk<sup>1,2,8,11</sup>

Tissue clearing methods enable the imaging of biological specimens without sectioning. However, reliable and scalable analysis of large imaging datasets in three dimensions remains a challenge. Here we developed a deep learning-based framework to quantify and analyze brain vasculature, named Vessel Segmentation & Analysis Pipeline (VesSAP). Our pipeline uses a convolutional neural network (CNN) with a transfer learning approach for segmentation and achieves human-level accuracy. By using VesSAP, we analyzed the vascular features of whole C57BL/6J, CD1 and BALB/c mouse brains at the micrometer scale after registering them to the Allen mouse brain atlas. We report evidence of secondary intracranial collateral vascularization in CD1 mice and find reduced vascularization of the brainstem in comparison to the cerebrum. Thus, VesSAP enables unbiased and scalable quantifications of the angioarchitecture of cleared mouse brains and yields biological insights into the vascular function of the brain.



Todorov, M. I. *et al.* Machine learning analysis of whole mouse brain vasculature. *Nat Methods* 17, 442–449 (2020).

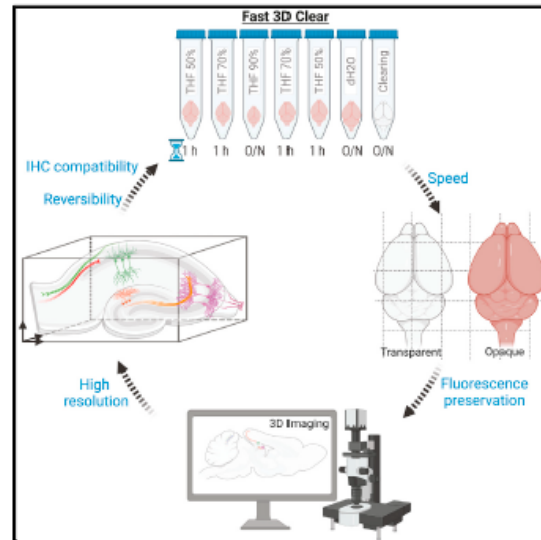


Cell Reports  
**Methods**

Report

**A fast, aqueous, reversible three-day tissue clearing method for adult and embryonic mouse brain and whole body**

Graphical abstract



Authors

Stylios Kosmidis, Adrian Negrean, Alex Dranovsky, Attila Losonczy, Eric R. Kandel

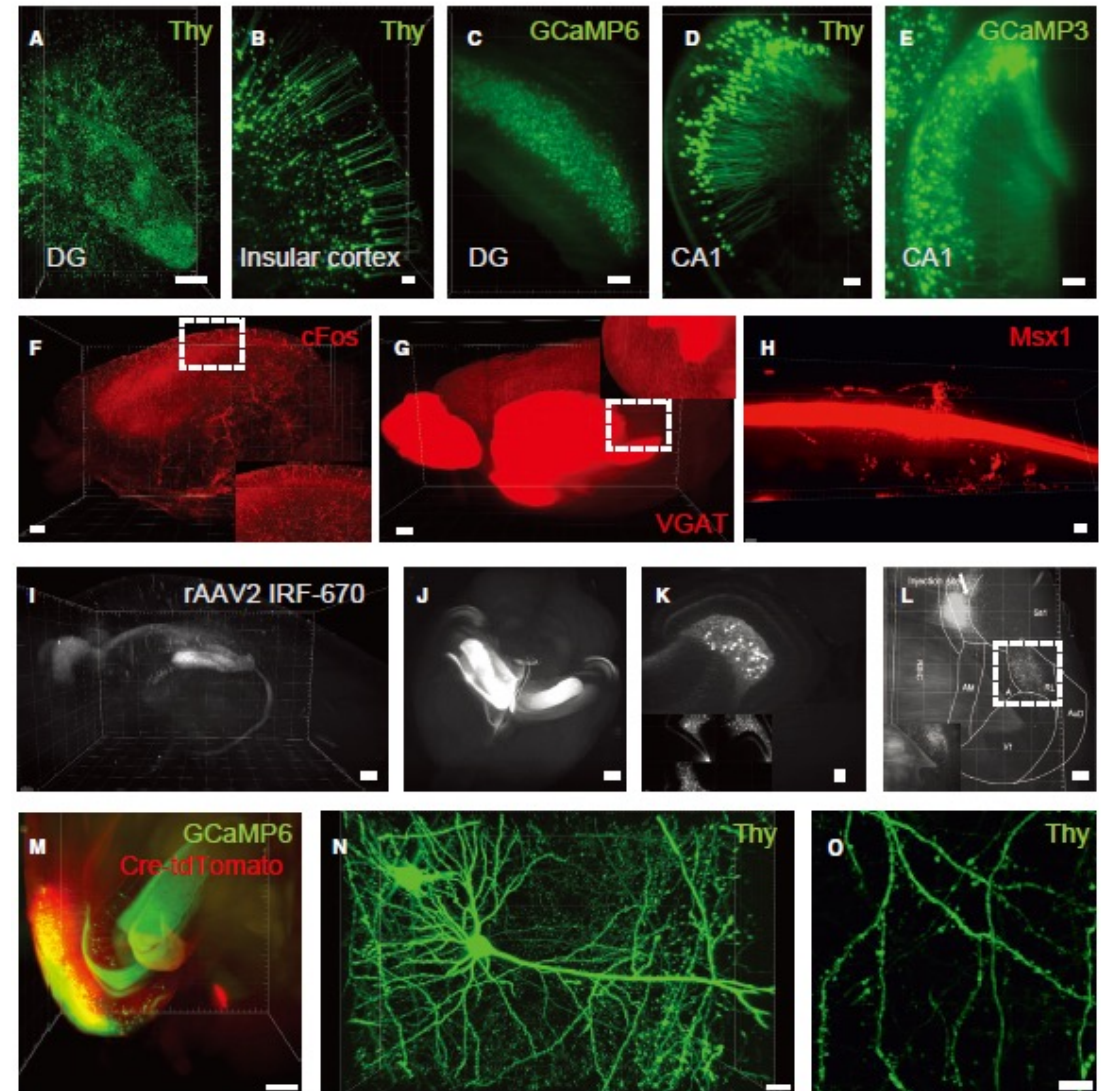
Correspondence

erk5@columbia.edu (E.R.K.), sk3440@columbia.edu (S.K.)

In brief

Tissue clearing enables the study of cells as units and as components of a network within intact organs. Kosmidis et al. develop an easy and speedy method for clearing large tissues and visualizing individual cells and their connections within the brain in 3D.

Kosmidis, S., Negrean, A., Dranovsky, A., Losonczy, A. & Kandel, E. R. A fast, aqueous, reversible three-day tissue clearing method for adult and embryonic mouse brain and whole body. *Cell Reports Methods* 1, 100090 (2021).



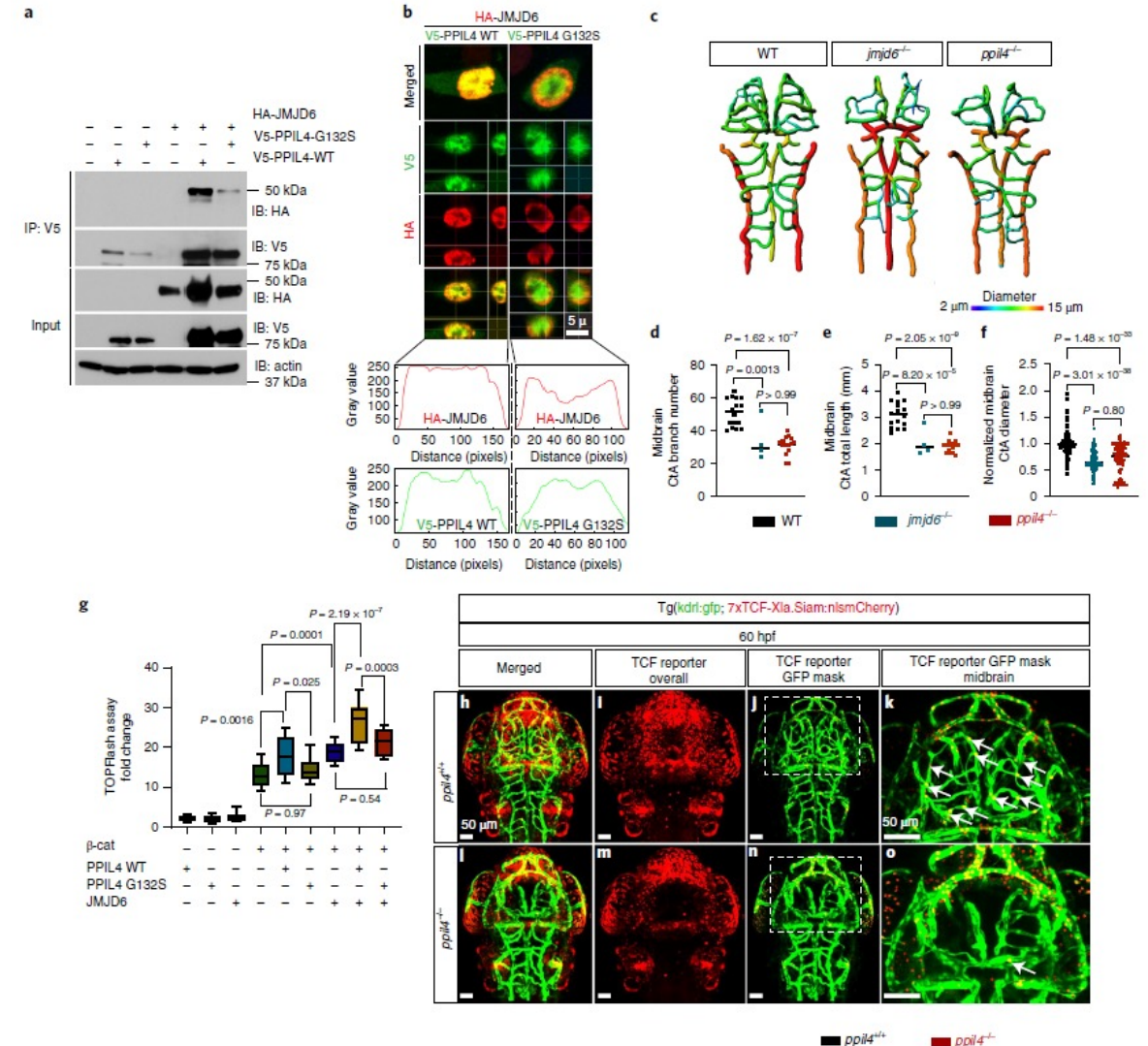


## PPIL4 is essential for brain angiogenesis and implicated in intracranial aneurysms in humans

Tanyeri Barak<sup>1,2,3,4,18</sup>, Emma Ristori<sup>2,5,18</sup>, A. Gulhan Ercan-Sencicek<sup>1,2,3,4</sup>, Danielle F. Miyagishima<sup>1,2,3,4</sup>, Carol Nelson-Williams<sup>2</sup>, Weilai Dong<sup>2,6</sup>, Sheng Chih Jin<sup>2,6,7</sup>, Andrew Prendergast<sup>5</sup>, William Armero<sup>2,5</sup>, Octavian Henegariu<sup>1,2,3,4</sup>, E. Zeynep Erson-Omay<sup>1,2,3,4</sup>, Akdes Serin Harmanci<sup>1,2,3,4</sup>, Mikhael Guy<sup>8</sup>, Batur Gültekin<sup>1</sup>, Deniz Kilic<sup>1</sup>, Devendra K. Rai<sup>1,2,3,4</sup>, Nükte Goc<sup>1</sup>, Stephanie Marie Aguilera<sup>1</sup>, Burcu Gülez<sup>1</sup>, Selin Altinok<sup>1</sup>, Kent Ozcan<sup>1</sup>, Yanki Yarman<sup>1</sup>, Süleyman Coskun<sup>1,2,3,4</sup>, Emily Sempou<sup>9</sup>, Engin Deniz<sup>9</sup>, Jared Hintzen<sup>5</sup>, Andrew Cox<sup>2</sup>, Elena Fomchenko<sup>1</sup>, Su Woong Jung<sup>10</sup>, Ali Kemal Ozturk<sup>11</sup>, Angeliki Louvi<sup>1,4</sup>, Kaya Bilgüvar<sup>2,4,12</sup>, E. Sander Connolly Jr.<sup>13</sup>, Mustafa K. Khokha<sup>2,9</sup>, Kristopher T. Kahle<sup>1,4,15,16</sup>, Katsuhito Yasuno<sup>1,2,3,4</sup>, Richard P. Lifton<sup>2,6</sup>, Ketu Mishra-Gorur<sup>1,2,3,4</sup>, Stefania Nicoli<sup>2,5,17</sup> and Murat Günel<sup>1,2,3,4</sup>

Intracranial aneurysm (IA) rupture leads to subarachnoid hemorrhage, a sudden-onset disease that often causes death or severe disability. Although genome-wide association studies have identified common genetic variants that increase IA risk moderately, the contribution of variants with large effect remains poorly defined. Using whole-exome sequencing, we identified significant enrichment of rare, deleterious mutations in *PPIL4*, encoding peptidyl-prolyl *cis-trans* isomerase-like 4, in both familial and index IA cases. *Ppil4* depletion in vertebrate models causes intracerebral hemorrhage, defects in cerebrovascular morphology and impaired Wnt signaling. Wild-type, but not IA-mutant, *PPIL4* potentiates Wnt signaling by binding *JMJD6*, a known angiogenesis regulator and Wnt activator. These findings identify a novel *PPIL4*-dependent Wnt signaling mechanism involved in brain-specific angiogenesis and maintenance of cerebrovascular integrity and implicate *PPIL4* gene mutations in the pathogenesis of IA.

Barak, T. *et al.* *PPIL4* is essential for brain angiogenesis and implicated in intracranial aneurysms in humans. *Nat Med* 27, 2165–2175 (2021).





nature neuroscience

ARTICLES

<https://doi.org/10.1038/s41593-022-01091-9>

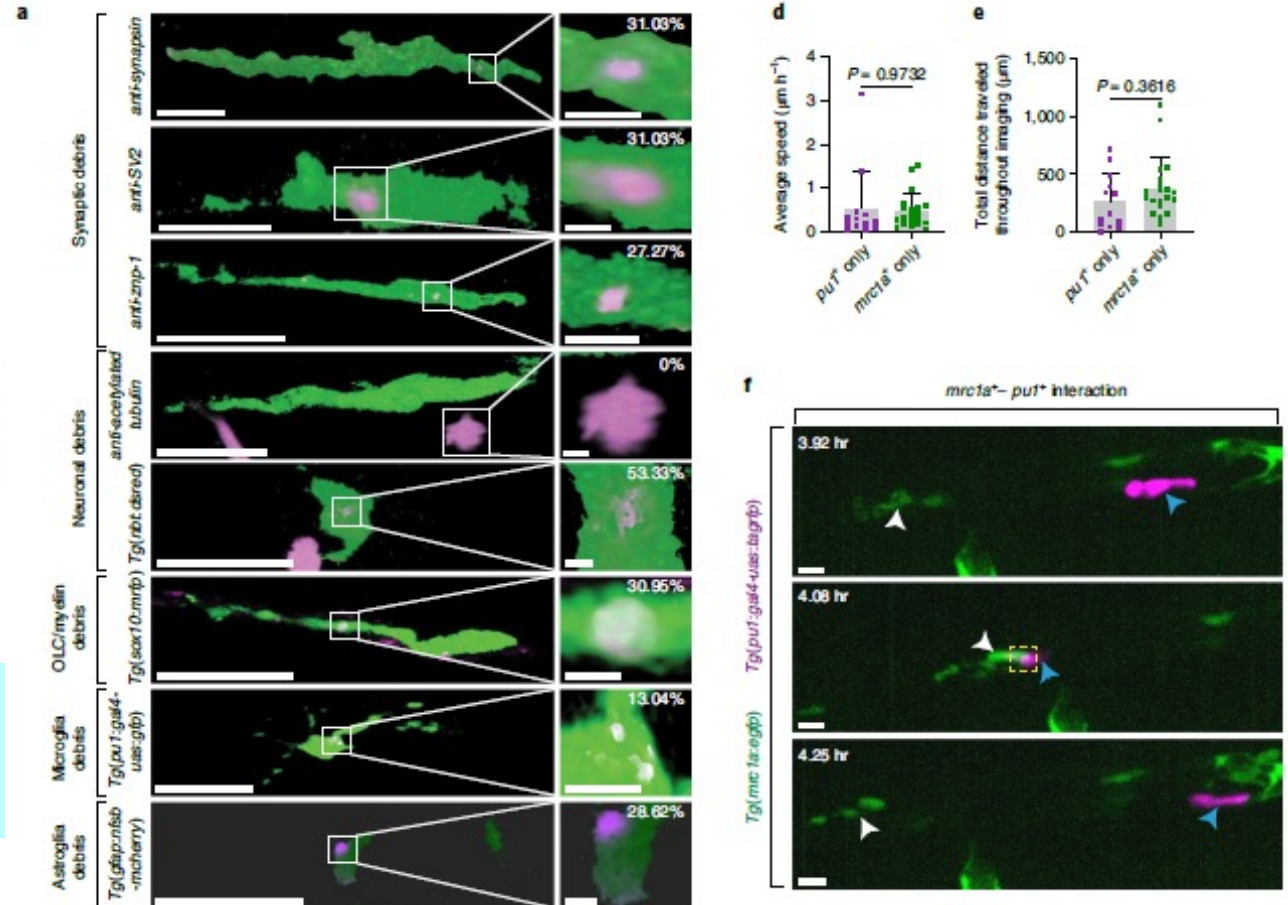
Check for updates

## The embryonic zebrafish brain is seeded by a lymphatic-dependent population of *mrc1*<sup>+</sup> microglia precursors

Lauren A. Green<sup>1,2,3</sup>, Michael R. O’Dea<sup>1,3</sup>, Camden A. Hoover<sup>1,2</sup>, Dana F. DeSantis<sup>1,2</sup> and Cody J. Smith<sup>1,2</sup>

Microglia are the resident macrophages of the CNS that serve critical roles in brain construction. Although human brains contain microglia by 4 weeks gestation, an understanding of the earliest microglia that seed the brain during its development remains unresolved. Using time-lapse imaging in zebrafish, we discovered a *mrc1a*<sup>+</sup> microglia precursor population that seeds the brain before traditionally described microglia. These early microglia precursors are dependent on lymphatic vasculature that surrounds the brain and are independent of *pu1*<sup>+</sup> yolk sac-derived microglia. Single-cell RNA-sequencing datasets reveal *Mrc1*<sup>+</sup> microglia in the embryonic brains of mice and humans. We then show in zebrafish that these early *mrc1a*<sup>+</sup> microglia precursors preferentially expand during pathophysiological states in development. Taken together, our results identify a critical role of lymphatics in the microglia precursors that seed the early embryonic brain.

Green, L. A., O’Dea, M. R., Hoover, C. A., DeSantis, D. F. & Smith, C. J. The embryonic zebrafish brain is seeded by a lymphatic-dependent population of *mrc1*<sup>+</sup> microglia precursors. *Nat Neurosci* (2022) doi:10.1038/s41593-022-01091-9.



## nature metabolism

Explore content ▾ About the journal ▾ Publish with us ▾ Subscribe

[nature](#) > [nature metabolism](#) > [articles](#) > [article](#)

Article | [Published: 28 November 2022](#)

### Maternal diet disrupts the placenta–brain axis in a sex-specific manner

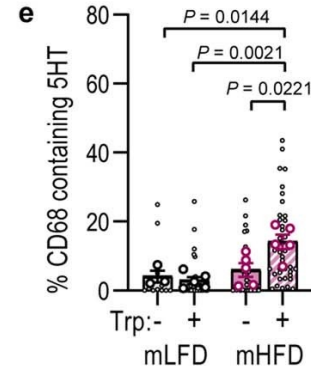
[Alexis M. Ceasrine](#), [Benjamin A. Devlin](#), [Jessica L. Bolton](#), [Lauren A. Green](#), [Young Chan Jo](#), [Carolyn Huynh](#), [Bailey Patrick](#), [Kamryn Washington](#), [Cristina L. Sanchez](#), [Faith Joo](#), [A. Brayan Campos-Salazar](#), [Elana R. Lockshin](#), [Cynthia Kuhn](#), [Susan K. Murphy](#), [Leigh Ann Simmons](#) & [Staci D. Bilbo](#)

[Nature Metabolism](#) **4**, 1732–1745 (2022) | [Cite this article](#)

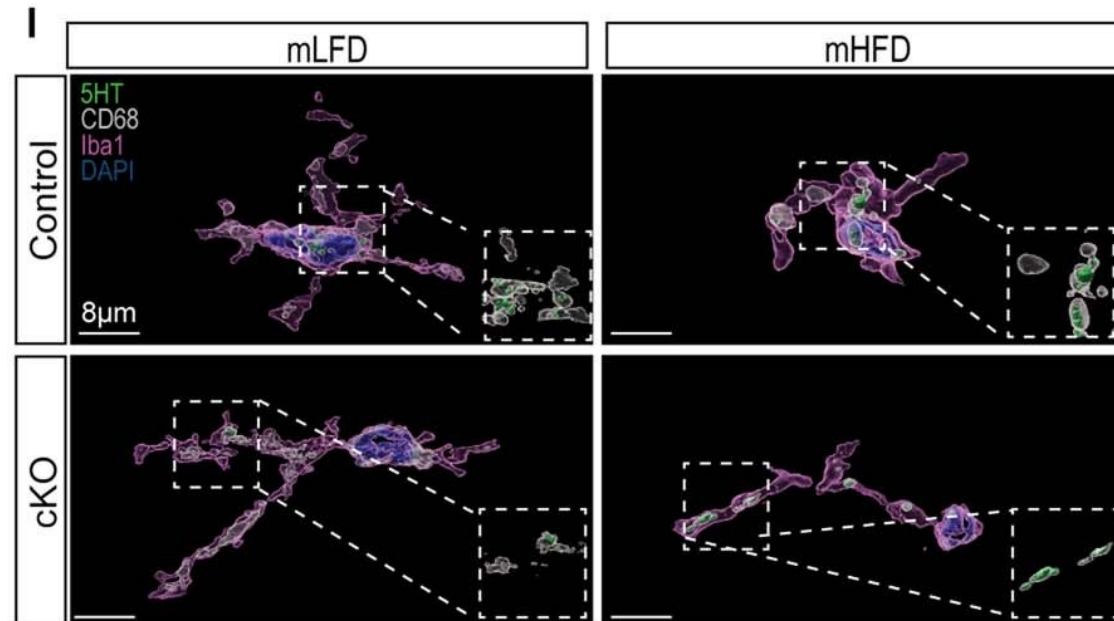
3865 Accesses | 1 Citations | 220 Altmetric | [Metrics](#)

#### Abstract

High maternal weight is associated with detrimental outcomes in offspring, including increased susceptibility to neurological disorders such as anxiety, depression and communicative disorders. Despite widespread acknowledgement of sex biases in the development of these disorders, few studies have investigated potential sex-biased mechanisms underlying disorder susceptibility. Here, we show that a maternal high-fat diet causes endotoxin accumulation in fetal tissue, and subsequent perinatal inflammation contributes to sex-specific behavioural outcomes in offspring. In male offspring exposed to a maternal high-fat diet, increased macrophage Toll-like receptor 4 signalling results in excess microglial phagocytosis of serotonin (5-HT) neurons in the developing dorsal raphe nucleus, decreasing 5-HT bioavailability in the fetal and adult brains. Bulk sequencing from a large cohort of matched first-trimester human samples reveals sex-specific transcriptome-wide changes in placental and brain tissue in response to maternal triglyceride accumulation (a proxy for dietary fat content). Further, fetal brain 5-HT levels decrease as placental triglycerides increase in male mice and male human samples. These findings uncover a microglia-dependent mechanism through which maternal diet can impact offspring susceptibility for neuropsychiatric disorder development in a sex-specific manner.



**Extended Fig 7e**, **IMARIS** reconstruction quantification from female e14.5 dorsal raphe nucleus microglia. Statistics shown for animal averages (large circles), small circles are individual microglia. (n = 3 mLFD, 5, mLFD+Trp, 6 mHFD, 5 mHFD+Trp from 3 litters/diet).



**Extended Fig 7f**, **IMARIS** reconstructions from female mLFD and mHFD control and cKO e14.5 DRN. Statistics ran for animal averages (large circles), small circles are individual microglia. (n = 7 mLFD control, 5 mLFD cKO, 5 mHFD control, and 4 mHFD cKO from 7 mLFD and 5 mHFD litters)